A Comparison of Weighted and Fuzzy Overlays in Mapping Landslide Susceptibility, South-Central Front Range, Colorado

by

Patricia L. Lee

A Thesis Presented to the
FACULTY OF THE USC DORNSIFE COLLEGE OF LETTERS, ARTS AND SCIENCES
UNIVERSITY OF SOUTHERN CALIFORNIA
In Partial Fulfillment of the
Requirements for the Degree
MASTER OF SCIENCE
(GEOGRAPHIC INFORMATION SCIENCE AND TECHNOLOGY)

May 2023

Copyright © 2023 Patricia L. Lee

To my family, who have always had my best interests at heart

Acknowledgements

My gratitude goes to Dr. Sedano for ensuring I did not stray too far into the weeds and for guidance when I needed it. I am also grateful to my work wife Dr. Caekaert for bouncing ideas with me whenever I need a sounding board and giving me sound advice. To my dearest friends and my classmates turned friends, thank you for your help and support.

Table of Contents

List of Tables

List of Figures

Abbreviations

AHP	Analytical hierarchy process
AOI	Area of interest
DEM	Digital elevation model
ELECTRE	ELimination Et Choix TRaduisant la REalité
GIS	Geographic information systems
GISci	Geographic information science
GIS-MCDA	Geographic information science-multiple criteria decision analysis
LiDAR	Light Detecting And Ranging
LR	Logarithmic Regression
LULC	Land use/land cover
MAUT	Multi-attribute utility theory
MCDA	Multiple criteria decision analysis
MS	Mean and standard deviation
MSL	Mean sea level
NDVI	Normalized difference vegetation index
NOAA	National Oceanic and Atmospheric Administration
PROMETHEE	Preference Ranking Organization METHod for Enrichment Evaluations
SPI	Stream power index
STI	Sediment transportation index
SWR	Soil water retention
TPI	Topographic position index
TWI	Topographic wetness index

VC	Vegetation coverage
US	United States
USDA	United States Department of Agriculture
USGS	United States Geological Survey

Abstract

Landslide susceptibility mapping incorporates variables such as slope, precipitation, and lithology, among others, alongside a wide range of different methodologies in order to generate maps that may aid in landslide prediction. Criteria in the literature is expansive and varied, and the weighting methods used equally so. Weighted overlay and fuzzy overlay were chosen and compared using a select number of criteria as a means of testing which method would yield a better, more accurate result. Between the two, fuzzy overlay appears to be the more accurate of the two methods after evaluating the outputs, and this is due to the ways in which the two methods classify criteria. Of the eight criteria used, slope has been the most influential criterion for both methods with lithology coming in as a surprisingly strong factor for the weighted overlay and drainage systems as a strong influence for the fuzzy overlay. This influence is reflected in the locations of areas of higher landslide susceptibility and reveal that weighting and bias have definite effects on the outputs. There then exists a circular influence between the outputs shaping decisions that may affect large numbers of people and decisionmakers' opinions affecting criteria emphasis. Of the two methods used, fuzzy overlay produced less biased results than weighted overlay, as the emphasis used in weighted overlay are highly subjective and influenced by the user.

Chapter 1 Introduction

Landslides are natural phenomena that cause extensive damage to property and loss of life across the globe (AMERICAN GEOSCIENCES INSTITUTE n.d.; USGS n.d.; Wayllace et al. 2019; Wieczorek and Leahy 2008). They are not easy to predict, as they have various triggers and mechanisms of movement (Highland 2008; Korup 2017). Researchers use geographic information science (GIS) to not only image the before and after of a landslide event (Petley 2012) but also to create predictive maps and models on landslide severity and frequency (Lai and Tsai 2019; Qiu and Mitani 2017; Saha et al. 2005; Tan et al. 2020; Zhou et al. 2021). The purpose of this project is to compare landslide susceptibility results of two methodologies, weighted overlay and fuzzy overlay, to understand how differences in weighting methods affects the results. An overview of the different criteria used in the literature is covered, as well as what variables were included in the analyses. The results of the two methods are then compared along with limitations of this study as well as how projects like this impact society.

1.1. Background

The combination of geographical information science and geology makes logical sense, as both fields convey information primarily through the use of maps. Studies viewing landslides through the combined lenses of geology and GIS have been done before, and research and modelling within the geoscience realm has prioritized the effects of precipitation and groundwater on landslide initiation and movement (Bogaard et al. 2007; Shou and Chen 2021; Wayllace et al. 2019). Many studies on various geologic properties of landslides that are not strictly “spatial” and do not employ GIS exist, such as studies of water saturation and pore pressure (De Maio et al. 2020; Schulz et al. 2009; Viesca and Rice 2012; Wang and Sassa 2009),

soil composition and geology (Blońska et al 2018; Donnarumma et al. 2013; Park 2015), and slope angle (Çellek 2020; Coe et al. 2004; Iwahashi et al. 2002; Zakaria et al. 2017).

A variety of models have been used for landslide hazard and prediction ranging from heuristic fuzzy approach to machine learning (Ercanoglu and Gokceoglu 2001; Feizizadeh and Blaschke 2012; Feizizadeh and Blaschke 2014; Francioni et al. 2019; Kavzoglu et al. 2013; Lai and Tsai 2019; Palcic and Lalic 2009; Stanley and Kirschbaum 2021; Zhou et al. 2021). Multiple criteria decision analysis (MCDA) has been the most frequently used method to determine locations of highest landslide risk. There are multiple methods within MCDA to weight criteria, and each method has its strengths and weaknesses. Here, the weighted overlay method was used to rank and weigh criteria and a fuzzy overlay was used as comparison.

This project utilized a number of criteria that have been used for landslide susceptibility mapping and evaluation. A digital elevation model (DEM) is an important dataset for this project, as from this one piece of data, slope may also be derived. As far as properties of the natural environment go, geology, precipitation, and rivers have been shown to be important factors that were used (Ayalew and Yamagishi 2004; Chen and Li 2020; Du et al. 2014; Erener et al. 2016; Feizizadeh and Blaschke 2013; Feizizadeh and Blaschke 2014; Lai and Tsai 2019; Mallick et al. 2018; Patil et al. 2020; Roccati et al. 2021; Shou and Chen 2021). Data on the built environment includes roads, to analyze proximity of landslide risk to areas of human habitation and activity.

1.2. Study Area

The study area is a 10,947 square mile portion of Colorado that covers most of the Front Range just to the west of the urbanized metroplex of Denver, Boulder, and Fort Collins. This area was chosen because the presence of the Rocky Mountains renders it particularly prone to

landslides. The Front Range is a smaller mountain belt within the Rocky Mountains that lies directly west of the Denver area (Figure 1).

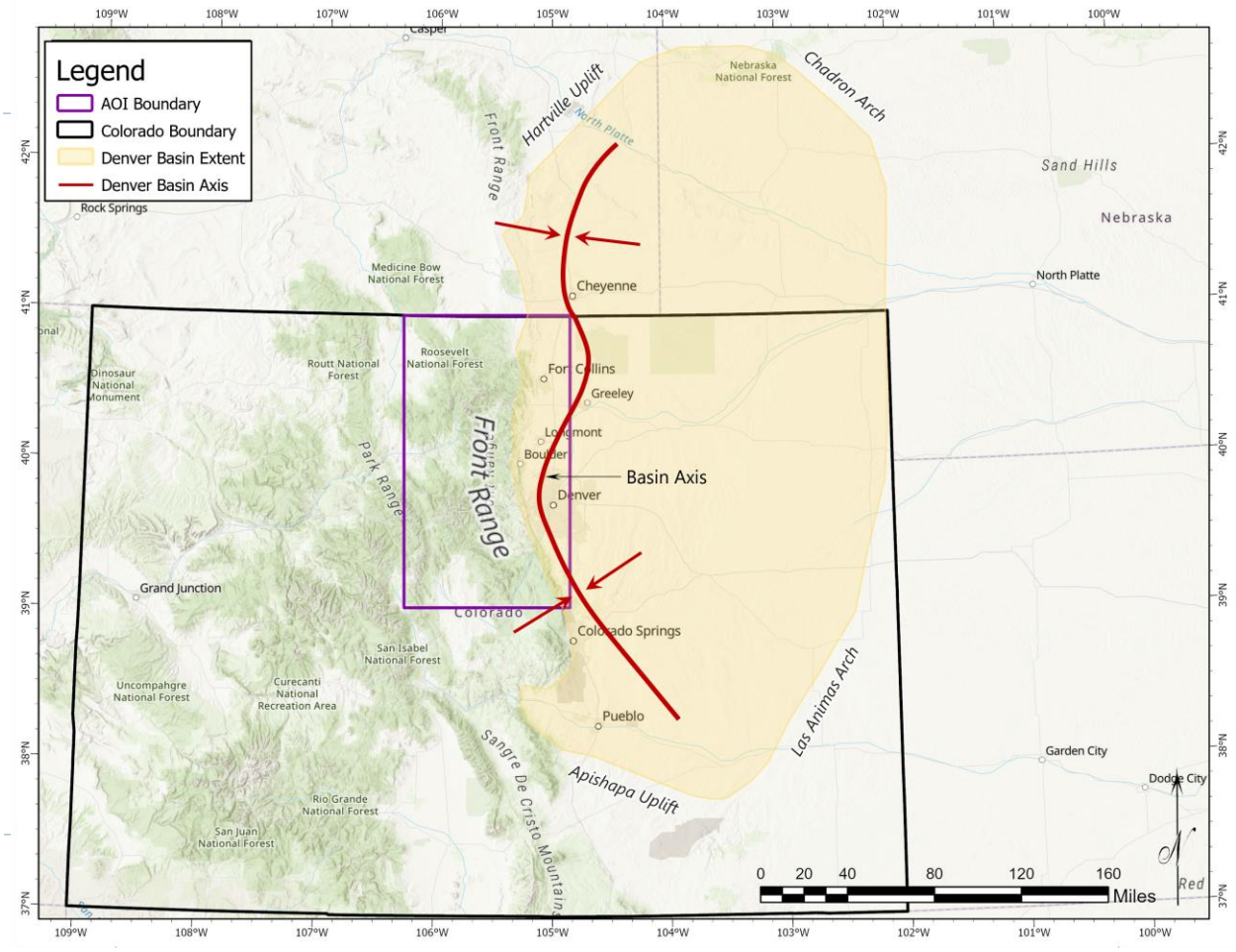

Figure 1 Schematic diagram of the geometry of the Denver Basin

Its boundary demarcates a five-mile buffer around three counties that encompass the majority of the predicted high-hazard locations: Larimer, Boulder, and Jefferson Counties. Figure 1 shows the locations of predicted landslide hazards as generated by the United States Geological Survey (USGS), along with population centers within Colorado borders. The predicted locations tend to coincide with areas of relatively significant elevation change (Figure 2).

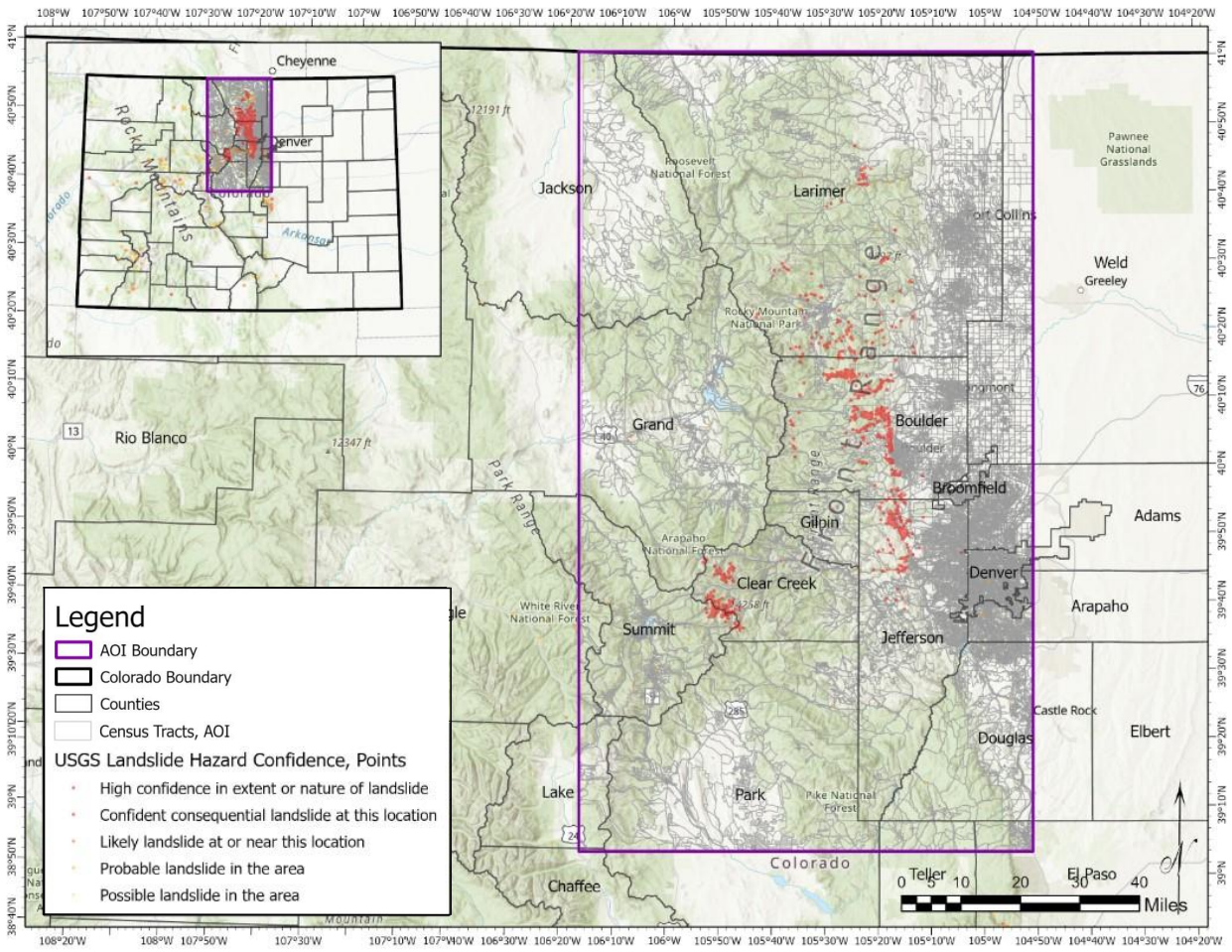

Figure 2 Area of interest location and detail

The goal of this project is to produce detailed analyses of potential landslide susceptibility locations using both weighted and fuzzy overlays. These results are compared not only to each other, but also to the landslide susceptibility inventory generated by the USGS.

1.3. Motivation

Landslides are significant natural hazards around the globe, and the US has its fair share of landslides (Regmi et al. 2013). According to the USGS, landslides account for 25-50 deaths in the US each year (USGS, n.d.; Wieczorek and Leahy 2008) and between $2-4 billion in annual losses (AMERICAN GEOSCIENCES INSTITUTE, n.d.; Wayllace et al. 2019). The ability to predict landslide events, like volcanic eruptions and earthquakes, can save numerous lives as

well as decrease damage to property and infrastructure (Winter et al. 2019). Other natural disasters, such as wildfires, earthquakes, tsunamis, and volcanic eruptions (Korup 2012), or rapid changes in weather (Huggel et al. 2012) also have a tendency to affect landslide frequency. Therefore, it is important to have a baseline understanding of topographies that are more susceptible to landslides in different environments.

Prediction of landslide occurrences may be improved upon with improved integration of GISci and geology. The field of geology covers a sizable range of topics of study, among them the wholesale study of the various kinds of landslides, including composition, failure mechanisms, and movement mechanics (Çellak, 2020; Çellak, 2021; Cerri et al. 2020; Chen et al. 2016; Donati et al. 2019; Donnarumma et al. 2013; Hu and Bürgmann 2020; Di Maio et al. 2020; Clague and Stead 2012; Glade et al. 2005; Highland 2008; Martel 2004). Many of these studies observe landslides strictly through the lens of geology, though the integration of GIS into geologic studies has increased as technology has developed (e.g., Ali et al. 2021; Bragagnolo et al. 2020; Chen and Li 2020; Feizizadeh and Blaschke 2013; Feizizadeh and Blaschke 2014; Francioni et al. 2019; Kavzoglu and Colkesen 2012; Mallick et al 2018; Saha et al. 2005; Zhou et al. 2021). Many of these studies have incorporated geology into spatial modeling to further landslide susceptibility mapping. However, they may still be lacking in the comparison between the two weighting methods, as well as an analysis on how bias affects the results.

1.4. Importance

There are many variables that go into the process that both affected and are affected by the opinions of the decisionmakers. Variables are weighted according to what are believed to be more or less important, and this relative subjectivity is integrated into the results. The availability

of data, as well as the quality of data, also affects results. These results then may be incorporated into land surveys for future infrastructure and urban expansion.

The utility of landslide susceptibility mapping cannot be overstated, particularly in regions prone to landslides. The ability to predict where landslides might occur is an area of study that is continually growing, and the environmental impacts of these natural occurrences can be felt for years after an event. This project aims to look at the differences between two variations on MCDA: weighted overlay and fuzzy overlay. These two methods were chosen due to their widespread usage, and this project aims to compare the results within the AOI with various criteria.

Research into landslide susceptibility mapping has yielded a number of different criteria depending on the location, data available, and if there is a specific aspect of landslide susceptibility that is being focused on. Bias in criteria selection or methodological decisions must be considered when building a project and generating results, and these results may affect people who live and work within the study area in question. The number of criteria reviewed for this project far exceeds the number used. Some of the reviewed criteria are location-specific to the studies conducted, and ultimately the results of this project are pertinent to the AOI alone. This project does not aim to test models that address global landslide susceptibility mapping.

Many factors had to be considered over the course of this project. How this project would contribute to both the scientific community as well as the wider general populace was a key component in determining the subject matter and study area. The results of this project were meant to be a practical and useful piece of information to aid in more accurate and precise potential landslide location determinations.

1.5. Overview

The remainder of this thesis is split into four chapters. Chapter 2 details previous work done that is related to this project, delving into more depth with regards to landslides, landslide susceptibility mapping, utilized criteria, and criteria weighting. Chapter 3 discusses the methodology used in this project, including data acquisition, research design, data preparation, and data processing. Chapter 4 focuses on the material results from the project. And finally, Chapter 5 dives into the analyses of the project results, as well as its impact on the scientific community.

Chapter 2 Related Work

Landslides are hazards that have increasingly posed potential threats to mankind (Glade and Crozier 2005). With ever-expanding urbanization encroaching on areas of unpopulated wilderness, increasing numbers of people are living in environments prone to landslides (AMERICAN GEOSCIENCES INSTITUTE, n.d.; USGS, n.d.; Winter et al. 2019), and therefore it becomes ever more important to both understand and forecast how and where landslides form. Geoscientists have reconstructed historical landslides in order to get a better grasp on landslide susceptibility prediction (Ebertardt 2012; Regmi et al. 2014; Reid et al. 2012), and the USGS maintains an extensive inventory of historic landslides in the US. Predicting landslide locations is done through the use of models constructed with specific criteria in mind – conditions that are necessary for landslide initiation. Geoscientists, therefore, have generated a number of various model types used for landslide susceptibility mapping. Understanding the overall processes that initiate landslides and what conditions are necessary for initiation is a primary point of interest for this project.

2.1. Regional Setting

The study area covers a small central-western portion of the Denver Basin that lies directly to the east of the Front Range. The present-day basin formed as a result of the uplift of the Front Range, with eroded sediment from the mountain belt loading down the western edge of the basin (Figure 3). The sediment weathered and eroded from the Front Range is deposited at the base of the mountains, which in turn causes that side of the basin to sink—hence the fact that the Denver Basin is what geologists would call an asymmetric basin. The Front Range consists primarily of uplifted formations that range from the Precambrian to the present – the Precambrian basement is predominately granite, the Paleozoic and Mesozoic layers consist

primarily of alternating siliciclastic and carbonate rocks, and the Cenozoic rocks are composed of mixed-source sedimentary rocks (Knepper 2002).

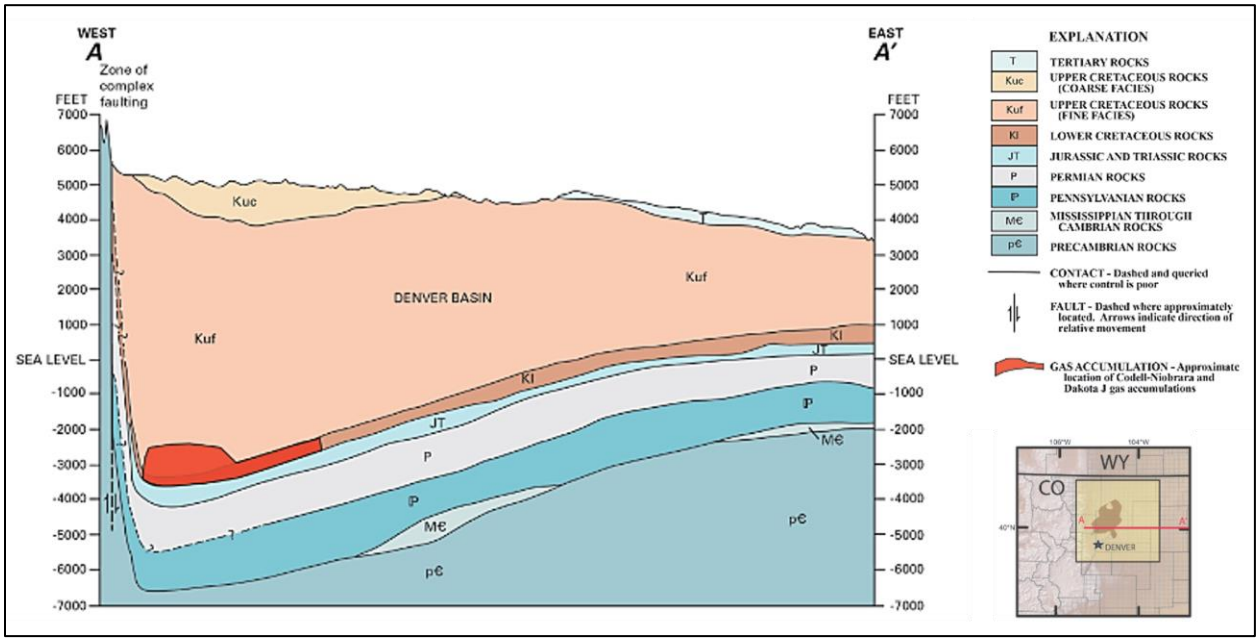

Figure 3 Cross-section of the Denver Basin (Nelson and Santus 2011)

The uplift of the modern Rocky Mountains, the mountain belt of which the Front Range is a part of, began during the late Pennsylvanian period, around 300 million years ago. The Denver basin was a shallow basin for most of its lifespan up until the Paleogene (65-45 Ma), when the Laramide orogeny uplifted the modern Rocky Mountains, causing sediment from the mountains to deposit and depress the western end of the basin (Nelson and Santus 2011). The Front Range is one of many smaller mountain belts that make up the greater Rocky Mountains.

The metropolitan areas of Denver, Boulder, and Fort Collins sit just to the east of the Front Range, near the axis of the basin. The locations of the cities themselves do not directly suffer from the effects of landslides, though their corresponding suburbs to the west – particularly where they press into the foothills of the Front Range – tend to feel said effects more frequently due to proximity to potential landslide hazard locations.

Ott (2020) and Suchet et al. (2003) indicate that intrusive igneous rocks, metamorphic rocks, and siliciclastic sedimentary rocks weather the slowest, while carbonate sedimentary rocks weather the fastest. In between these endmembers are extrusive igneous rocks and rocks consisting of a mix of igneous, metamorphic, and sedimentary rocks. Unconsolidated lithology consists of material that has already been eroded and mixed with other sediments that, size-wise, are more likely to be easily transportable. As the Front Range consists of Precambrian granite – an intrusive igneous rock – at its core with Paleozoic and Mesozoic siliciclastic and carbonate rocks above, the softer carbonates likely eroded before the siliciclastic rock and granite.

2.2. Landslide Overview

The term "landslide" encompasses a wide range of mass movement, be it slope failure or otherwise due to gravity (Highland 2008; Korup 2012; Yamagishi 2017). Highland (2008) and Yamagishi (2017) break down the term landslide into different classifications based on movement type and involved material. Different terms to describe displacement of land masses/material include avalanche, fall, flow, slide, slump, spread, and topple (Clague and Roberts 2012; Highland 2008; Yamagishi 2017), and each of these terms have their own set of criteria that differentiates how they are named. Landslides have a variety of triggering mechanisms, some of which include earthquakes, heavy precipitation, snowmelt, and erosion (Korup 2012). For purposes of this project, the term "landslide" refers primarily to mass movements of earthen material that is categorized as a flow (spatially continuous movement of material where surface of shear is short-lived, closely-spaced, usually not preserved), slide (cohesive, relatively undeformed material moves over surface of rupture or relatively thin zones of intense shear strain), or fall (detachment of rock and soil from a steep slope along a surface with little no shear displacement) (Highland 2008).

2.2.1. Landslide Anatomy

A failure surface, or sliding surface, is the plane on which the bulk of a landslide's material travels over (Highland 2008; Martel 2004). The surface itself is a plane of weakness where gravity is able to overcome the shear frictional forces keeping the material above it immobile and may be planar or curved (Martel 2004). These failure surfaces may be visible on the surface and are known as rupture surfaces (Highland 2008).

A landslide consists of multiple features, though terminology can differ even when referring to the same feature. The surface of rupture, also known as the sliding surface, is the main surface on which the loose debris travels upon. The head of a landslide is the term used to describe the area furthest upslope where material has shifted, while the toe of a landslide represents the material that has traveled furthest downslope. Scarps form at or near the head of the landslide due to tension, and tension fractures may form on the flanks of the landslide. Material that has traveled downslope may buckle if there is a decrease in the travel velocity, forming ripples or ridges on the surface.

2.2.2. Landslide Triggers and Characterization

Landslides occur due to a variety of triggering mechanisms, both natural and artificial (Korup 2012). In places with high amounts of precipitation, rainwater can saturate the soil and turn it into mud, which then slumps downhill due to decreased structural integrity (Highland 2008). Volcanic eruptions, along with earthquakes that may or may not be associated with said eruptions, can destabilize the uppermost layer of earthen material due to the excessive vibrations caused by such events (Korup 2012). Time and erosion may initiate slope failure simply due to gravity (Clague and Roberts 2012). Manmade structures, such as roads, may also cause landslides both during the construction process – destabilization of the surface due to

construction equipment and explosives, if bedrock is needed to be cleared – and post construction – the resultant excavated road is a surface of high change in relief (Highland 2008).

Regmi et al. (2014) performed a study that focused on characterizing landslides in Colorado. In their paper, they described two different types: smaller, surficial landslides and larger, deep-seated landslides. According to the authors, these two kinds of landslides have a temporal aspect to size: evidence of shallow landslides are modern-aged and small- to large-sized, while evidence of large, deep-seated landslides are much older in age (hundreds to thousands of years old). Shallow small- to medium-sized landslides tend to be located in areas of steeper slope and are dominated by sedimentary rock close to rivers, while large-sized landslides trend along areas of flatter slope (Cruden and Varnes 1996; Regmi et al. 2014; Wieczorek and Leahy 2008). Shallow landslides have a sliding base that generally lies at the boundary between soil and bedrock, and pore water plays a major role in the initiation of a landslide (Regmi et al. 2014). Deep-seated landslides have been determined to be older due to the fact that they tend to have dense vegetation cover (Regmi et al. 2014). Shou and Chen (2021) imply that collapse and movement mechanics tend to dictate the type of landside the occurs.

Of the landslides that have occurred in modern times in the state of Colorado, the Slumgullion earthflow in southwestern Colorado has been the most heavily studied (Amitrano et al. 2019; Gomberg et al. 1995; Gomberg et al. 2011; Madison et al. 2019). This nearly four-kilometer-long landslide has been in motion for approximately 350 years at a rate of up to two centimeters per day (Amitrano et al. 2019; Madison et al. 2019), giving scientists a natural laboratory on landslide kinematics. The lithology and hydrology of the Slumgullion area has been extensively studied, and the scale of the landslide has given rise to various “sections” within the total length that act semi-independently of the whole, therefore allowing geoscientists

to study temporal and mechanical differences within the Slumgullion (Gomberg et al. 1995; Gomberg et al. 2011; Madison et al. 2019). This research has tremendously increased knowledge on landslide mechanics, and that translates into generalized landslide susceptibility mapping.

2.3. Criteria Employed in Landslide Prediction

For this project, a spread of forty-two papers (Table 1) were used to determine what criteria were most frequently used in landslide susceptibility efforts. These studies varied widely in terms of location: the studies were spread out within fourteen different countries across the globe.

Table 1 Literature references (in alphabetical order)

Number	Reference
1	Ali et al. 2020
2	Ayalew and Yamagishi 2004
3	Bragagnolo et al. 2020
4	Chen and Chen 2021
5	Chen and Li 2020
6	Chen et al. 2015
7	Du et al. 2017
8	Ercanoglu and Gokceoglu 2015
9	Erener et al. 2016
10	Feizizadeh and Blaschke 2013
11	Feizizadeh et al. 2014
12	Ghorbanzadeh et al. 2019
13	Huggel et al. 2012
14	Kavzoglu et al. 2013
15	Korup 2012
16	Lehmann et al. 2019
17	Lombardo and Mai 2018
18	Mallick et al. 2018
19	Nandi and Shakoor 2009
20	Nohani et al. 2019
21	Patil et al. 2019
22	Pawluszek and Borkowski 2016
23	Pham et al. 2020
24	Pourghasemi et al. 2012
25	Pourghasemi et al. 2020
26	Regmi et al. 2014
27	Rengers et al. 2016
28	Roccati et al. 2021
29	Roodposhti et al. 2016
30	Roy and Saha 2019
31	Roy et al. 2019
32	Saha et al. 2005
33	Saito et al. 2009
34	Schulz et al. 2009
35	Shou and Chen 2021
36	Vahidnia et al. 2010
37	Vakhshoori and Zare 2016
38	Vojtekova and Vojtek
39	Wayllace et al. 2019
40	Zhao et al. 2017
41	Zhou et al. 2021
42	Zhu et al. 2014

A multitude of various criteria were used in landslide susceptibility modeling, ranging from atmospheric to geologic and everything in between. These criteria were used depending on the purpose of the model being used. Landslide susceptibility is dependent on a number of factors, though lithology, slope, and groundwater level are three of the most heavily studied parameters (Regmi et al. 2014; Schulz et al. 2009; Wayllace et al. 2019; Zhou et al. 2021), though they are certainly not the only parameters taken into consideration. Attributes such as elevation, aspect, soil composition, land use, stream power index (SPI), and topographic wetness index (TWI) have also been used in landslide susceptibility studies (Highland 2008; Kavzoglu et al. 2013; Martel 2004; Saha et al. 2005; Schulz et al. 2009). Natural disasters and changes in weather (Huggel et al. 2012; Korup 2012) have also been studied with regards to landslide initiation frequency, and vegetation cover is one of the lesser-known factors studied in landslide frequency (Lehmann 2019; Rengers et al. 2016).

The criteria authors working in landslide susceptibility mapping chose include various attributes specific to not only their study areas, but to certain aspects of their study that they either wanted to emphasize or had particular access to. For example, Chen et al. (2015) utilized evaporation rates and soil water retention in their study – a criterion that no other study referenced in this thesis has used. Roccati et al. (2021) used terracing and existing landslide proximity as criterion for their own study – factors which influence slope gradient and surface stability. The individual criteria, in the order listed in Table 2, are detailed in the following sections, organized by criteria category.

Table 2 Landslide susceptibility criteria used in the literature

Category	Criteria	Description	References	Tally
Topography	Elevation	Vertical distance from a given baseline, usually mean sea level (MSL)	1, 2, 3, 4, 5, 6, 7, 8, 9, 10, 11, 14, 16, 17, 18, 19, 20, 21, 22, 23, 24, 25, 26, 27, 28, 29, 30, 31, 32, 33, 35, 36, 37, 38, 40, 42	36
	Aspect	Direction a slope faces, usually measured in degrees from north	1, 2, 3, 4, 5, 7, 8, 9, 10, 11, 12, 14, 17, 18, 19, 20, 21, 22, 23, 24, 25, 27, 28, 30, 31, 32, 33, 35, 37, 38, 40, 42	32
	Slope	Angle of inclination of a surface	1, 2, 3, 4, 5, 7, 8, 9, 10, 11, 14, 17, 18, 20, 22, 23, 24, 25, 26, , 30, 31, 32, 33, 35, 36, 37, 38, 40, 42	30
	Curvature	Derivative of elevation that calculates curvature of a surface	1, 3, 4, 5, 12, 17, 20, 23, 24, 25, 33, 40	12
	Geomorphology	Classification of landforms with regards to erosional properties (with respect to landslide studies)	18, 21, 22, 26, 31, 40	6
	Slope Length	Distance of a consistent angle of inclination of a surface	24, 26	2
	Roughness	Slope derivation via moving standard deviation filter	22	1
	Shaded Relief	A hypothetical illumination value of the surface	22	1
	Topographic Position Index (TPI)	Calculated difference between cell elevation and mean elevation of neighboring cells	22	1
	Desiccation Height	Depth from the summit level (summit level minus elevation)	33	1
	Undesiccation Height	Height above river level (elevation minus river level)	33	1
	Slope Shape	Measure for the shape of each pixel	42	1

Category	Criteria	Description	References	Tally
Hydrology	Drainage Proximity	Proximity to a fluvial network	1, 4, 5, 6, 7, 9, 10, 11, 12, 13, 15, 18, 19, 20, 21, 22, 23, 24, 25, 26, 28, 29, 30, 31, 35, 36, 37, 38, 40	29
	Precipitation	Rainfall in a given area	1, 5, 6, 10, 11, 13, 14, 15, 16, 18, 19, 21, 31, 34, 37, 39, 40, 41	18
	Topographic Wetness Index (TWI)	A function of the slope and upstream contributing area per unit width orthogonal to flow direction	1, 3, 4, 5, 14, 17, 22, 24, 25, 31	10
	Stream Power Index (SPI)	Potential for flow erosion at a given point on the surface	1, 4, 5, 17, 22, 24, 31	7
	Drainage Density	Calculated density of fluvial network in a given area	6, 11, 14, 29, 32	5
	Sediment Transportation Index (STI)	A function of slope and upstream catchment area	1, 4, 5, 31	4
	Solar Radiation	Radiant energy for a specific location and date	1, 22	2
	Evaporation	Sum of evaporation from water, soil, and plants	6	1
	Water Conditions	A classification on whether or not slip surfaces are wet	8	1

Category	Criteria	Description	References	Tally
Subsurface	Lithology	Geologic composition of the underlying bedrock	1, 2, 3, 4, 5, 7, 9, 10, 13, 14, 15, 17, 18, 21, 22, 23, 24, 25, 26, 28, 29, 30, 31, 32, 33, 34, 36, 38, 39, 40	30
	Lineament Proximity	Proximity to faults or fractures in the underlying bedrock	1, 2, 5, 7, 9, 10, 11, 12, 17, 18, 20, 21, 23, 24, 25, 29, 30, 31, 32, 35, 36, 37, 38	23
	Soil Composition	Composition of the top soil	4, 5, 9, 16, 18, 25, 30, 31, 34	9
	Depth of Soil	Depth of the top soil	8, 9, 23, 39	4
	Seismic Zone	Categorization on whether or not area is in a seismically active zone	13, 15, 21, 31, 41	5
	Major Structure Proximity	Proximity to major geologic structural features	21, 32	2
	Soil Water Retention (SWR)	Ability of soil to absorb and retain free flowing water	6	1
	Soil Liquidity Index	Index describing water content required to liquify soil	19	1
	Dip Slope Index	Index describing topographic surfaces which slope in the same direction	35	1

Category	Criteria	Description	References	Tally
Surface	Land Use/Land Cover (LULC)	Categorization of how surface is utilized	1, 3, 4, 5, 6, 8, 9, 10, 11, 12, 13, 14, 17, 18, 19, 20, 21, 22, 24, 25, 28, 29, 30, 31, 32, 36, 37, 38	28
	Road Proximity	Proximity to a road	1, 2, 4, 5, 9, 10, 11, 13, 14, 20, 21, 22, 23, 24, 25, 28, 31, 35, 37	19
	Vegetation Coverage	Percentage of vegetation coverage	4, 5, 7, 13, 15, 16, 17, 18, 20, 21, 25, 30, 31, 35, 37	15
	Erodibility	Ability of top soil to be eroded	9, 18, 19	3
	Settlement Proximity	Proximity to an urbanized environment	13, 21, 28	3
	Existing Landslides Proximity	Proximity to a previous landslide location	15, 26, 28	3
	Terracing	Presence of terraced surfaces	28	1
	Landslide-Rainfall Index	Correlation between cumulative rainfall and rainfall intensity at different landslide locations	35	1

2.3.1. Topography

Topography forms the basis of all landslide modeling. Without surface data, landslide susceptibility modeling would not be possible. Different types of topographic data were utilized in the various studies, with some forms being derivatives from others. A number of topographic data are usually derived from DEMs (Ali et al. 2021; Ayalew and Yamagishi 2004; Chen and Chen 2021; Chen and Li 2020; Chen et al. 2015; Mallick et al. 2018; Nohani et al, 2019; Pawluszek and Borkowski 2016; Pham et al. 2020; Pourghasemi et al. 2020; Roodposhti et al. 2016; Roy and Saha 2019; Saito et al. 2009; Vahidnia et al. 2010; Vojtekova and Zare 2016; Zhao et al. 2017) and are discussed below.

2.3.1.1. Elevation

Elevation is the vertical distance from a given baseline, usually mean sea level (Dempsey 2020), and elevation is an interpolated surface representation of DEMs (Du et al. 2014; Erener et al. 2014). This vertical distance changes depending on surface features, such as mountains and valleys above sea level. Chen et al. (2015) indicate that regions with low relative elevation throughout are more prone to inundation, and that areas with a steeper topography have a lower probability of flooding since water can be drained downslope.

2.3.1.2. Slope

Certain conditions need to be met in order for a landslide to occur, the least of which is a slope gradient. Difference in elevation has a negative correlation with slope stability (Çellak, 2020; Kayastha 2015), and this factor is one of the most commonly used in landslide susceptibility modeling, as reported by Çellak (2013), Dağ (2007), and Hasekioğullari (2011). Çellak (2020) also mentions how slope plays an important role in lithological and soil properties, such as permeability, cohesion, strain, and shear and normal stress, as well as hydrological properties dealing with groundwater flow and saturation. Coe et al. (2004) reported that around

ninety-six percent of landslides within their study area had slopes between sixteen to forty-four degrees. Patil et al. (2020) found in order of highest to lowest frequency of landslides occurring on slope angle ranges in their study area: 30° – 40°, 20° – 30°, 10° – 20°, 40° – 50°, < 10°, 50° – 60°, 60° – 70°, > 70°. It is with their analysis that the ranking of slopes was determined for this project.

2.3.1.3. Aspect

Erener et al. (2016) define aspect as a slope's orientation using compass degrees, i.e., 0° through 360°, with 0° and 360° both being due north, a property that may contribute to landslide susceptibility modeling by implying which slopes are more likely to be affected by atmospheric conditions, such as wind and precipitation, as well as amount of sunshine received (Pourghasemi et al. 2012). Ghorbanzadeh et al. (2019) goes so far as to say that aspect is one of the most important topographical features that can be used in landslide susceptibility studies. Aspect is calculated based on the derived slope values.

2.3.1.4. Curvature

Curvature, as defined by Ghorbanzadeh et al. (2019) and Pourghasemi et al. (2012), is a slope or aspect's rate of change with respect to a particular direction. This criterion is particularly useful in landslide susceptibility mapping because curvature defines topographic features as concave, convex, or flat. Chen and Chen (2021) split curvature into five groups; Chen and Li (2020), Lombardo and Mai (2018), Pourghasemi et al. (2020), and Saito et al. (2005) broke up curvature into two categories for further distinction.

2.3.1.5. Geomorphology

Geomorphology refers to the landscape of an area that includes not only static surface features, but also temporal aspects to the landscape, including seasonal changes (Mallick et al.

2018). Roy et al. (2019) use geomorphology to classify surface features into regions that not only include lithological and soil composition, but also hydrological components.

2.3.1.6. Slope length

Slope length was a criterion that Pourghasemi et al. (2012) utilized, wherein this parameter was a measurement of slope steepness and length. It was used as a means to measure soil loss and sediment transport capacity overland through the use of a fluid.

2.3.1.7. Roughness

Pawluszek and Borkowski (2017) utilize roughness as a criterion. Roughness, as defined by the authors, is a derivative from a slope map and applies a moving standard deviation filter with a defined kernel size. Typically, rougher areas tend to indicate areas affected by landslides, and the degree of roughness may correlate with specific types of landslide activities. Roughness can be used to generate landslide inventory maps (McKean and Roering 2004).

2.3.1.8. Shaded relief

Shaded relief is, as defined by Pawluszek and Borkowski (2017), a hypothetical surface illumination that works by visualizing shaded relief from eight different sun directions. Similar in function to solar radiation, this data may be derived from DEMs.

2.3.1.9. Topographic position index

Topographic position index (TPI) is the calculated difference between the elevation of one raster cell and the mean elevation of its surrounding cells (Pawluszek and Borkowski 2017). This criterion identifies different topographic features based on the sharpness of edges, such as ridges and valleys.

2.3.1.10. Desiccation height

Saito et al. (2009) use this criterion as a means of approximating ideal erosion volumes and heights for both the past and the future. They define desiccation height as summit level minus elevation (Dis), or depth from the summit level.

2.3.1.11. Undesiccation height

Undesiccation height, as defined by Saito et al. (2009) is the height above the river level, or elevation minus river level. This criterion, like desiccation height, is used to approximate ideal past and future erosion volume or height. Saito et al. (2009) further mention a correlation between relief and slope angles to the standard deviation of undesiccation height. High relief and steep slopes tend to have high standard deviation while low relief and flatter slopes correlate to low standard deviation. The formulas to calculate the average undesiccation height in order to get the standard deviation of undesiccation height are:

$$Udis_{av} = \frac{1}{N}\sum_{d} Udis \quad (1)$$

$$Udis_{sd} = \frac{1}{N}\sum_{i}((Udis - Udis_{av})^2)^{\frac{1}{2}} \quad (2)$$

where *Udis* is measured undesiccation height, $Udis_{av}$ is average undesiccation height, $Udis_{sd}$ is the standard deviation of undesiccation height, and *N* is the population size.

2.3.1.12. Slope shape

Zhu et al. (2014) describe slope shape in terms of curvature: whether or not slopes are flat, straight, convex, concave, or a combination thereof. They stated that areas with upper convex, lower concave slopes are more likely to have landslide activity. The authors decided upon slope shape instead of curvature because slope shape takes the shape of the entire slope into account, whereas curvature measures the shape of a slope of a single pixel independently of its neighbors.

2.3.2. Hydrology

Hydrology, for the purposes of this project, covers everything that pertains to water with respect to landslide susceptibility. This includes, atmospheric, terrestrial, and subterranean water, as water in all locations affect landslide initiation and propagation – water is generally the lubricant that allows a landslide to travel on a slip surface (Wayllace et al. 2019). It can also be the cause of slope failure – either by, again, due the fact that it can act as a lubricant, or by weight should a soil absorb enough (Rotaru et al. 2007). Either way, reaching a critical saturation point can tip a slope from being stable to unstable, thus giving rise to slope failure and consequently, a landslide.

2.3.2.1. Drainage proximity

Many studies have used drainage proximity as one of their criterion (Chen et al. 2016; Du et al. 2017; Erener et al. 2016; Feizizadeh et al. 2014; Ghorbanzade et al. 2019; Mallick et al. 2018; Pawluszek and Borkowski 2016; Pourghasemi et al. 2012; Roodposhti et al. 2016; Roy and Saha 2019; Roy et al. 2019; Vahidnia et al. 2010; Vakhshoori and Zare 2016; Zhao et al. 2017). Weighting was done based on buffered distances to the nearest river or stream. Du et al. (2016) point out how slope instability can develop as a result of river incision, hence the increase of landslide susceptibility with drainage proximity.

2.3.2.2. Precipitation

A number of studies utilized precipitation as their means of gauging rainfall in their study area. Chen et al. (2015) used daily rainfall, while Ali et al. (2021), Chen and Li (2020), Feizizadeh et al. (2014), Vakhshoori and Zare (2016), and Zhao et al. (2017) used average annual rainfall. Feizizadeh and Blachke (2013) and Mallick et al. (2018) used a 30-year meteorological data, while Nandi and Shakoor (2009) used annual cumulative rainfall.

Regarding precipitation patterns, it has been noted that rainfall has a tendency to increase with elevation, a trend that has been termed the orographic effect (Daly et al. 1993).

2.3.2.3. Drainage density

Chen et al. (2015), Feizizadeh et al. (2014), and Roodposhti et al. (2016) utilized drainage density in their studies. Chen et al. (2015) defined drainage density as the length of rivers for a given area. As mentioned by Du et al. (2016), the presence of a river can influence slope stability, and therefore knowing what the drainage density is within a study area is crucial. Kavzoglu et al. (2012) list the formula for drainage density as:

$$D_y = \sum L/A \quad (3)$$

where D_y is the drainage density, L is stream length, and A is the catchment area.

2.3.2.4. Stream power index

Stream power index (SPI) is defined as flow erosion potential at a given surface point (Pawluszek and Borkowski 2017; Roy et al. 2019) and is calculated with a formula Pourghasemi et al. (2012) cited in their study:

$$SPI = As \times \tan\beta \quad (4)$$

where As is catchment area and β the local slope in degrees.

2.3.2.5. Topographic wetness index

Pourghasemi et al. (2012), Pawluszek and Borkowski (2017), and Roy et al. (2019) define TWI as a factor used to quantify topographic control on hydrologic processes. TWI is a function of the slope and upstream contributing area per unit width orthogonal to flow direction:

$$TWI = \ln\frac{As}{\tan\beta} \quad (5)$$

where *As* is the area that is drained through a certain point, and β the slope at the point of drainage.

2.3.2.6. Sediment transportation index

Sediment transport index (STI) is a factor used to measure how an area directly contributes to sediment discharge – it quantifies the process of erosion and deposition. Roy et al. (2019) include the equation for STI in their study:

$$STI = (m+1) \times \left(\frac{As}{22.13}\right)^{m} \times \sin\left(\frac{B}{0.0896}\right)^{n} \quad (6)$$

where *As* is the catchment area, *B* the local slope in degrees, the contributing area exponent *m* is usually set to 0.4, and the slope exponent *n* to 0.0896.

2.3.2.7. Solar radiation

Pawluszek and Borkowski (2017) define solar radiation – more specifically, area solar radiation (ASR) – as a derivative of slope and aspect. This criterion combines radiant energy from the sun with the sun angle and direction for a given location. Ali et al. (2021) describe higher amounts of solar radiation being indicative of greater availability of soil and rock pore space – hence a lower probability of landslide occurrence. Both Pawluszek and Borkowski (2017) and Ali et al. (2021) essentially use solar radiation as a means of measuring evaporation.

2.3.2.8. Evaporation

Evaporation, as defined by Chen et al. (2015), is the sum of water, soil, and plant evaporation. This criterion takes into account evapotranspiration from plants and evaporation from surface water, though Chen et al. (2015) point out that this parameter is more critical during the summer when evapotranspiration rates are higher due to seasonal rainfall and longer hours of sunlight.

2.3.2.9. Water condition

Ercanoglu and Gokceoglu (2002) factored water condition – the amount of moisture found on a given surface – into their study. They used a simple classification for assessing water condition, as dense vegetation and mountainous terrain sometimes prevented direct observation. Four categories were used: landslide susceptibility is high if water condition is wet, moderate if water condition is dripping or flowing, low if water condition is damp, and a non-issue if water condition is dry.

They caveated their observations by stating that water conditions in the same area change with the seasons, and that the observations they used were what had been noted specifically at the time the study was being conducted.

2.3.3. Subsurface

The subsurface category consists of any criteria that deals with data beneath the Earth's surface. These data include lithology, lineaments, various soil properties, and seismic activity, to name a few. Subsurface data is primarily collected by geologists, geophysicists, hydrologists, soil scientists, though data collection is not restricted to these professions. In terms of landslide susceptibility mapping, subsurface data is important because a large part of why landslides occur and where they occur is dictated by subsurface properties.

2.3.3.1. Lithology

Lithology is a key component of landslide susceptibility mapping, as geology affects not only the subsurface, but the surface as well. The lithological composition of an area tends to dictate not only subsurface properties such as porosity, permeability and fluid composition (Schulz et al. 2009; Wayllace et al. 2019), but it also affects surficial properties such as topography, rates of weathering and erosion, and soil composition (Ott 2020). Because geology is such a key component of landslide susceptibility mapping, a significant number of the authors

referenced in this study have used lithology as one of their key criteria. Vojtekova and Vojtek (2020) went one step further and used geology as a proxy for permeability.

2.3.3.2. Lineament proximity

Lineaments, in the geological and geographical sense, comprise surface features that are generally indicative of subsurface structures, such as elongated hills and valleys. Florinsky (2016) states that lineaments are usually associated with linear subsurface features such as faults and fractures, and to a lesser extent, mechanical deformation – fracturing or folding – or zones of higher permeability. Lineaments indicate planes of weakness in the subsurface, areas that may slip with enough pressure or lubrication, resulting in landslides if they are close to the surface, or earthquakes if they are deep within the Earth's crust. Landslides may also result as an event secondary to an earthquake, thus further reinforcing the correlation between landslide activity and lineament proximity.

2.3.3.3. Soil composition

Soil composition is largely a result of the lithology of a region, as the soil's minerals are primarily sourced from their parent rocks. Different soil compositions have different properties, such as soil depth, land use type, and level of erosion, and certain soil compositions correlate more readily to landslide frequency (Erener et al. 2016; Pourghasemi et al. 2020). Pourghasemi et al. (2020) also indicate that variation in soil composition changes the permeability and strength of a slope surface.

2.3.3.4. Soil water retention

Chen et al. (2015) identify soil water retention (SWR) as the amount of water a soil can store after some sort of precipitation or inundation event. Dependent on the soil composition, as well as types of vegetation on the surface, SWR may change depending on the season. Chen et al. (2015) include the formula for calculating SWR:

$$SWR_i = SWR_0 \left(\frac{100}{CN_i} - 1\right) \quad (7)$$

where CN_i is an integer between 0 to 100 that is determined by hydrologic soil properties and ground cover conditions, and SWR_0 is a scaling factor dependent on the unit of measurement.

2.3.3.5. Depth of soil

Erener et al. (2016) utilizes depth of soil in their study by classifying soil depth into four categories: very deep, deep, shallow, and very shallow. The authors of this paper have discovered that for their study area in northwestern Turkey, landslides occurred most frequently in the very deep category, in which soil depth was over 90 cm and the occurrence rate was 78%.

2.3.3.6. Seismic zone

Roy et al. (2019) used seismic zones as a criterion – seismic zones meaning areas where there is ongoing tectonic activity, primarily in the form of earthquakes. Given that their study area was in western Bengal in the foothills of the Himalaya Mountains, earthquakes are not uncommon to the region and therefore likely serve as triggers to landslides that occur in the area.

2.3.3.7. Major structure proximity

Patil et al. (2020) used the proximity to major structures as a criterion, their chief focus being thrust faults. Saha et al. (2005) also denote importance to proximity to major tectonic structures, most notably thrust faults. Both Patil et al. (2020) and Saha et al. (2005) single out thrust faulting in particular because of the fact that their study areas are in the Himalaya Mountains, where active thrust faults routinely generate earthquakes.

2.3.3.8. Soil liquidity index

Soil liquidity index was used by Nandi and Shakoor (2009) quantifies the amount of water needed in a soil to change it from a solid state to a plastic based on soil composition. The equation for soil liquidity is:

$$LI = (Wn - PL)/(LL - PL) \quad (8)$$

where *LI* is the liquidity index, *Wn* is water content, *PL* plastic limit, and *LL* liquid limit.

2.3.4. Surface

Surface data plays a large role in landslide susceptibility mapping. Of the data used in landslide susceptibility studies, surface information changes the most frequently. This is due to the fact that surface attributes are and have been anthropomorphically shaped in timescales that can easily fit within an average human's lifespan. The changes wrought on the surface therefore heavily affect surface properties that, in turn, affect the probability of a landslide occurring.

2.3.4.1. Land use/land cover

Land use/land cover (LULC) were a significant component of many studies. Pourghasemi et al. (2020) mention how land use can affect hydrological and mechanical slope stability properties. Human activity is generally the cause of multiple triggers that contribute to climate change, and changes in LULC is a means of mapping how anthropogenic activity affects natural process, landslides included (Mallick et al. 2018).

2.3.4.2. Road proximity

Studies have revealed a correlation between landslide activity and the presence of roads in mountainous regions (Erener et al. 2016; Feizizadeh et al. 2014; Pawluszek and Borkowski 2017; Pourghasemi et al. 2012; Roy et al. 2019). This is due to the fact that the construction of roads requires the excavation of rock and soil, which subsequently weakens slope integrity (Pawluszek and Borkowski 2017). Nohani et al. (2019) point out that road construction on slopes more than 10 degrees are more prone to landslide activity.

2.3.4.3. Vegetation coverage

Du et al. (2017) and Mallick et al. (2018) both use vegetation coverage (VC) in their studies, as it was noted that increased vegetation cover negatively affected landslide frequency. Mallick et al. (2018) calculated VC from Landsat-8 satellite imagery. Du et al. (2017)'s VC data was derived from Landsat ETM+ imagery, and both Du et al. (2017) and Roy et al. (2019) used normalized difference vegetation index (NDVI) to calculate VC as follows:

$$NDVI = \frac{IR - R}{IR + R} \quad (9)$$

$$VC = \frac{NVDI - NVDI_{soil}}{NVDI_{veg} - NVDI_{soil}} \quad (10)$$

where *NVDI* is the normalized difference vegetation index, *IR* the infrared portion of the electromagnetic spectrum, *R* the red portion of the electromagnetic spectrum, $NVDI_{soil}$ the NVDI of uncovered soil, and $NVDI_{veg}$ the NVDI for pure vegetation.

2.3.4.4. Erodibility

Erener et al. (2016) and Mallick et al. (2018) measure the ability of sediment to be eroded from the soil. This erosion includes consideration of ease of soil transport due to infiltration and runoff. The equation Mallick et al. (2018) used for this calculation is:

$$K = 0.0293(0.65 - D_G + 0.24D_G^2) \quad (11)$$

$$exp\left\{-0.0021\left(\frac{OM}{f_{clay}}\right) - 0.00037\left(\frac{OM}{f_{clay}}\right)^2 - 4.02f_{clay} + 1.72f_{clay}^2\right\}$$

$$D_G = -3.5f_{clay} - 2.0f_{silt} - 0.5f_{sand} \quad (12)$$

where *K* is the soil erodibility factor, D_G is geometric mean radius, *OM* is the percentage of organic matter, f_{sand} the percentage of sand, f_{silt} the percentage of silt, and f_{clay} the percentage of clay.

2.3.4.5. Settlement proximity

Patil et al. (2020) used settlement proximity by weighting inside a Landslide Numerical Risk Factor geospatial model, though no detail as to how they weighted settlement proximity was given. Roccati et al. (2021) used a buffer distance of ten meters and broke down "settlement" into further categories: buildings, other manufacts, and retaining walls.

2.3.4.6. Existing landslide proximity

Roccati et al. (2021) also considered the existence of pre-existing landslide deposits, which may be indicative of higher slope instability. The authors separated previous landslides into four categories: active/reactivated/suspended landslides, dormant landslides, inactive/stabilized landslides, and area affected by widespread shallow landslides.

2.3.4.7. Terracing

Roccati et al. (2021) take terraced surfaces into account with regards to slope stability. They discuss how terracing both improves and worsens slope stability, depending on amounts of rainfall and runoff, as well as vegetation growth. Vegetation increases slope stability, while rainfall and runoff decreases slope stability.

2.3.4.8. Landslide-rainfall index

Shou and Chen (2021) define this criterion as the correlation between cumulative rainfall and rainfall intensity at different landslide locations, and the dataset is used to predict the landslide-rainfall index at a chosen location. As shown in Figure 4, L1 and L2 indicate the upper and lower thresholds for a dataset, which is then used to generate a rectangular bound for the data. Midpoints are then used to determine the slopes for L1 and L2, and a line perpendicular to L1 and L2's slopes is used to determine d_1 and d_2, which are the distances between a chosen point and L1 and L2, respectively. The equation for the landslide-rainfall index (I_d) is:

$$I_d = d_2/(d_1 + d_2) \quad (13)$$

where d_1 is the distance from L1 and d_2 is the distance from L2.

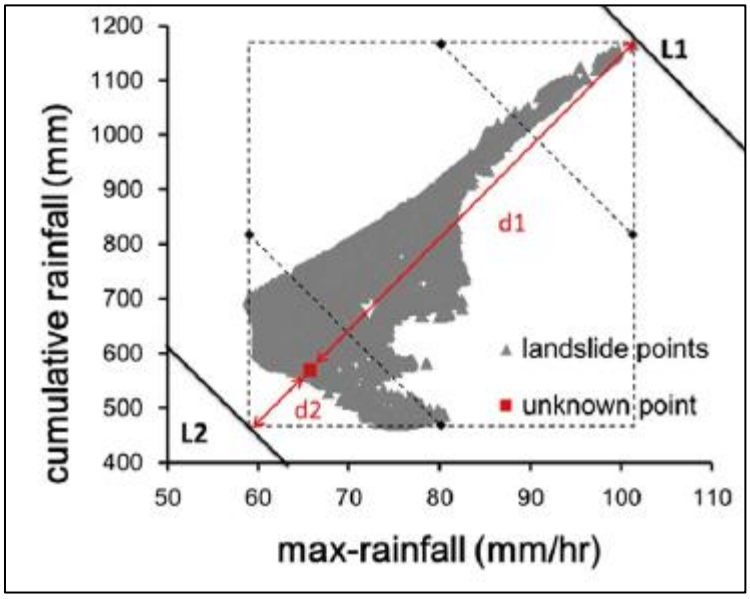

Figure 4 How landslide-rainfall index is graphically calculated (Shou and Chen 2021).

2.4. Modeling Methods

Landslide susceptibility mapping is a generalized term used to denote spatial analysis regarding landslide susceptibility, and a number of studies have utilized various methods for generating landslide susceptibility models. Criteria and methodologies have differed among these studies, but several specific criteria and susceptibility analysis methods have been utilized more frequently than others.

Multiple-criteria decision analysis (MCDA) and logistic regression (LR) were some of the more commonly used modeling methods used. Other methods are briefly covered, though their usage within landslide susceptibility mapping is much less frequent than that of MCDA and LR.

2.4.1. Multiple-Criteria Decision Analysis

MCDA is a decision-making model that utilizes weights to determine the importance of criteria relative to one another in order to achieve a result that best fits the criteria used, and it is this method that was used for this project. The MCDA process requires several key components: the decision maker, evaluation criteria, and decision alternatives (Malczewski and Rinner 2015). MCDA is a frequent choice for environmental suitability studies, as it provides a systematic means of incorporating decision maker priorities and various criteria and outputs various alternatives which the decision maker can then select from (Huang et al. 2011; Jankowski 1995). Different studies utilized different methods for generating landslide susceptibility models and maps. MCDA, logistic regression, and machine learning were some of the modeling methods used. MCDA, as mentioned before, stands for multi-criteria decision analysis, and this method is dependent upon using a weighting scheme to determine the importance of one criterion against another.

MCDA with regards to GIS can be a powerful tool if properly utilized. GIS on its own analyzes and visualizes spatial data, while MCDA provides a structure and weighted criteria for decision making. The combination of the two (commonly referred to as GIS-MCDA) complement each other, as the combination allows for decision-making to occur while taking into consideration spatial data (Feizizadeh and Blaschke 2013). Malczewski and Rinner (2015) argue that the purpose of using GIS-MCDA is to provide options with geographical input to aid decision makers in developing and making better-informed solutions to the problem that required an MCDA in the first place, as opposed to yielding a single solution. GIS-MCDA is therefore a powerful, systematic tool that offers options to assistance in solving a problem with spatial information that supports the decision maker's ability to come to a decision that not only incorporates spatial data, but also their own value judgments.

Under the umbrella of MCDA are a number of different methods to weight criteria. Of these, analytical hierarchy process (AHP) is the most widely used method (see, e.g., Ahmed 2015; Chen et al. 2015; Feizizadeh and Blaschke 2013; Feizizadeh and Blaschke 2014; Pawluszek and Borkowski 2017; Pourghasemi et al. 2012; Roccati et al. 2021; Roy and Saha 2019; Vojtekova and Vojtek 2020), though de Montis et al. (2005), Huang et al. (2011), Malczewski (2004), Malczewski and Rinner (2015), and Triantaphyllou and Baig (2005) discuss other weighting methods as well. Of these papers that discuss different weighting methodologies, AHP was discussed in all five papers. ELimination Et Choix TRaduisant la REalité (ELECTRE) was mentioned in three out of five, and multi-attribute utility theory (MAUT) and Preference Ranking Organization METHod for Enrichment Evaluations (PROMETHEE) were each discussed in two of the five papers listed. These methods are described in the following paragraphs.

AHP was developed by Saaty in 1980. A hierarchy of criteria is created before paired comparison ratios are used to determine how criteria are weighted (de Montis et al. 2005; Huang et al. 2011; Malczewski 2004; Malczewski and Rinner 2015; Triantaphyllou and Baig 2005). AHP has found wide usage in suitability analyses and conflict resolution (Saaty 1987). ELimination Et Choix TRaduisant la REalité (ELECTRE) was developed in 1968 by Roy (de Montis et al. 2005; Huang et al. 2011; Malczewski and Rinner 2015). This method compares the concordance and discordance of paired alternatives, wherein if one criterion is determined to be better than the one its being compared to, it receives a higher rank, or weight. MAUT, developed by Churchman, Ackoff, and Arnoff in 1957, allows for multiple objectives, qualitative data, and intangible factors to be considered in the weighting process (de Montis et al. 2005; Huang et al. 2011). It allows for the comparison of risky outcomes through computed expected utility.

PROMETHEE is similar to ELECTRE in that it also uses a ranking scheme and paired alternatives. Unlike ELECTRE, PROMETHEE ranks the paired alternatives based on criterion type and threshold values (Huang et al. 2011; Malczewski and Rinner 2015).

This project intends to use two methods that fall under the MCDA umbrella: weighted overlay and fuzzy overlay. The two overlays utilize multiple criteria in which each criterion is weighted or ranked in terms of importance. Weighted overlay works by breaking criteria into sub-criteria and reclassifying them according to importance before then weighing the criterion itself in relation to other criteria. Roslee et al. (2017) and Hassan et al. (2020) utilize weighted overlay in spatial suitability analyses with the former focused on landslides in Pahang, Malaysia and the latter on agricultural land in Pakistan. Both studies use weighted overlay to determine spatial susceptibility or suitability based on the rankings they assigned to criteria. Fuzzy overlay, unlike weighted overlay, substitutes assigned ranks with fuzzy memberships. There are seven different memberships: fuzzy Large, fuzzy Small, fuzzy Linear, fuzzy Near, fuzzy Gaussian, fuzzy mean and standard deviation (MS) Large, and fuzzy MS Small. Each membership reclassifies a criterion based on what sub-criteria are considered more important than others. Once each criterion has an associated fuzzy membership, a fuzzy overlay method is chosen. There are five methods: fuzzy *And*, fuzzy *Or*, fuzzy *Product*, fuzzy *Sum*, and fuzzy *Gamma*, and each one emphasizes specific aspects of the resultant combination of fuzzy memberships. Hasanloo et al. (2019) and Baidya et al. (2014) use fuzzy overlays to analyze flood risk and land resources.

With how many varied weighting methods there are, both weighted overlay and fuzzy overlay seem to be ideal candidate methods for decision making with multiple criteria. Malczewski (2004) points out that data – particularly spatial data – has inherent inaccuracy and

imprecision due to ambiguity in inputted data, be it from scaling or from user preferences. The fact that data formatting is not standardized means that different data sources have different levels of accuracy and precision (Malczewski 2004). De Montis et al. (2005) indicates that the choice of weighting method by the decision maker may or may not be the best fit for whatever problem they are trying to solve, and Steele et al. (2009) furthers this argument by suggesting that weighting individual criterion is subjective because ranks are defined by the decision maker. While MCDA in general is a popular and widely used method for decision-making that involves multiple criteria, there are certainly other methods that exist to generate similar outputs.

2.4.2. Logistic Regression

Logistic regression (LR) is a multiple criteria regressive analysis in which the dependent variable may be neither continuous nor quantitative, and the relationship with several independent variables is explored (Lee 2005). It is a method that is used in predictive analysis, utilizes binary dependent variables, and generates nonlinear models (Kavzoglu et al. 2012; Lee 2005). This method was used by Du et al. (2014), Erener et al. (2016), Kavzoglu et al. (2012), and Lee (2005) as a means of comparing different methodologies. Ayalew and Yamagishi (2004) and Lombardo and Mai (2018), in contrast, use LR as their sole means of analyzing landslide susceptibility.

LR is calculated based on a general linear model equation:

$$P = \frac{1}{(1 + e^{Z})} \quad (14)$$

where P is event probability, e is the base of the natural logarithm, and Z is a value that ranges from -∞ to +∞, and Z is defined by the following equation:

$$D_G = -3.5f_{clay} - 2.0f_{silt} - 0.5f_{sand} \quad (15)$$

$$Z = B_0 + B_1X_1 + B_2X_2 + \cdots + B_nX_n \quad (16)$$

where B is the model's intercept, n is the number of independent variables, and B_n is the coefficient that measures X_n, which is the contribution of an independent variable. The dependent variable in LR is expressed as:

$$D_G = -3.5f_{clay} - 2.0f_{silt} - 0.5f_{sand} \quad (17)$$

$$Logit(p) = \ln\left(\frac{p}{1-p}\right) = 1/1 + e^{B_0 + B_1X_1 + B_2X_2 + \cdots + B_nX_n} \quad (18)$$

where p is the dependent variable probability and $p/(1-p)$ is the likelihood ratio.

The advantage of using LR in susceptibility analysis is that the dependent variable only outputs as one of two values: 0 or 1, and the results can be interpreted as a probability that ranges from 0 to 1. If the result is closer to 0, then it has a lower probability of success, whereas if the result is closer to 1, the odds of the result occurring is higher (Kavzoglu et al. 2012).

2.4.3. Other Methods

Aside from MCDA and LR, a number of other modeling methods exist. Of the studies referenced for this project, over twenty different modeling methods were utilized for landslide susceptibility mapping. These other methods have been summarized in Table 3.

Table 2 Weighting schemes used in other studies

Method	Study
Artificial neural network	Vahidnia et al. 2010
Analytic network process	Ali et al. 2021
Association rule mining	Erener et al. 2016
Convolutional neural network	Ghorbanzadeh et al. 2019; Li 2020
Frequency ratio	Vakhshoori and Zare 2016
Fuzzy logic	Ercanoglu and Gokceoglu 2002; Roy and Saha 2019; Vakhshoori and Zare 2016
Fuzzy membership function	Roodposhti et al. 2016
Heuristic fuzzy approach	Stanley and Kirschbaum 2017
Fuzzy interference system	Vahidnia et al. 2010
Information value method	Du et al. 2014; Saha et al. 2005
Landslide nominal susceptibility factor	Saha et al. 2005
Landslide numerical risk factor	Roy and Saha 2019
Long short-term memory	Li et al. 2021
Naïve Bayes	Ali et al. 2021
Machine learning	Lai and Tsai 2019
Monte Carlo	Feizizadeh and Blaschke 2013
Ordered weighted average	Feizizadeh and Blaschke 2012; Feizizadeh and Blaschke 2013
Random forest	Ali et al. 2021; Ghorbanzade et al. 2019; Lai and Tsai 2019
Shannon entropy	Roodposhti et al. 2016; Zhao et al. 2017
Support vector machine	Ghorbanzadeh et al. 2019; Li et al. 202; Roy et al. 2019; Vakhshoori and Zare 2016
Support vector machine regression	Kavzoglu et al. 2012
Variable weight combination	Li et al. 2021
Weight of evidence	Nohani et al. 2019; Roy et al. 2019
Weighted linear combination	Feizizadeh and Blaschke 2012; Feizizadeh and Blaschke 2013

Chapter 3 Methodology

This project aims to generate a model in which landslide susceptibility maps are created through the use of weighted criteria. Two different methods for weighting were used to analyze the data: weighted overlay and fuzzy overlay. The base data used for these different methods are identical but are differentiated due to respective geoprocesses, and weighting was determined using previous studies as a guide.

3.1. Research Design

The purpose of this project is to not only generate a model in which landslide susceptibility locations may be predicted, but to also determine what criteria weigh more heavily in determining landslide initiation. Data of all types have been used in a variety of studies that used a number of methods, though this project did not use the complete list of criteria detailed in Chapter 2.

For this project, Esri's ArcGIS Pro is the primary software used in modeling landslide susceptibility in the south-central Front Range. The data for this project were collected and formatted before undergoing susceptibility analysis. Two methods – weighted overlay and fuzzy overlay – were used, resulting in maps that can then be compared to determine the most accurate predictions. These two methods were chosen to allow for repeatability and to test how different methods affect results. A simplified workflow is shown in Figure 5.

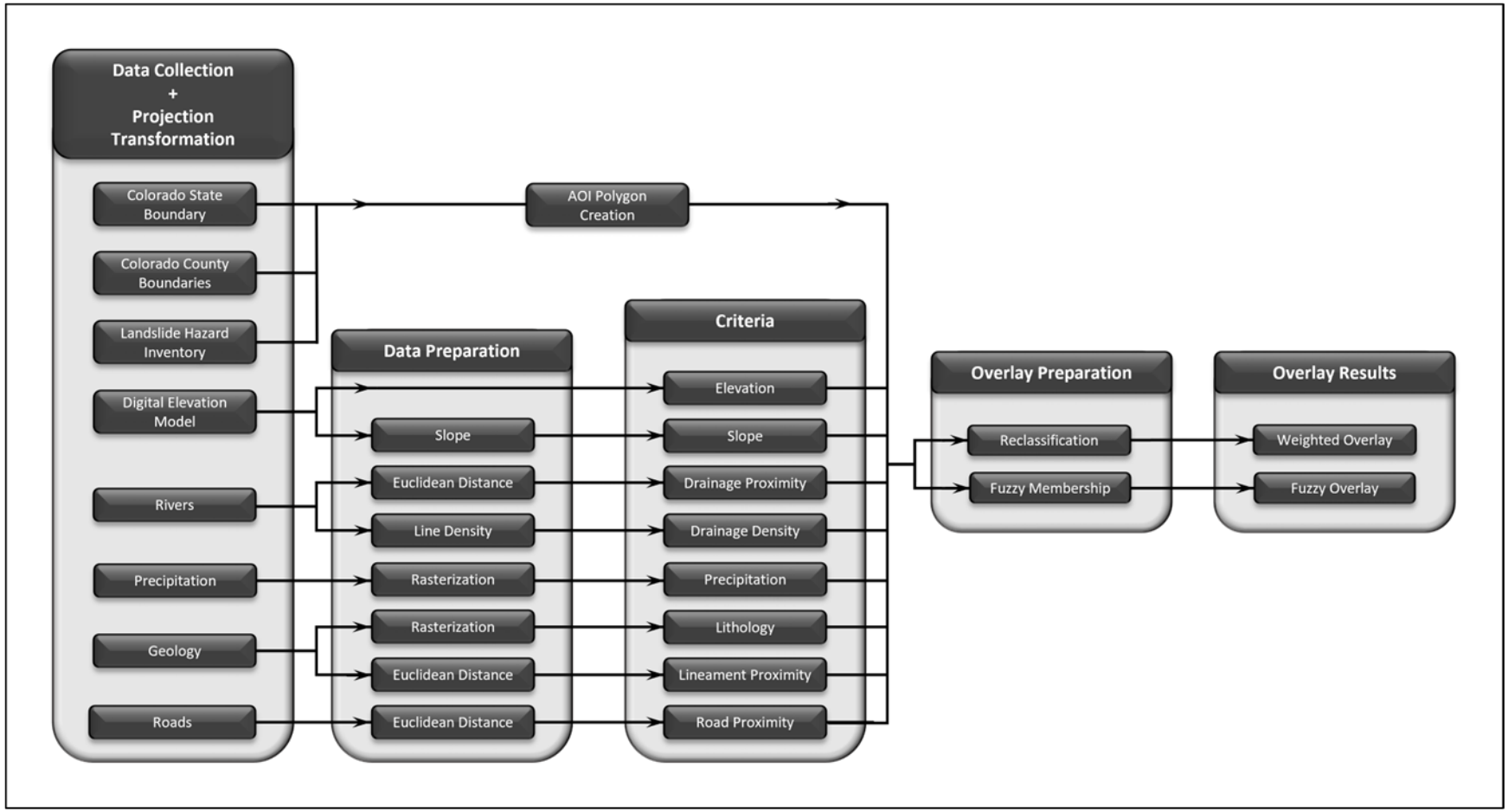

Figure 5 Project workflow

The DEM was chosen to be used as the basis for both the scale and the snap raster because of its high resolution and coverage area. Any generated rasters would be created using the 10-meter resolution of the DEM, as well as the bounds. Other snap rasters were considered, but the DEM was ultimate chosen due to the fact that it is the base upon which almost all of the other analyses build upon.

A map projection was selected for the project, chosen based on what projection best fit the AOI: in this case, NAD 1983 UTM Zone 13N. NAD 1983 Colorado State Plane Central FIPS 502 was considered but not used due to the fact that the three Colorado State Plane projections focus on latitudinal bands of the state, as opposed to longitudinal bands (USA Contiguous Albers Equal Area Conic USGS). As landslides vary in size and scale, data with the highest resolution was used as the snap raster. For this project, the data with the highest resolutions available were elevation and slope at ⅓ arc-second (10-meter), and elevation was selected as the snap raster. Subsequent rasters generated from various shapefiles retained the same resolution as the snap raster.

3.2. Choice of Study Area

The study area was chosen based on several factors, the first of which was the average frequency of landslide occurrences. Colorado has a high incidence rate of landslides that originate from the western half of the state that lies within the bounds of the Rocky Mountains. The fact that the state has a long history of recorded landslides further made it a feasible candidate study location, and the USGS also has multiple marked locations marked as “high risk” for landslide activity. The fact that the Colorado Geological Survey also had landslide data on their website also helped in determining what area to focus on for this study.

42

Once the initial data was downloaded, an AOI was selected based on data coverage, and this location was determined using the USGS's landslide hazard inventory and county boundaries. Areas in the landslide inventory with a high density of high confidence in landslide activity were focused on first. The region with the highest density of likely landslide locations encompasses the Front Range in north-central Colorado. The *Pairwise Buffer* tool was used to generate a buffer of five miles around county boundaries, and the bounds of the AOI were drawn using points determined by the buffers of three counties: Larimer, Boulder, and Jefferson Counties (Figure 6). These counties were chosen due to the fact that a majority of the high-risk landslide hazard locations from the landslide inventory fell within these counties. Initially, these three counties were to be the AOI for this project, but the cluster of high confidence that straddled Clear Creek and Summit Counties to the west-southwest of the three counties could not be ignored, and so the AOI was expanded to follow latitudinal and longitudinal lines. Once the AOI was established, the rest of the data was clipped to the AOI for ease of use.

43

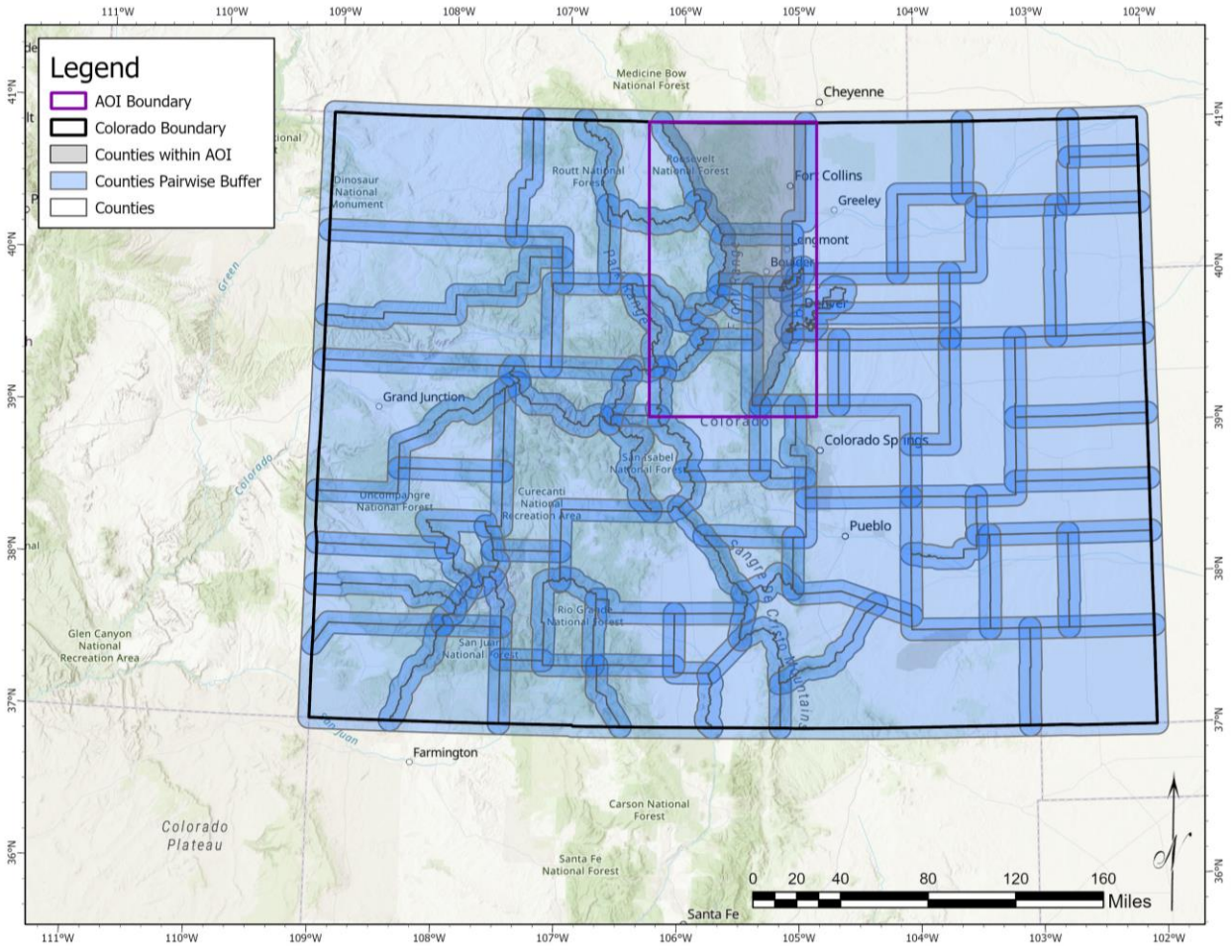

Figure 5 Buffers on Colorado county boundaries with the three chosen counties (Larimer, Boulder, and Jefferson) lightly shaded in grey

3.3. Criteria Selection and Data Preparation

Eight different criteria were used for this study: elevation, slope, precipitation, drainage proximity, drainage density, lithology, lineament proximity, and road proximity. These criteria were chosen based on a combination of usage in the literature, data availability, and AOI coverage (Table 4). Each of the criteria covered in 2.3 was searched to see if the associated data could be included in this project and, if found, retained if the data coverage extended over the whole of the AOI. Five different data sets were used to generate the eight criteria that were ultimately used in this project. The data come from different sources and in different formats,

some of which required more preparation than others. The following sections detail these criteria and data preparation processes.

Table 3 Variables employed and raw data utilized for this project

Criteria	Data	Format	Source	Description
Elevation	DEM	geoTIFF	USGS	DEM with coverage across the contiguous US
Slope	DEM	geoTIFF	USGS	DEM with coverage across the contiguous US
Precipitation	Precipitation	shapefile	USDA	Averaged annual rainfall by state from 1981 to 2010
Drainage Proximity	Rivers	shapefile	NOAA	Rivers and streams within the contiguous US
Drainage Density	Rivers	shapefile	NOAA	Rivers and streams within the contiguous US
Lithology	Geology	shapefile	USGS	Geologic units and faults with attribute data by state
Lineaments	Geology	shapefile	USGS	Geologic units and faults with attribute data by state
Road Proximity	Roads	shapefile	Colorado, USCB	Major roads and highways within the state of Colorado

3.3.1. Elevation

Elevation ranking was taken from a number of sources, as almost every study included elevation as one of their criteria. Many of the studies observed a correlation between landslide frequency and higher elevation (Ayalew and Yamagishi 2004; Chen and Li 2020; Du et al. 2017; Feizizadeh and Blaschke 2013; Feizizadeh et al. 2014; Mallick et al 2018; Patil et al. 2019; Roodposhti et al. 2016; Shou and Chen 2021; Vakhshoori and Zare 2016), though the number of studies that detailed their ranking categorization were few and far in between.

Elevation was derived from a series of DEMs downloaded from the USGS. The USGS has multiple resolutions available to the public that cover the entirety of the contiguous US and the state of Alaska. The ⅓ arc-second (10-meter) resolution was chosen for this project because of all the resources searched, it was the highest-resolution DEM available that covered the entire

45

extent of the AOI. The DEM used in this project consisted of a mosaic of smaller geoTIFFs 1° × 1° in size that were combined using the *Merge* tool, and the color bar for the resultant DEM was normalized into a single uniform color bar for better visualization. Elevation that was then clipped to fit the AOI was derived from the merged DEM (Figure 7). Within the AOI, the elevation ranged from 1,438 meters to 4,356 meters (4,717.8 feet to 14,291.3 feet).

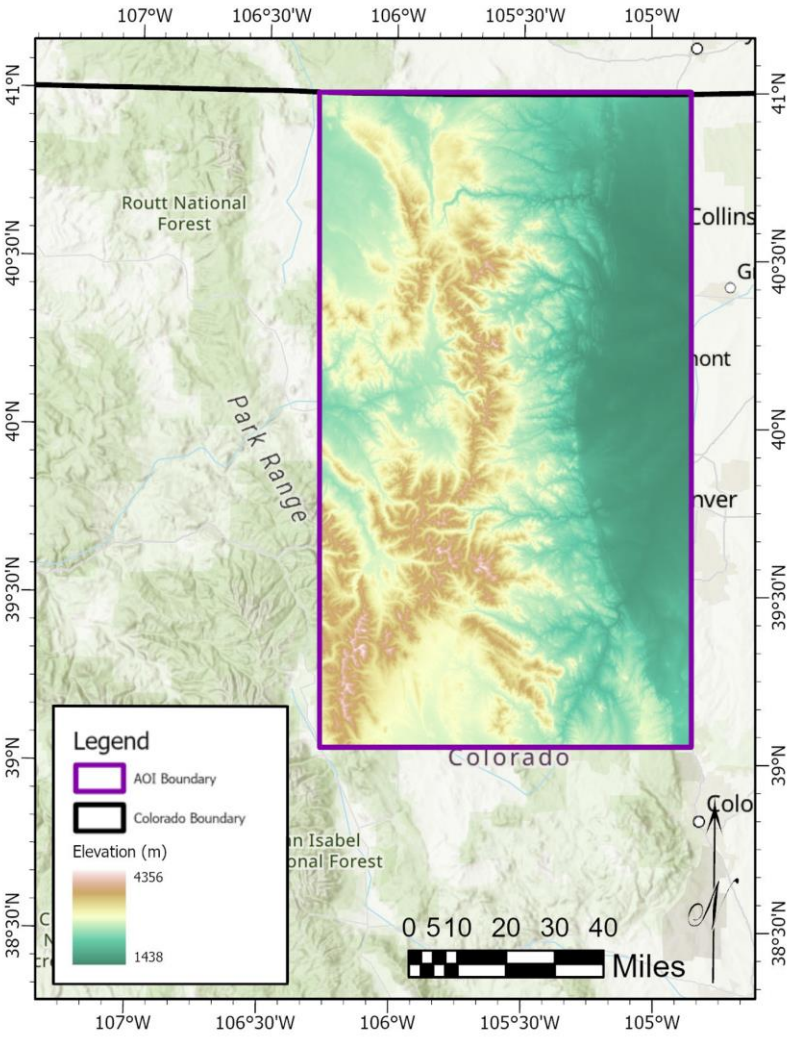

Figure 6 Elevation in meters

46

3.3.2. Slope

Slope was derived from the merged DEM (Figure 8). Within the AOI, the slope ranged from 0° to 85.1° For slope ranking, Patil et al. (2019) and Çellek (2020) indicated that slope gradients of between roughly 20° to 40° experienced landslides the most frequently, with landslide frequencies tapering off as slopes both decreased below 20° and increased greater than 40°.

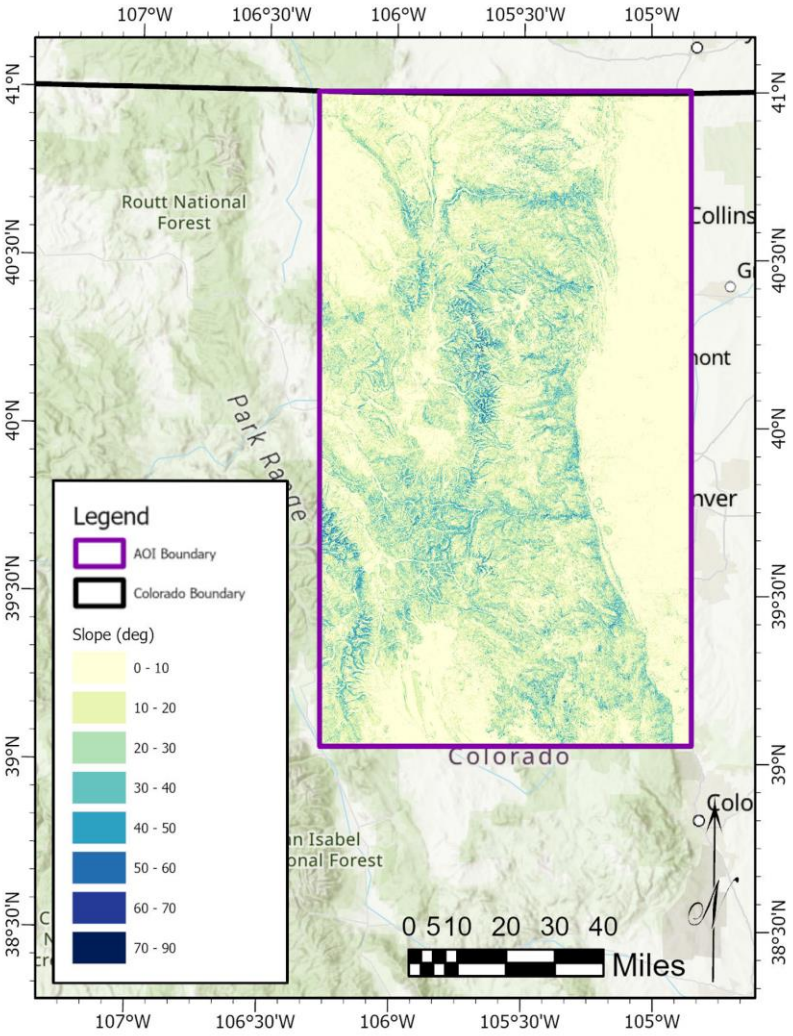

Figure 7 Slope in degrees derived from elevation

47

3.3.3. Precipitation

Precipitation was chosen as a criterion due to the frequency of its use in other studies, as well as the fact that the data was readily available. The data consists of averaged annual rainfall in inches that date from 1981 to 2010. The data was sourced from the USDA and was downloaded as a shapefile that covered the entire state. The clipped AOI data has a range of 10 inches to 52 inches (Figure 9). Precipitation was a somewhat common criterion used, and studies found a correlation between higher landslide frequencies and increased amounts of rainfall (Ali et al. 2020; Chen et al. 2015; Feizizadeh and Blaschke 2013; Feizizadeh et al. 2014; Nandi and Shakoor 2009; Roy et al. 2019; Zhao et al. 2017).

48

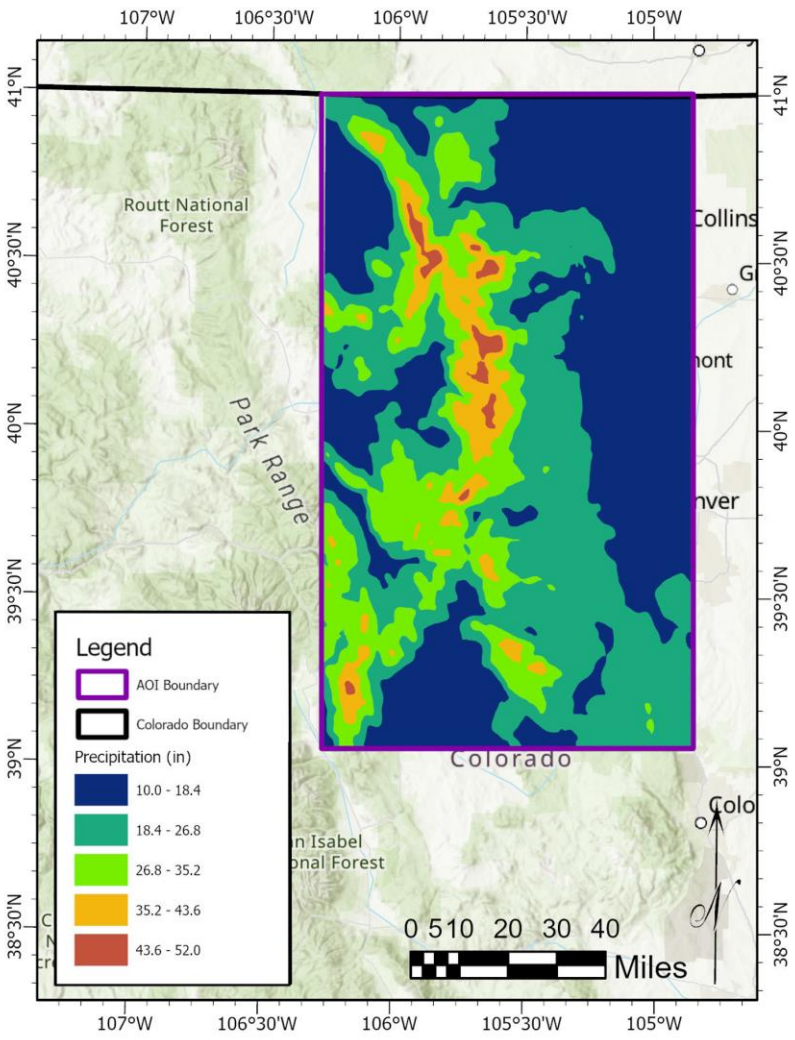

Figure 8 Precipitation in inches

3.3.4. Drainage Proximity

A shapefile of major rivers in the contiguous US was downloaded from the NOAA (Figure 12). This shapefile covers the contiguous United States and includes portions of rivers and streams that originate in Canada. Drainage systems data was easily accessible and drainage proximity factored into a number of studies (Ali et al. 2020; Erener et al. 2016; Ghorbanzadeh et al. 2019; Nandi and Shakoor 2009; Nohani et al. 2019; Roccati et al. 2021; Vahidnia et al. 2010), which revealed a correlation between distance from rivers and streams and landslide frequency.

The shapefile was clipped to the AOI and the *Euclidean Distance* tool was used to generate distance buffers, which is shown in Figure 10.

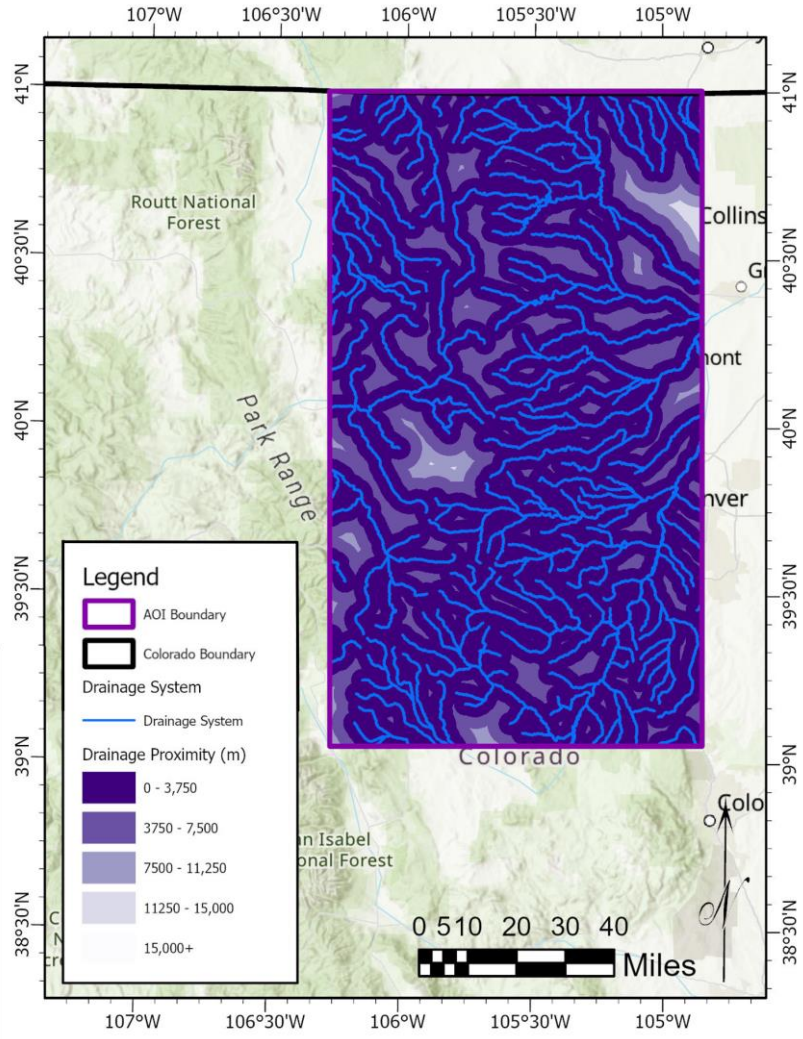

Figure 9 Drainage proximity in meters with clipped drainage systems superimposed

3.3.5. Drainage Density

Drainage density used the same shapefile as drainage proximity and was generated with the aid of the *Line Density* tool (Figure 12). Drainage density was, unfortunately, not as well documented in the literature, and Saha et al. (2019) was the only one to detail how they categorized the river density criterion.

50

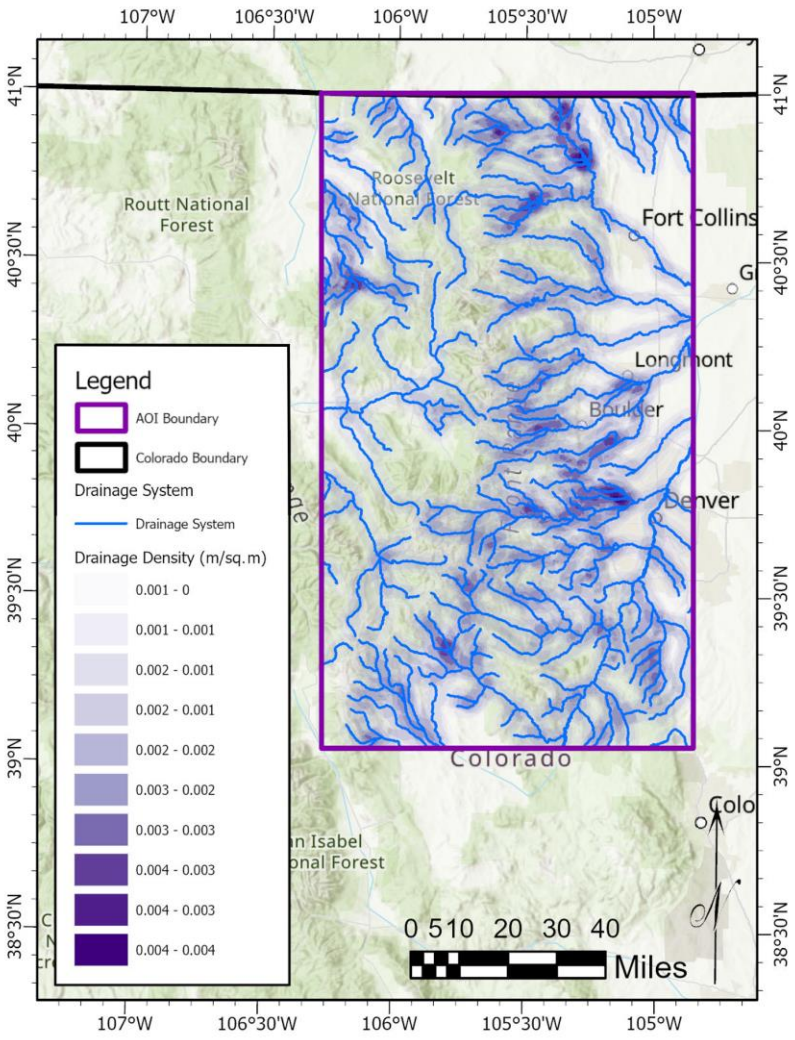

Figure 10 Drainage density in meters/meters squared with clipped drainage systems superimposed

51

3.3.6. Lithology

Geology was downloaded from the USGS. The shapefile covered the whole of the state of Colorado before being clipped to the AOI (Figure 12). The different lithological compositions were then visualized according to the associated key. Lithology was used as a criterion in many studies (Ali et al. 2020; Chen and LI 2020; Du et al. 2017; Kavzoglu and Colkeson 2013; Lombardo and Mai 2018; Pham et al. 2020; Roy and Saha 2019; Roy et al. 2019; Saha et al. 2005; Zhao et al. 2017). Despite the frequency of its use, however, Ott (2020) was the only

author to categorize lithologies by erodibility, and the rankings used in this project are based on Ott (2020)'s work.

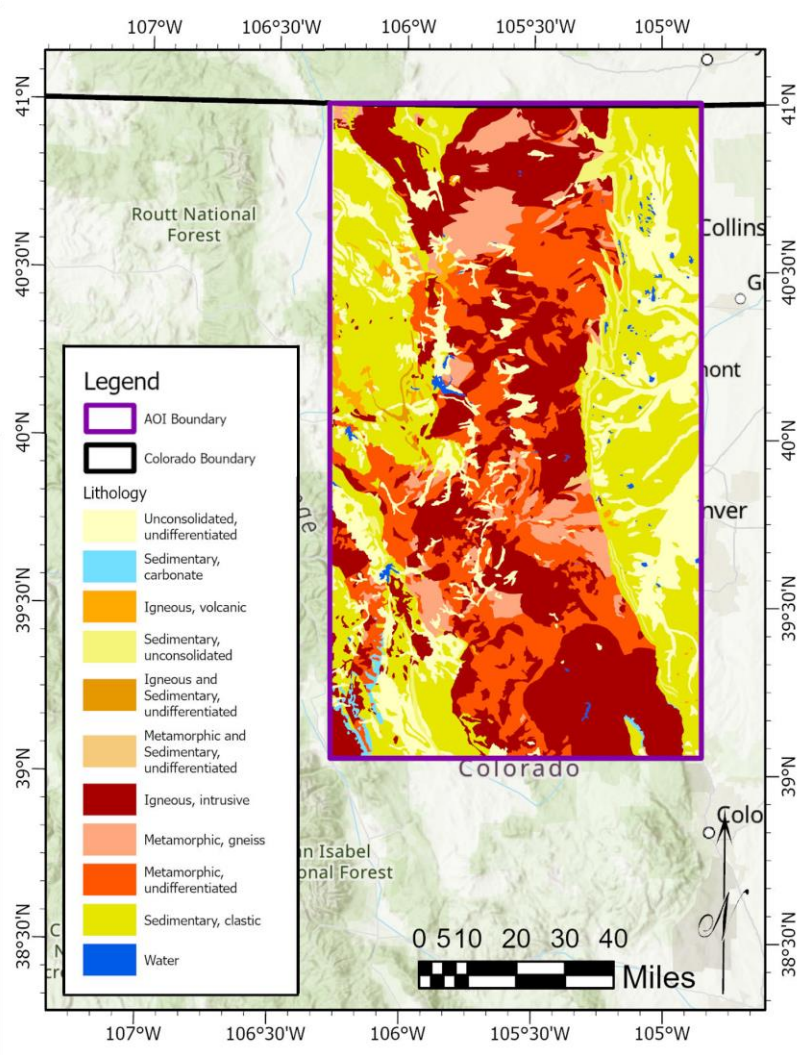

Figure 11 Lithologic classifications

3.3.7. Lineament Proximity

The lineament shapefile covered the entirety of Colorado and was color-coded according to standard geological map key colors (Figure 13). Lineament proximity was used in several studies, and many studies determined a correlation between lineament proximity and landslide

52

frequency (Chen and Li 2020; Erener et al. 2016; Ghorbanzadeh et al. 2019; Mallick et al. 2018; Pham et al. 2020; Vakhshoori and Zare 2016).

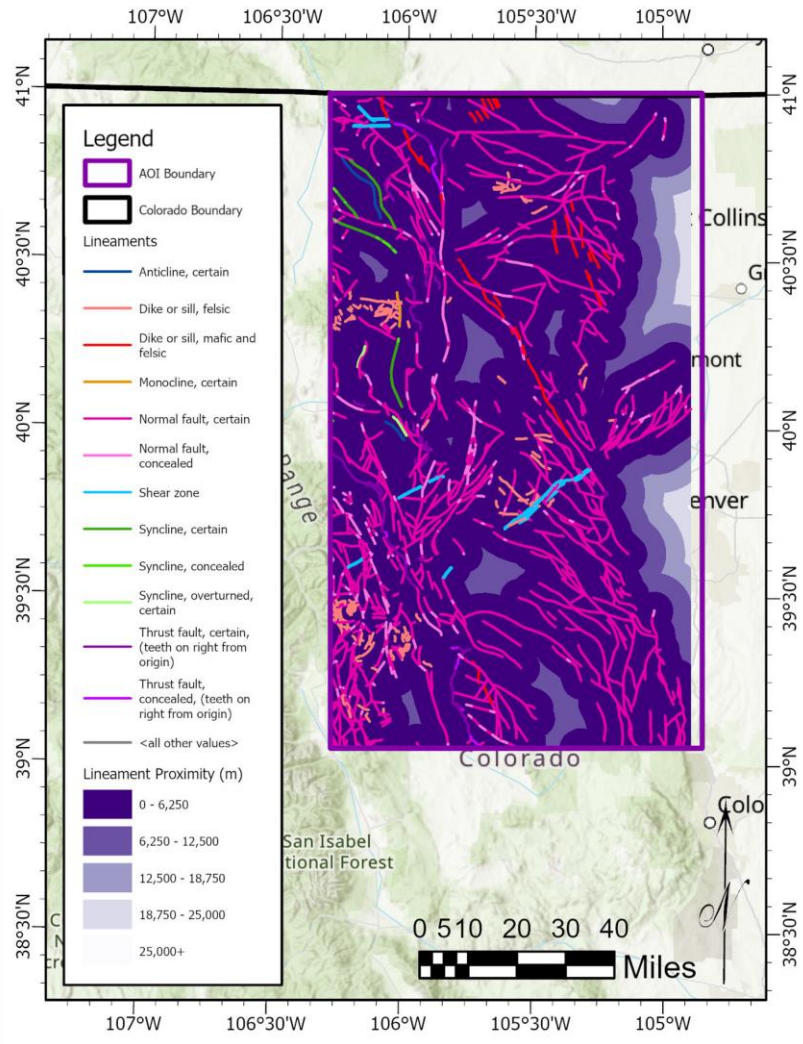

Figure 12 Lineament proximity in meters with lineaments superimposed

3.3.8. Road Proximity

Road data was provided by both the US Census Bureau and the state of Colorado in the form of shapefiles. A shapefile consisting of primary and secondary roads within Colorado was downloaded from the Census Bureau while a shapefile containing major streets came from the Colorado government. These two shapefiles were merged in order to form a more complete reference for transportation passages throughout the state using the *Merge* tool before being

clipped to the AOI bounds (Figure 14). Road proximity was included in a number of studies because the construction of roads – particularly in areas of dynamic topographical change – have a tendency to destabilize slope gradients by way of creating extremely steep slopes in order to create enough space level enough to build a road. This abrupt change in slope greatly increases the chances of slope failure, which in turn may develop into a landslide (Ayalew and Yamagishi 2004; Chen and Chen 2021; Nohani et al. 2019; Pawluszek and Borkowski 2016; Shou and Chen 2021).

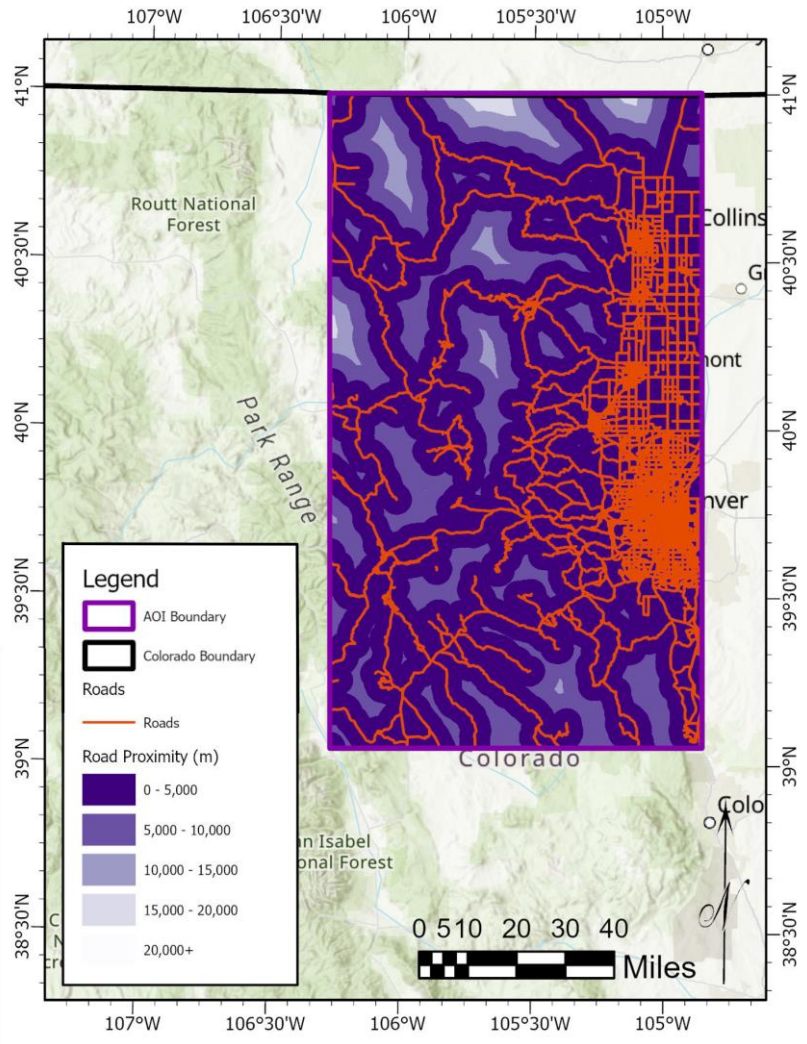

Figure 13 Road proximity in meters with clipped roads layer superimposed

54

3.3.9. Unselected Criteria

As mentioned in Chapter 2, landslide susceptibility mapping can and does utilize a variety of different criteria. Some of those mentioned had been intended for use in this project, but for various reasons ended up being discarded. The five criteria that were planned but rejected were aspect, LULC, soil composition, water saturation, porosity, and population/census tracts. Aspect was derived from elevation but was dropped due to insufficient data on what cardinal direction landslides tended to occur on within the AOI and therefore an appropriate weighting scheme would not be possible for the AOI. While data for LULC that covers the entire extent of the AOI exists, it was not discovered until the analysis was already completed. Soil composition had missing attributes in the attribute table that rendered the data inadequate for the purposes of this project. Water saturation data was spread out throughout the AOI, but the data points were sparce enough and spread out far enough that interpolation and extrapolation were not feasible. The data for porosity downloaded in a format that required additional processing outside the scope of this project to be used.

3.4. Weighted Overlay

Weighted overlay is but one of many MCDA methods that take into account criterion ranks and value functions (Malczewski and Rinner 2015). Weighted linear combination, weighted linear average, weighted summation, and simple additive weighting are other names this method is known by. This process is straight forward in that it is based on assumptions of additivity and linearity, in which the former indicates criteria are independently preferential of each other. The latter assumes that the preferential weight of a criterion is constant on every level it is considered in.

3.4.1. Reclassification of Criteria

For the weighted overlay, the data needed to be reclassified into a uniform scaling. The *Reclassification* tool was used here to change the scales from their original values to a 1 to 5 ranking with 5 being of high importance and 1 being of low importance. The breakup of ranking categories is described in further detail by criteria.

3.4.1.1. Elevation

Elevation was reclassified according to height above sea level. In this case, the higher the elevation, the greater the ranking, as there is a rough correlation between landslide activity and elevation (Clague and Roberts 2012). Table 5 shows the cutoff values for each rank, and Figure 15 is a visual representation of the reclassified elevation.

Table 4 Elevation reclassification ranks and cutoffs

Elevation	Rank	Cutoff
(meters)	5	<3500
	4	3000
	3	2500
	2	2000
	1	1500

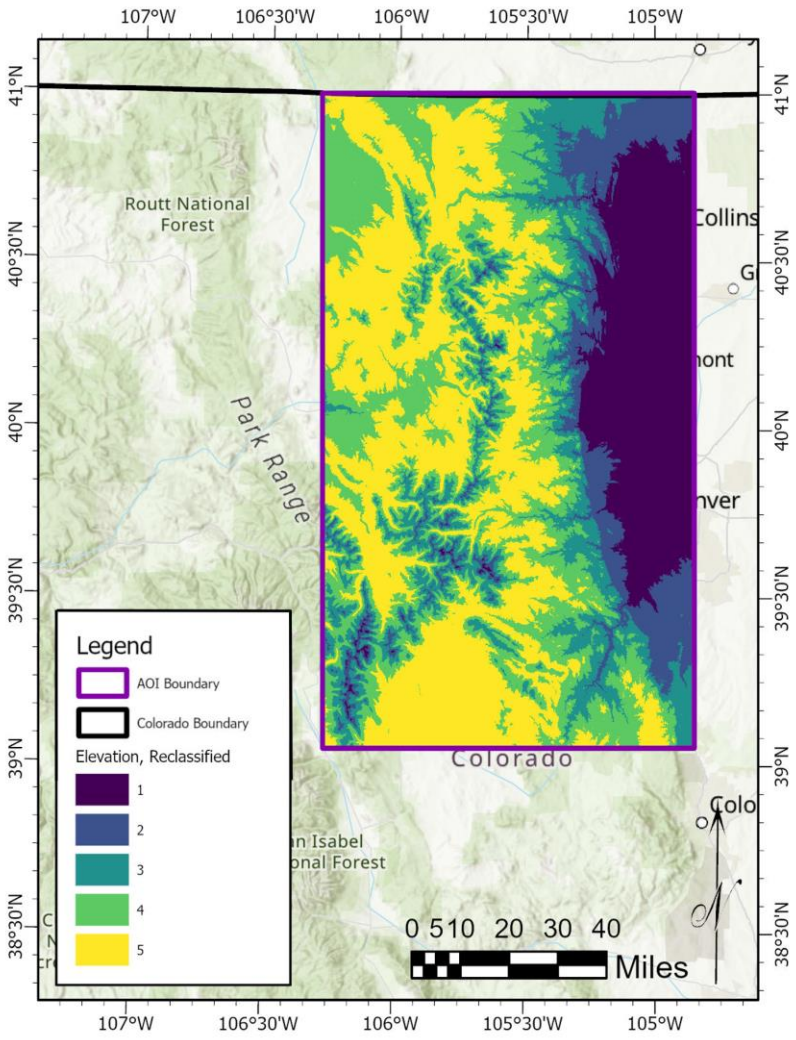

Figure 14 Reclassified elevation

3.4.1.2. Slope

The reclassification of slope utilized the cutoffs of several studies (Chen and Chen 2021; Chen and Li 2020; Feizizadeh and Blaschke 2013; Vakhshoori and Zare 2016) for the rank cutoffs used in this project. The ranking of these cutoffs were based on Patil et al. (2020)'s statistics for their study area. Table 6 breaks down the slope cutoffs for each rank and Figure 16 is a visual representation of reclassified slopes.

Table 5 Slope reclassification ranks and cutoffs

Slope	Rank	Cutoff
(degrees)	5	20-30
	5	30-40
	3	10-20
	3	40-50
	2	0-10
	2	50-60
	1	60-70
	1	<70

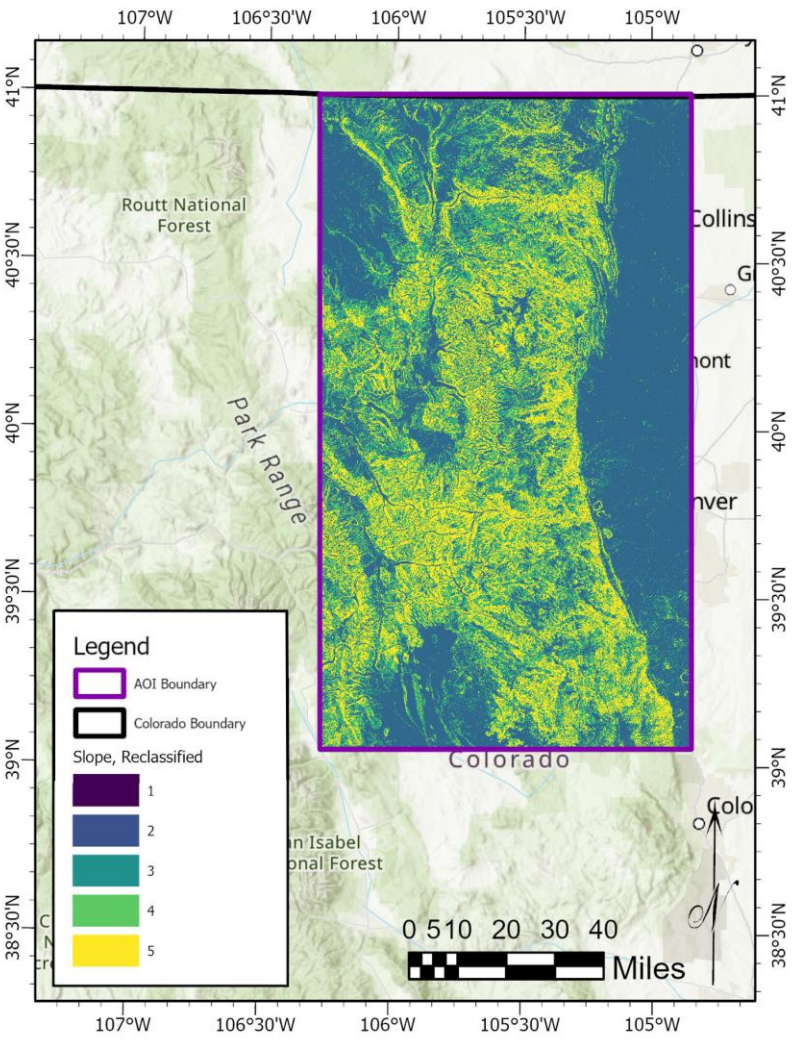

Figure 15 Reclassified slope

3.4.1.3. Precipitation

The reclassification of precipitation was a simplistic scaling using the minimum and maximum averaged rainfall in the shapefile. In order to reclassify precipitation, the shapefile had to be rasterized. The *Polygon to Raster* tool was used for this process. The cutoffs were equally distributed within that range with a higher rank given to increased average rainfall (Ali et al. 2020; Nandi and Shakoor 2009). The cutoffs are summarized in Table 7 and visualized in Figure 17.

Table 6 Precipitation reclassification ranks and cutoffs

Precipitation	Rank	Cutoff
(inches)	5	>50
	4	50
	3	37.5
	2	25
	1	12.5

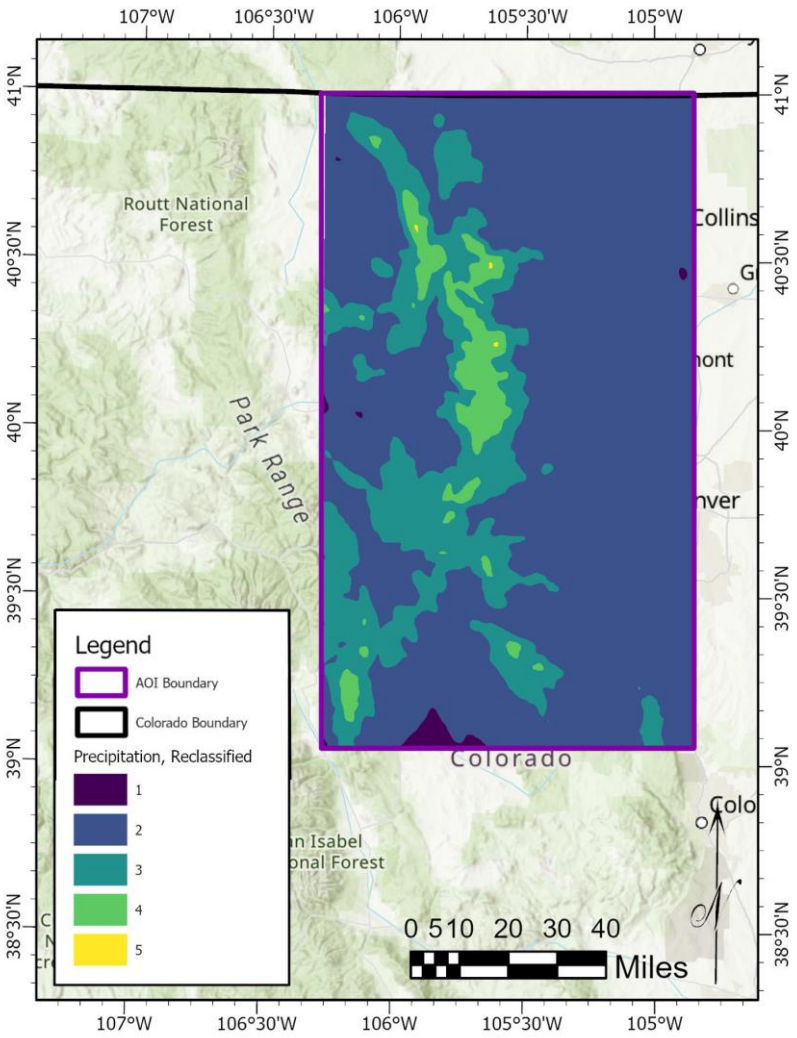

Figure 16 Reclassified precipitation

3.4.1.4. Drainage Proximity

Reclassification of drainage proximity required the use of the *Euclidean Distance* tool. The cutoffs were chosen based on work from Chen and Chen (2021), Erener et al. (2016), Patil et al. (2019), and Zhao et al. (2014). Table 8 shows the ranking cutoffs and Figure 18 visualizes these rankings.

Table 7 Drainage proximity reclassification ranks and cutoffs

Drainage Proximity	Rank	Cutoff
(meters)	5	3750
	4	7500
	3	11250
	2	15000
	1	>15000

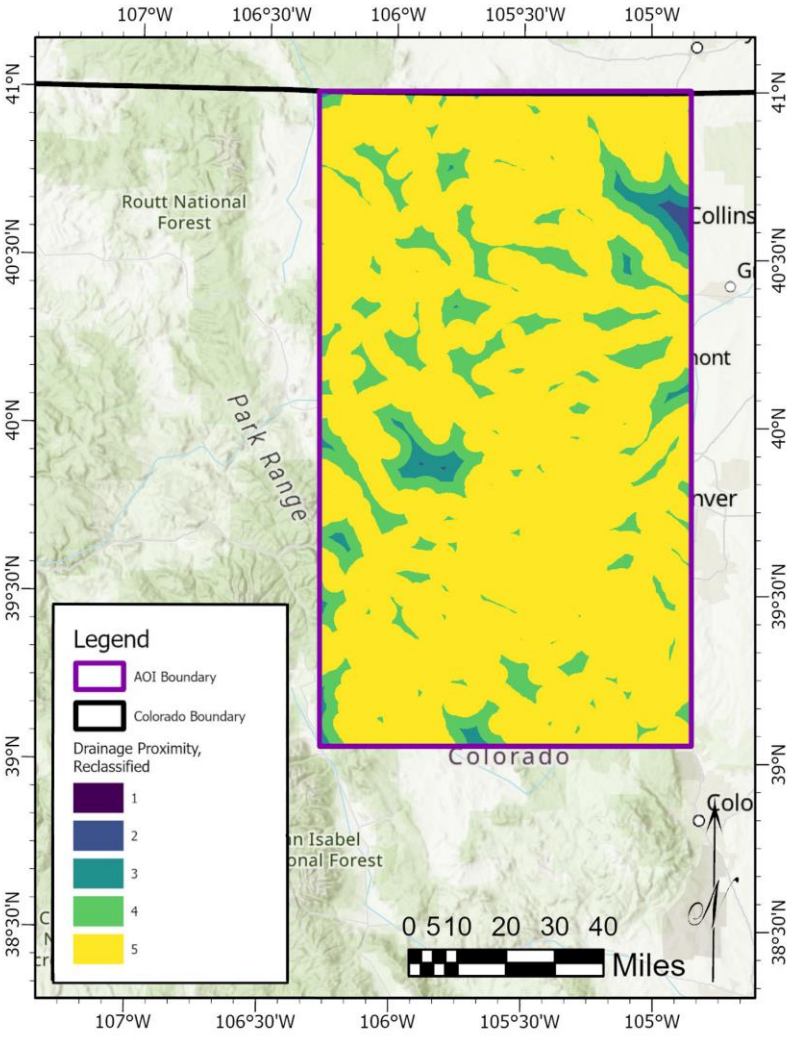

Figure 17 Reclassified drainage proximity

3.4.1.5. Drainage Density

Drainage density was not as commonly used in the literature, though Roodposhti et al. (2016) and Saha et al. (2005) use this criterion in their own studies. Table 9 delineates the cutoffs for the different ranks, while Figure 19 visualizes these cutoffs.

Table 8 Drainage density reclassification ranks and cutoffs

Drainage Density	Rank	Cutoff
(meters/square meters)	5	>4
	4	4
	3	3
	2	2
	1	1

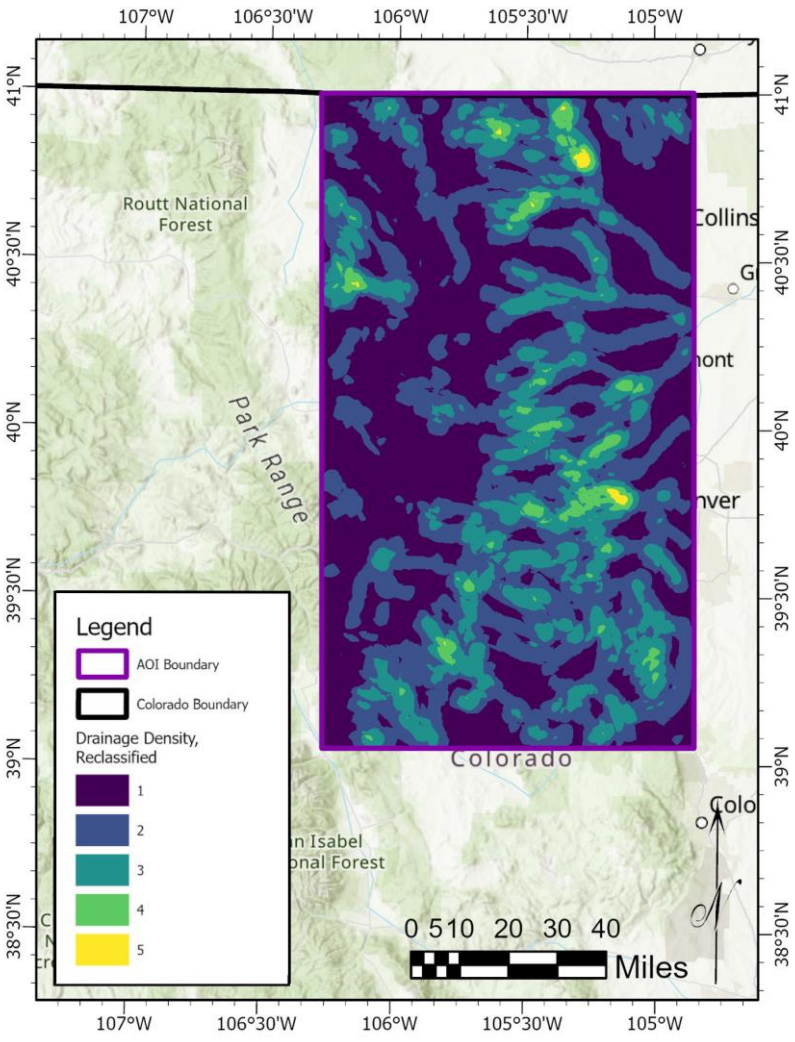

Figure 18 Reclassified drainage density

3.4.1.6. Lithology

Lithology required a different approach to reclassification because the symbology used for this shapefile is not numerical. Ott (2020) summarized the erodibility of different lithologic compositions, and the rankings were generated based on that author's work. The shapefile used for lithology also had to be converted to a raster in order to be reclassified, and therefore the *Polygon to Raster* tool was used. The *Fuzzy Membership* tool was then used to assign rankings to the different lithologies. The breakdown of ranks is shown in Table 10 and visualization is featured in Figure 20.

Table 9 Lithology reclassification ranks and categories

Lithology	Rank	Category
	5	Unconsolidated, undifferentiated
	4	Sedimentary, carbonate
	3	Igneous, volcanic
	3	Sedimentary, undifferentiated
	2	Igneous and Sedimentary, undifferentiated
	2	Metamorphic and Sedimentary, undifferentiated
	1	Igneous, intrusive
	1	Metamorphic, gneiss
	1	Metamorphic, undifferentiated
	1	Sedimentary, clastic
	N/A	Water

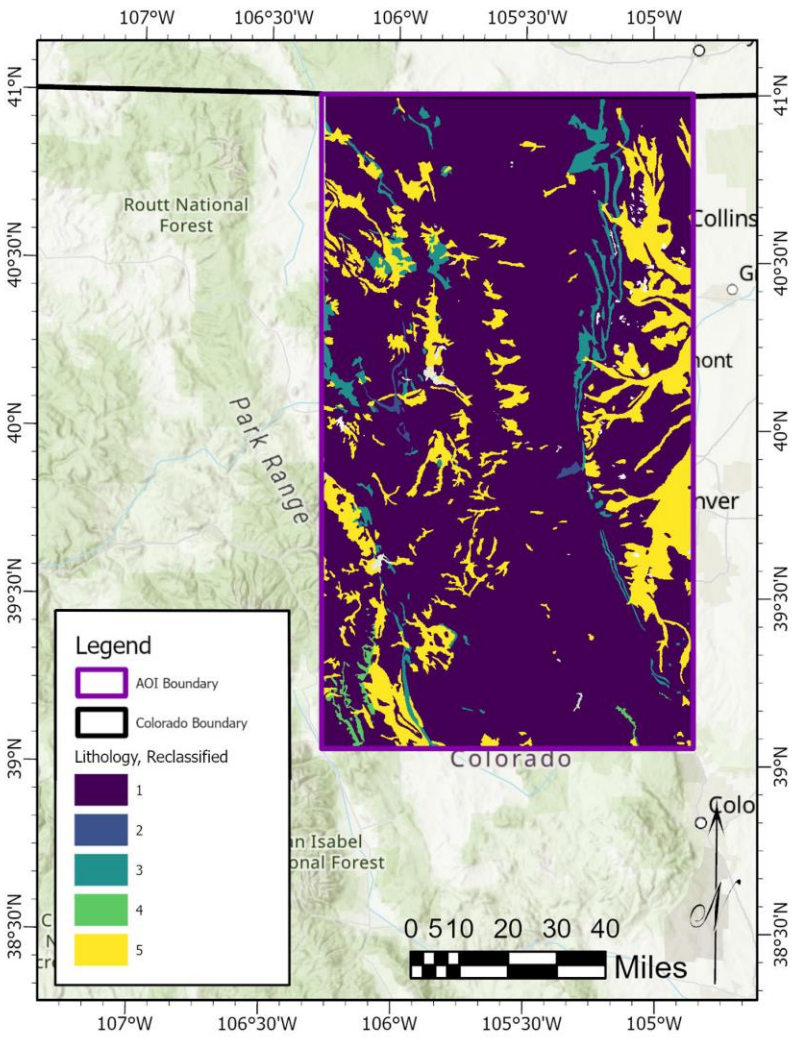

Figure 19 Reclassified lithology

3.4.1.7. Lineament Proximity

The reclassification of lineaments was relatively simplistic, as it only required the use of the *Euclidean Distance* tool to generate proximity buffers. The buffer cutoffs were guided by studies such as Ali et al. (2020), Du et al. (2017), Erener et al. (2016), Nohani et al. (2019), Roy et al. (2019), and Vojtekova and Vojtek (2020). Lineaments were used due to both the frequency of its use in other studies, as well as ease of access to the data. The cutoffs are shown in Table 11 and displayed in Figure 21.

Table 10 Lineament reclassification ranks and cutoffs

Lineament Proximity (meters)	Rank	Cutoff
	5	6250
	4	12500
	3	18750
	2	25000
	1	>25000

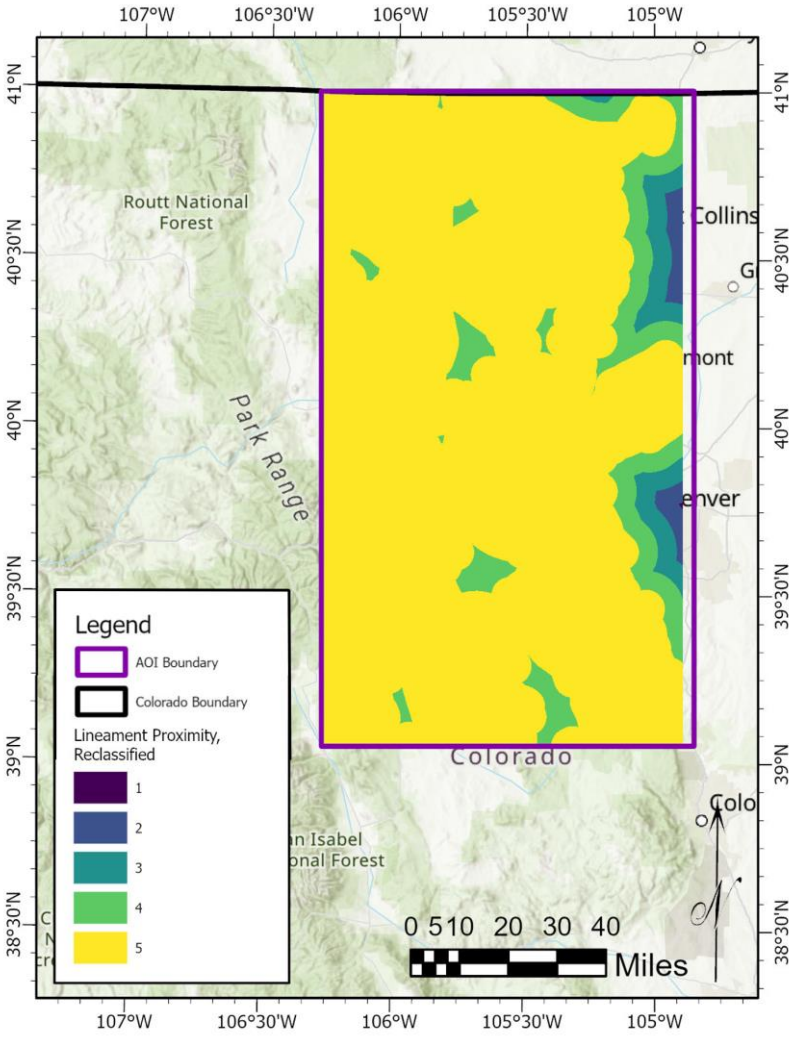

Figure 20 Reclassified lineament proximity

3.4.1.8. Road Proximity

Road proximity was a frequently used criterion in the literature (Ali et al. 2020; Ayalew and Yamagishi 2004; Feizizadeh and Blaschke 2013; Patil et al. 2019; Vakhshoori and Zare

2006). Reclassification was based distance from a road, and the cutoffs are shown in Table 12 and visualized in Figure 22.

Table 11 Road proximity reclassification ranks and cutoffs

Road Proximity	Rank	Cutoff
(meters)	5	5000
	4	10000
	3	15000
	2	20000
	1	>20000

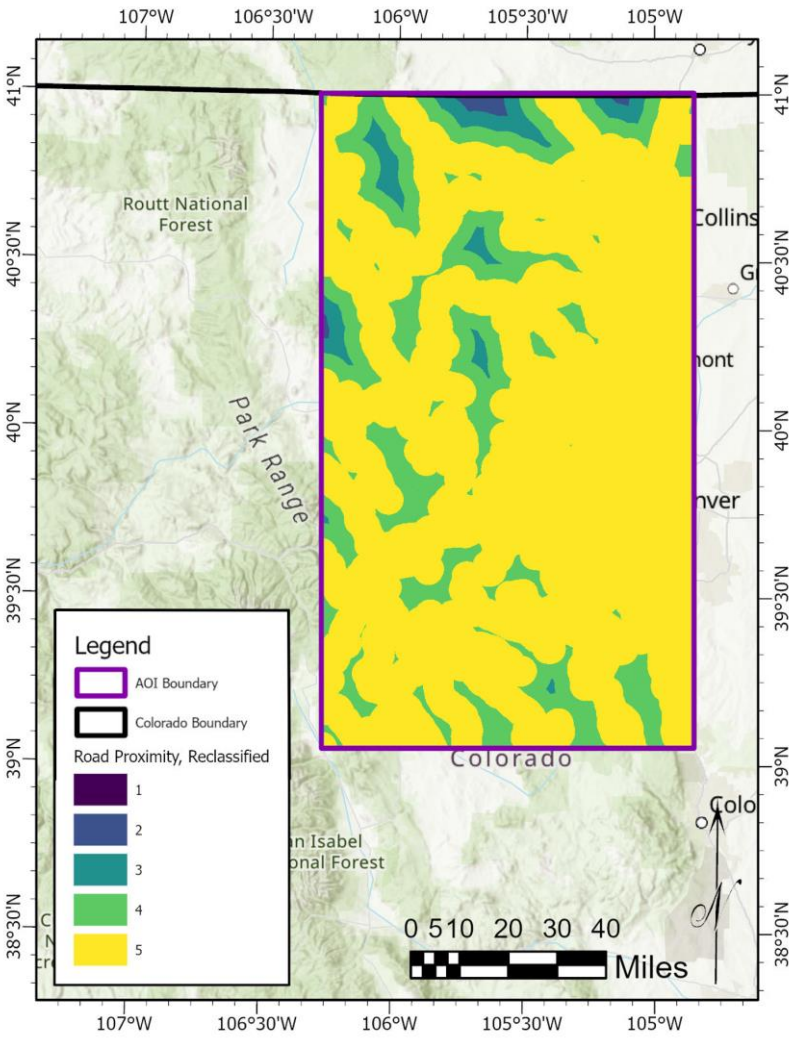

Figure 21 Reclassified road proximity

3.4.2. Weighting of Criteria

The *Weighted Overlay* tool was used to generate a landslide susceptibility map using the calculated ranks. The rankings in Tables 5-12 were used in the weighted overlay using the reclassified rasters and summarizes the criteria properties that went into the weighted overlay. Shit et al. (2016) utilized a weighted overlay for their study, and the equation for the weighted overlay is as follows:

$$S = \frac{\sum W_i S_{ij}}{\sum W_i} \quad (19)$$

where S is the spatial unit value in the output map, S_{ij} is the ith spatial class weight of jth factor map, and W_i is the weight ith factor map.

The criteria were ranked based on how previous studies weighted their chosen criteria, which is summarized in Table 13. Of the listed criteria, four studies provided the actual percentages each criterion was given for their work. Not all of the criteria used in this project were used within the four studies with given percentages. Feizizadeh and Blaschke (2014), for example included every criterion used in this study except river density.

Table 12 Criteria used for reclassification

Study	Slope	Aspect	Precipi-tation	Faults	Road Proximity	River Proximity	River Density
Ali et al. 2020	-/6.43/12.13/ 17.33/ 23.27+	-/69.78/ 143.39/ 215.59/ 287.79	-/800/900/ 1000/1250	0/2498/ 5333/8304/ 11680	0/100/219/ 362/557	0/103/211/ 327/479	-
Ayalew and Yamagishi 2004	-/4/16/31/ 46+	W/NW/NE/ SW/N/E/S/ SE/F	-	50/100/150	50/100/ 150	50/100/150	-
Bragagnolo et al. 2020	-/7.07/13.2/ 19.3/25.5+	0/60/180/ 270/359	-	-	-	-	-
Chen and Chen 2021	-/10/20/30/ 40/50/+	W/NW/NE/ SW/N/E/S/ SE/F	-	-	0/100/200/ 300/400/+	0/200/400/ 600/800/+	-
Chen and Li 2020	-/10/20/30/ 40/50/60/ 70/+	F/N/NE/E/S E/S/SW/W/ NW	-/1221.86/ 1502.36/ 1954.28/ 2639.95+	-/1000/2000/ 3000/4000+	0/200/400/ 600/800+	-/200/400/ 600/800+	-
Chen et al. 2015	-/2/4/6/8/+	-	-	-	-	200/400/600	-
Du et al. 2017	0/15/30/45+	F/N/NE/E/S E/S/SW/W/ NW	-/1000/1500/ 2000/2500/ 3000+	-/500/1000/ 1500/2000+	-/200/400/ 600/800/ 1000+	-/200/400/ 600/800/ 1000+	-
Ercanoglu and Gokceoglu 2015	-	-	-	-	-	-	-
Erener et al. 2016	0/5/10/15/ 20/25/30/35/ 40+	F/N/NE/E/S E/S/SW/W/ NW	-	0/500/1500/ 2500/3500/ 5000/6500/ 8000/9000+	0/100/200/ 300/400/ 500/700/ 900+	0/100/200/ 300/400/ 500/750/ 1000+	-
Feizizadeh and Blaschke 2013	0/10.1/20.1/ 30.1/40.1+	F/N/E/S/W	-/251/301/ 350/401+	0/1001/ 2001/3001/ 4000+	0/26/51/ 76/100+	0/51/101/ 151/200+	-
Feizizadeh et al. 2014	Continuous	F/N/NE/E/S E/S/SW/W/ NW	Continuous	Continuous	Continuous	Continuous	-
Ghorbanzadeh et al. 2019	Continuous	F/N/NE/E/S E/S/SW/W/ NW	-	-	-	-	-
Huggel et al. 2012	-	-	-	-	-	-	-
Kavzoglu et al. 2013	0/5/10/15/ 20/25/30/ 35+	F/N/NE/E/S E/S/SW/W/ NW		-	25	-	8
Korup 2012	-	-	-	-	-	-	-
Lehmann et al. 2019	-	-	-	-	-	-	-
Lombardo and Mai 2018	-	-	-	-	-	-	-
Mallick et al. 2018	Continuous	F/N/NE/E/S E/S/SW/W/ NW	Continuous	Continuous	-	Continuous	-

Study	Slope	Aspect	Precipi-tation	Faults	Road Proximity	River Proximity	River Density
Nandi and Shakoor 2009	0/7.1/14.1/ 21.1/35.1/ 42.1/49.1/ 56.1/63.1+	-	-/92.7/93.98/ 95.26/96.53/ 97.80/99.07/ 100.34/101. 61/102.67+	-	-	0/401/801/ 1201/1601/ 2001/2401/ 2801/3201/ 3601	-
Nohani et al. 2019	0/5/15/30/ 45+	F/N/E/S/W	-	0/100/200/ 300/400+	0/100/200/ 300/400+	0/100/200/ 300/400+	-
Patil et al. 2019	30/20/10/40/ -10/50/60/ 70+	-	80.14/89.26/ 97.24/107.9 6/120.95+	5000/10000/ 15000/ 20000/ 25000/ 30000/ 35000	5000/10000/ 15000/ 20000/ 25000	2000/4000/ 6000/8000/ 10000	-
Pawluszek and Borkowski 2016	Continuous	F/N/NE/E/S E/S/SW/W/ NW	-	-	-/50/100/ 150/200+	-/50/100/ 200/500+	-
Pham et al. 2020	0/14.54/ 29.09/43.63/ 58.18+	F/N/NE/E/S E/S/SW/W/ NW	-	0/101/201/ 301/401/ 500+	0/101/201/ 301/401/ 500+	0/101/201/ 301/401/ 500+	-
`Pourghasemi et al. 2012	0/6/16/31/ 51/70+	N/NE/E/SE/ S/SW/W/N W	-	0/100/200/ 300/400+	0/100/200/ 300/400/ 500+	-/100/200/ 300/400+	-
Pourghasemi et al. 2020	Continuous	F/N/NE/E/S E/S/SW/W/ NW	-	Continuous	Continuous	Continuous	-
Regmi et al. 2014	-	-	-	-	-	-	-
Rengers et al. 2016	-	-	-	-	-	-	-
Roccati et al. 2021	0/11/21/36/ 51/76/ 100+ (%)	F/N/NE/E/S E/S/SW/W/ NW	-	-	<5/>5	<10	-
Roodposhti et al. 2016	Continuous	F/N/NE/E/S E/S/SW/W/ NW	Continuous	Continuous	Continuous	Continuous	Continuous
Roy and Saha 2019	0/9.32/ 18.44/27.34/ 36.66+	F/N/NE/E/S E/S/SW/W/ NW	1877.38/ 1991.97/ 2090.45/ 2167/ 2239.06+	0/1.54/2085/ 4.2/5.75+	0/1.74/3.94/ 6.72/10.22+	0/0.42/1.1/ 1.66/2.26+	-
Roy et al. 2019	0/9.32/ 18.44/27.34/ 36+	F/N/NE/E/S E/S/SW/W/ NW	1877/1991/ 2090/2167/ 2239+	0/1.34/2.61/ 3.92/5.51+	0/1.74/3.94/ 6.79/10.28+	0/0.42/1.1/ 1.66/2.24+	-
Saha et al. 2005	-15/16/26/ 36/45+	F/N/NE/E/S E/S/SW/W/ NW	-	- 504/505/100 9/1513/ 2017/2521/ 3025+	-	-	-310/311/ 620+
Saito et al. 2009	-	-	-	-	-	-	-
Schulz et al. 2009	-	-	-	-	-	-	-
Shou and Chen 2021	-25/26/27/ 28/29/30+	-	Unstable/ 0/31/101/ 151/201/ Stable	-	-	-	-
Vahidnia et al. 2010	Continuous	Continuous	-	Continuous	-	Continuous	-

Study	Slope	Aspect	Precipi-tation	Faults	Road Proximity	River Proximity	River Density
Vakhshoori and Zare 2016	0/5/15/25/ 35/50+	F/N/NE/E/S E/S/SW/W/ NW	600/700/ 800/900/ 1000	0/200/400/ 600/1000+	0/250/600/ 750+	0/100/250/ 500+	-
Vojtekova and Vojtek 2020	0/2.1/5.1/ 15.1/35+	F/N/NE/E/S E/S/SW/W/ NW	-	-200/201/ 401/601/ 801+	-	-100/101/ 201/301/ 401+	-
Wayllace et al. 2019	-		-	-	-	-	-
Zhao et al. 2017	0/11/21/31/ 41/50+	F/N/NE/E/S E/S/SW/W/ NW	650/700/ 750/800/ 850/900/ 950/1000/ 1050+	-	-	0/201/401/ 600/1200+	-
Zhou et al. 2021	-	-	-	-	-	-	-
Zhu et al. 2014	-	-	-	-	-	-	-

The percentages were summed and normalized, as shown in Table 14, with missing values normalized to 0.

Table 13 Calculation of normalizing percentages

Criteria	Feizizadeh and Blaschke (2014)	Feizizadeh et al. (2014)	Kavzoglu et al. (2012)	Mallick et al. (2018)
Elevation	0.02	-	0.0265	-
Slope	0.141	0.177	0.29	0.261
Precipitation	0.172	0.062	-	0.178
River Proximity	0.112	0.13	-	-
River Density	-	0.101	0.0355	-
Lithology	0.21	0.15	0.3074	0.056
Lineament Proximity	0.124	0.092	-	0.128
Road Proximity	0.036	0.131	0.0181	0.103
Sum of Percentages	0.815	0.843	0.6775	0.726

ArcGIS Pro, however, requires that inputted percentages are entered as integers that sum up to 100%, and the sum of the percentages shown in the “Percentage” column second from the right in Table 15, which were rounded to two significant figures, did not equal 100% but rather 99%. To determine which criterion would receive the final 1%, the difference between the

percentages and the actual non-rounded results were calculated, and the criterion with the greatest negative difference received the additional 1%. These differences are shown in the "Difference" column to the far right in Table 15, and the criterion with the greatest negative difference was river density.

Table 14 Normalization of percentages with missing rounding percent

Criteria, Normalized	Feizizadeh and Blaschke (2014)	Feizizadeh et al. (2014)	Kavzoglu et al. (2012)	Mallick et al. (2018)	Averaged Percentage	Percentage	Difference
Elevation	0.024540	0.000000	0.039114	0.000000	0.015914	0.02	0.004086
Slope	0.173006	0.209964	0.428044	0.359504	0.292630	0.29	-0.002630
Precipitation	0.211043	0.073547	0.000000	0.245179	0.132442	0.13	-0.002442
River Proximity	0.137423	0.154211	0.000000	0.000000	0.072909	0.07	-0.002909
River Density	0.000000	0.119810	0.052399	0.000000	0.043052	0.04	-0.003052
Lithology	0.257669	0.177936	0.453727	0.077135	0.241617	0.24	-0.001617
Lineament Proximity	0.152147	0.109134	0.000000	0.176309	0.109397	0.11	0.000603
Road Proximity	0.044172	0.155397	0.026716	0.141873	0.092040	0.09	-0.002040
Sum of Percentages	1.000000	1.000000	1.000000	1.000000	1.000000	0.99	-0.010000

Once the additional 1% was added to river density, the total summed percentage resulted in 100%. Table 16 shows the finalized percentages given for each criterion.

Table 15 Missing percent added to variable with maximum negative difference

Criteria, Finalized	Percentage
Elevation	0.02
Slope	0.29
Precipitation	0.13
River Proximity	0.07
River Density	0.05
Lithology	0.24
Lineament Proximity	0.11
Road Proximity	0.09
Sum of Percentages	1.00

The finalized percentage results are shown in Table 17 along with the reclassified rankings for each criterion.

Table 16 Finalized reclassification ranks and percentages of criteria for weighted overlay

Criteria	Rank	Category	Percentage
Elevation (meters)	5	<3500	0.02
	4	3000	
	3	2500	
	2	2000	
	1	1500	
Slope (degrees)	5	20-30	0.29
	5	30-40	
	3	10-20	
	3	40-50	
	2	0-10	
	2	50-60	
	1	60-70	
	1	<70	
Precipitation (inches)	5	>50	0.13
	4	50	
	3	37.5	
	2	25	
	1	12.5	
River Proximity (meters)	5	3750	0.07
	4	7500	
	3	11250	
	2	15000	
	1	>150000	
River Density (length/unit area)	5	>4	0.05
	4	4	
	3	3	
	2	2	
	1	1	

Criteria	Rank	Category	Percentage
Lithology	5	Unconsolidated, undifferentiated	0.24
	4	Sedimentary, carbonate	
	3	Igneous, volcanic	
	3	Sedimentary, undifferentiated	
	2	Igneous and Sedimentary, undifferentiated	
	2	Metamorphic and Sedimentary, undifferentiated	
	1	Igneous, intrusive	
	1	Metamorphic, gneiss	
	1	Metamorphic, undifferentiated	
	1	Sedimentary, clastic	
	N/A	Water	
Lineament Proximity (meters)	5	6250	0.11
	4	12500	
	3	18750	
	2	25000	
	1	>25000	
Road Proximity (meters)	5	5000	0.09
	4	10000	
	3	15000	
	2	20000	
	1	>20000	

Reclassifying slope required knowledge of how frequently landslides occur at certain slope gradients. To that end, Patil et al. (2019) calculated what percentage of landslides occur within specific ranges, and the ranking scheme used correlates to frequency. Table 18 explains how ranks were calculated, and Table 1 shows the slope gradient ranges with frequency percentages and the corresponding ranks.

Table 17 Ranking for slope derived from frequency

Rank	Frequency (percent)
1	<1%
2	1%-10%
3	10%-20%
4	20%-30%
5	>30%

Table 18 Slope categorization by frequency

Slope (degrees)	Frequency (percent)	Rank
0°-10°	7.000%	2
10°-20°	15.000%	3
20°-30°	30.000%	5
30°-40°	31.000%	5
40°-50°	14.000%	3
50°-60°	3.000%	2
60°-70°	0.200%	1
<70°	0.001%	1

3.5. Fuzzy Overlay

Fuzzy overlay is different from weighted overlay in that fuzzy memberships are used in place of rankings. Different fuzzy memberships are used according to what aspect of a criterion is emphasized, and these are then put into a fuzzy function to yield a result. Depending on the type of function used, results again vary depending on what aspect of the results is to be highlighted.

3.5.1. Fuzzy Membership Layers

In addition to the criteria used in this project being reclassified and therefore used in a weighted overlay, the same criteria were also used in a fuzzy overlay. The criteria were processed with the *Fuzzy Membership* tool in order to prioritize certain aspects of each one. Different membership types were used for different criteria, based on what features ranked more important than others. The *Fuzzy Membership* tool transformed the data into a 0 to 1 scale based on what aspect of the criterion is considered more or less important, with 1 being most important and 0 being least important. The fuzzy membership type for each criterion is listed in Table 20.

Table 19 Fuzzy membership for each criterion

Category	Criteria	Fuzzy Membership
Topography	Elevation	fuzzy large
	Slope	fuzzy Gaussian
Hydrology	Precipitation	fuzzy large
	Drainage Proximity	fuzzy small
	Drainage Density	fuzzy large
Subsurface	Lithology	fuzzy large using reclassified data
	Lineament Proximity	fuzzy small
Surface	Road Proximity	fuzzy small

The equation for the fuzzy *Gaussian* operator was written out by Kritikos and Davies (2014) as:

$$\mu(x) = e^{-f1(x-f2)^2} \qquad (20)$$

where $\mu(x)$ is the membership value of category x, which is the observed variable value or crisp value, $f1$ is the standard deviation or spread, and $f2$ is the midpoint. The spread has a range from 0 to 1. All things being equal, the larger the $f1$ value, the narrower the spread, while the smaller the $f1$ value, the wider the spread, as seen in Figure 23.

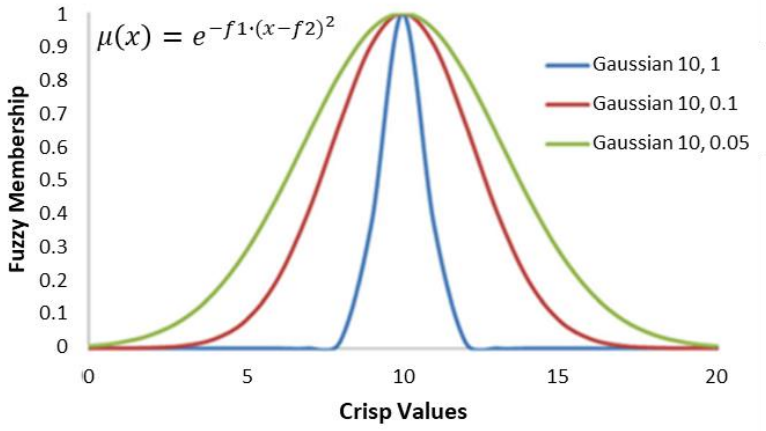

Figure 22 Visual of how fuzzy Gaussian transforms original data into a normal distribution with different spread values (Kritikos and Davies 2014)

3.5.1.1. Fuzzy large elevation

Fuzzy large was chosen as the fuzzy membership for elevation. Fuzzy large emphasizes larger values more heavily than smaller values, which would be equivalent to the reclassification scheme used in the weighted overlay (Figure 24).

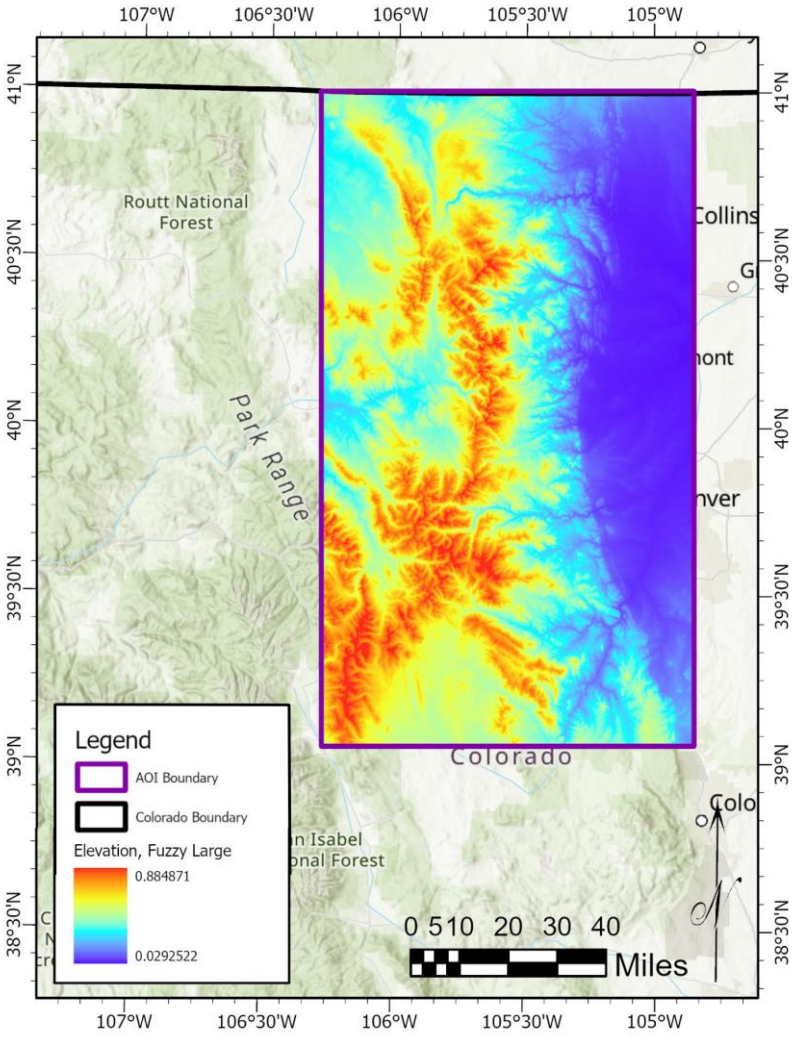

Figure 23 Fuzzy large elevation

3.5.1.2. Fuzzy Gaussian slope

Using the *Fuzzy Membership* tool on slope took some trial and error to ensure that the range of slope gradients were properly weighted. As mentioned before in 3.4.2, Patil et al. (2019) lists the frequency in which landslides occurred for given slope gradient ranges. Using their

landslide frequency statistics, the midpoint for the fuzzy Gaussian operator was 30, given that Patil et al. (2019) highest landslide frequency percentages ranged from 20° – 40°. A spread of 0.1 – the default – was used (Figure 25).

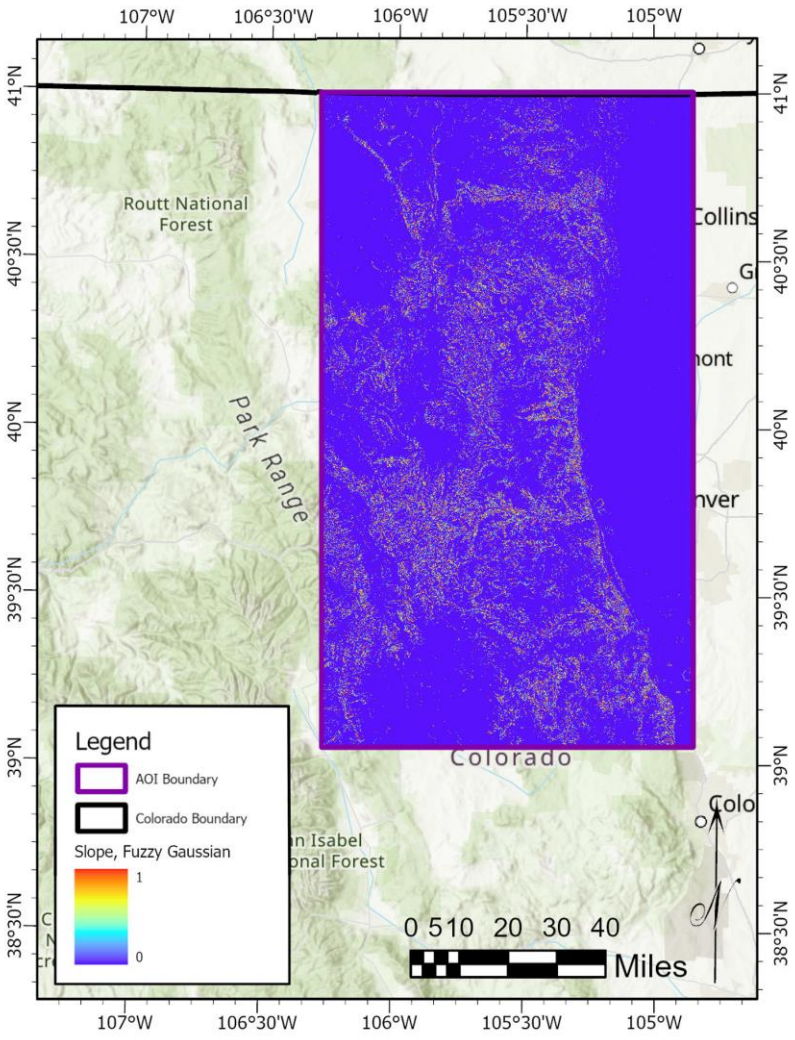

Figure 24 Fuzzy Gaussian slope

3.5.1.3. Fuzzy large precipitation

The precipitation raster generated for the *Weighted Overlay* tool was also required for the *Fuzzy Membership* tool. The fuzzy large operator was used to place emphasis on areas with higher average rainfall (Figure 26).

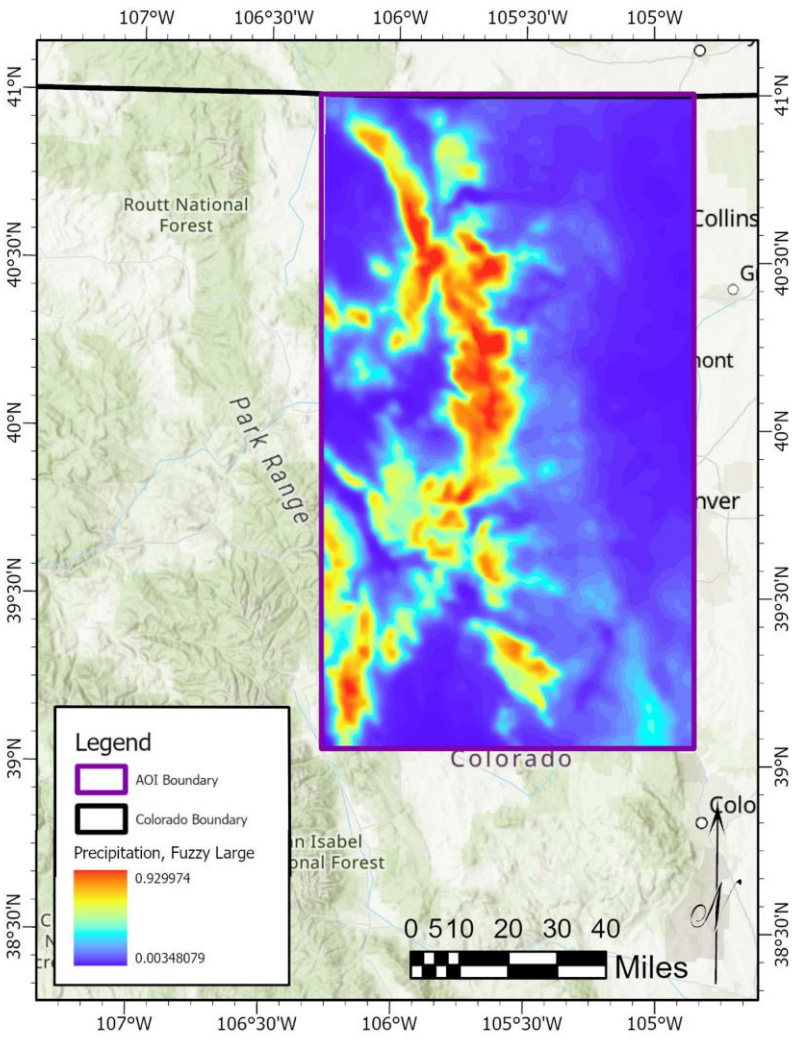

Figure 25 Fuzzy large precipitation

3.5.1.4. Fuzzy small drainage proximity

Drainage proximity utilized the fuzzy small operator (Figure 27). In this way, the *Fuzzy Membership* tool output would resemble that used for the weighted overlay in that the closer an area is to a drainage channel, the higher the landslide susceptibility.

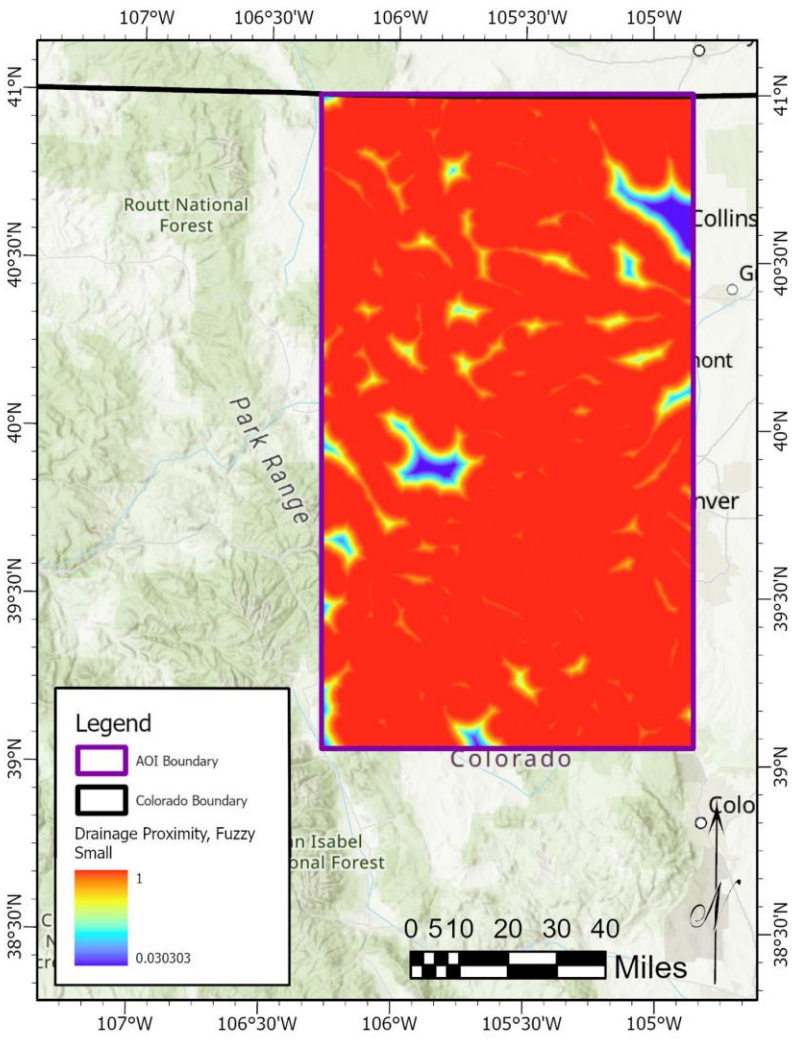

Figure 26 Fuzzy small drainage proximity

3.5.1.5. Fuzzy large drainage density

The output from using the *Line Density* tool to calculate drainage density resulted in a raster that had large data gaps where there were no rivers or streams. Because the *Fuzzy Membership* tool cannot run on a raster with data gaps, the *Reclassification* tool was used to convert areas with no data into areas with a data value of 0. The resultant raster was reclassified and then used to generate a fuzzy membership output using the fuzzy large operator (Figure 28).

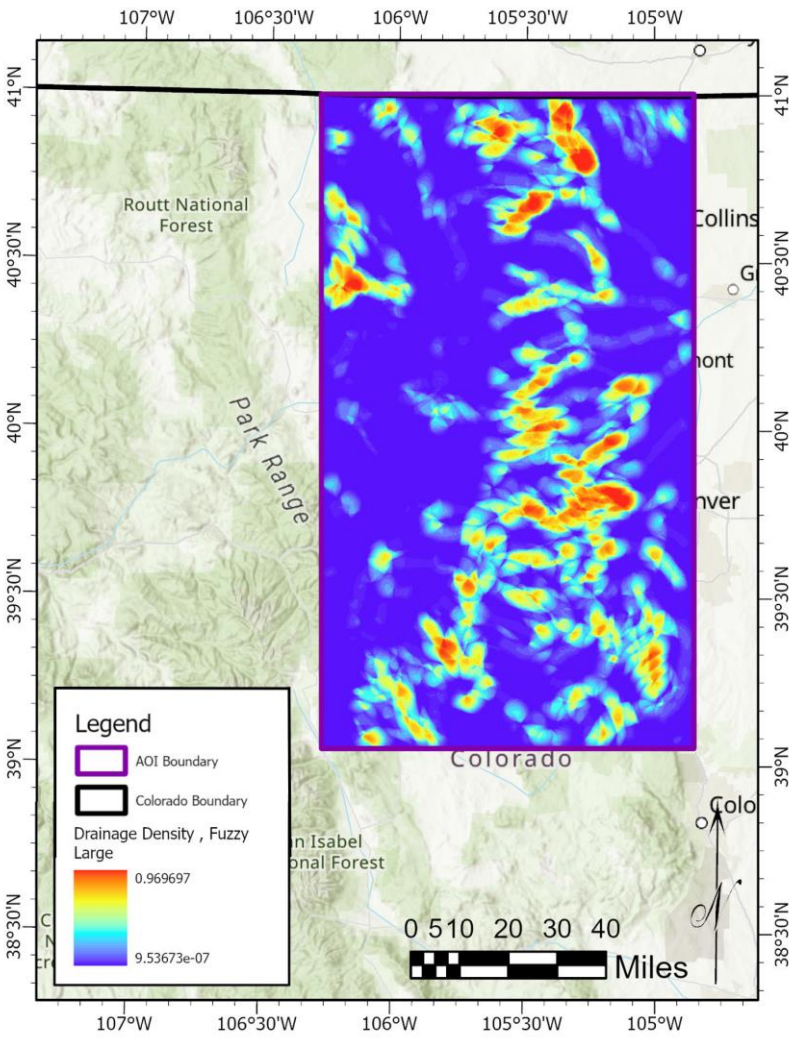

Figure 27 Fuzzy large drainage density

3.5.1.6. Fuzzy large lithology

The lithology raster used in the weighted overlay was also required for the *Fuzzy Membership* tool. Lithology also required preparation, though this was in the form of first determining which types of lithology weathered and eroded easiest. This data came from Ott (2020), and the different lithology types were reclassified using the same ranking method mentioned in 3.5.1 (Figure 29).

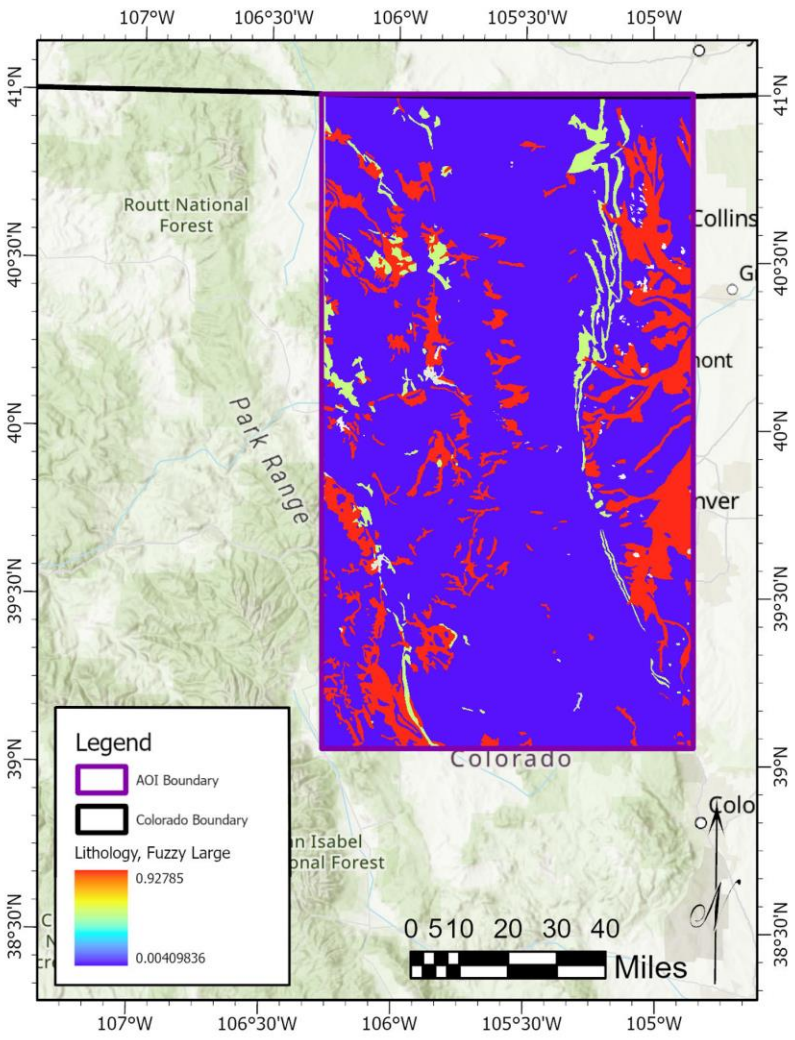

Figure 28 Fuzzy large lithology

3.5.1.7. Fuzzy small lineaments

The fuzzy small operator was used for lineament proximity (Figure 30). This follows the same rationale as the ranking used in the weighted overlay with a closer proximity indicating a higher risk of landslide activity (Chen and Li 2020; Nohani et al. 2019; Patil et al. 2019; Saha et al. 2005; Vakhshoori and Zare 2016).

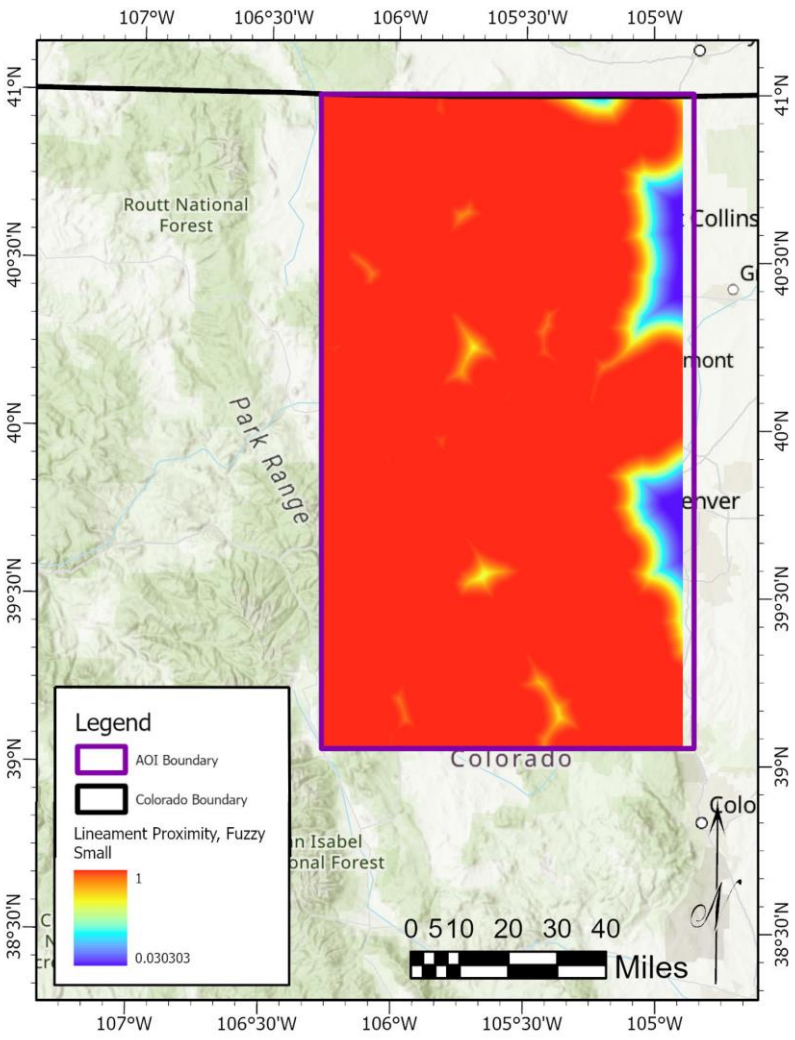

Figure 29 Fuzzy small lineament proximity

3.5.1.8. Fuzzy small road proximity

Road proximity also utilized the fuzzy small operator (Figure 31). The choice of fuzzy small for the fuzzy operator followed the same logic as the ranking in the weighted overlay of closer proximity to roads means increased landslide susceptibility (Erener et al. 2016; Patil et al. 2019; Vakhshoori and Zare 2016).

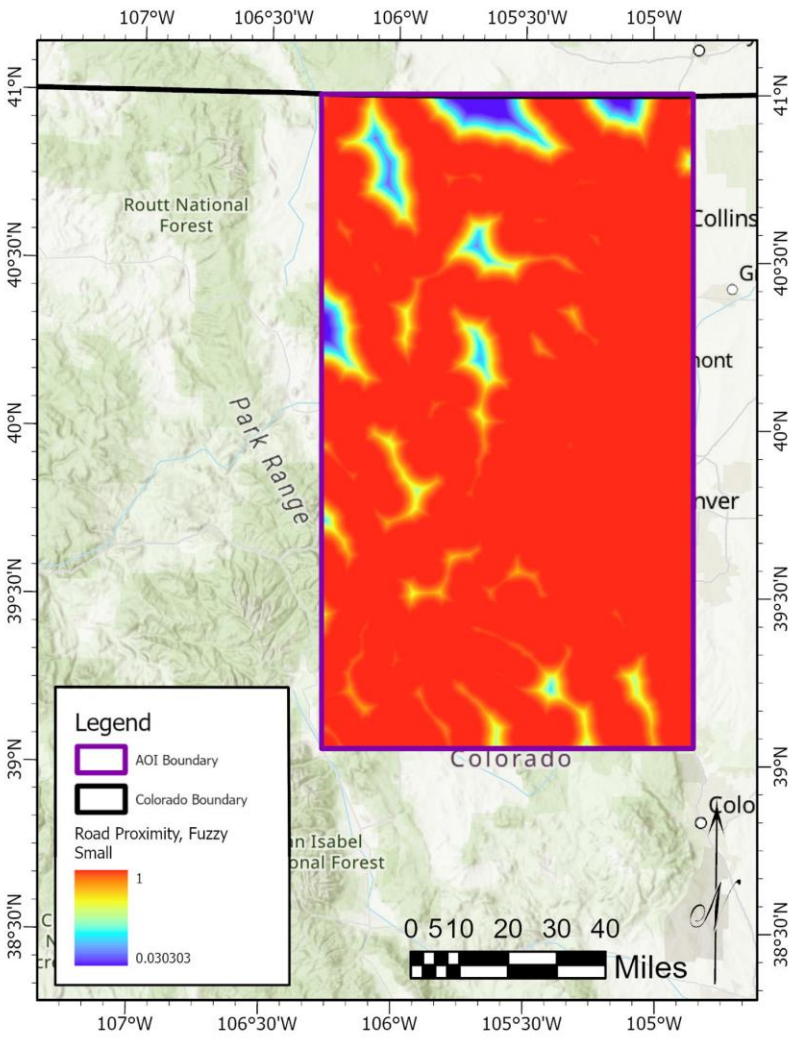

Figure 30 Fuzzy small road proximity

3.5.2. Selection of Fuzzy Overlay Method

The *Fuzzy Overlay* tool offers five different fuzzy overlay operators: *And*, *Or*, *Sum*, *Product*, and *Gamma*. The fuzzy membership-converted rasters (listed in Table 20) were used, and the fuzzy *Gamma* operator was selected after examining each preliminary result using the five operators on the default settings in ArcGIS Pro. The fuzzy *Gamma* function works by multiplying the fuzzy Algebraic *Sum* with the fuzzy Algebraic *Product*, of which both are raised to the power of γ. Vakhshoori and Zare (2016) explain how fuzzy *Gamma* is derived:

$$\mu_s(x) = 1 - \prod_{i=1}^{n} \mu_i\,(x) \quad (21)$$

$$\mu_p(x) = \prod_{i=1}^{n} \mu_i\,(x) \quad (22)$$

$$\mu_\gamma(x) = [\mu_s(x)]^\gamma \times\ [\mu_p(x)]^{1-\gamma} \quad (23)$$

where $\mu_s(x)$ is fuzzy Algebraic *Sum*, $\mu_p(x)$ fuzzy Algebraic *Product*, μ_γ fuzzy *Gamma*, γ a parameter in the range of 0 to 1, *n* the number of criteria being used, and $\mu_i(x)$ the map with a fuzzy membership function. The closer the output is to 1 the more susceptible an area is to having a landslide occur.

Changing γ values changes the results. A γ equal to 1 produces results that are identical to the results of fuzzy Algebraic *Sum*, while a γ equal to 0 yields results equal to the results of fuzzy Algebraic *Product*. Various values for γ were tested to determine what would be most appropriate for the final fuzzy *Gamma* γ value.

Fuzzy *Gamma* was chosen as the representative fuzzy overlay output for several reasons. Fuzzy *And* were not chosen because the data was not supposed to be completely exclusive by requiring all of the criteria to be present. Fuzzy *Or*, on the other hand, was too inclusive and skewed the results by overemphasizing areas with low landslide feasibility. Fuzzy *Sum*, similar to Fuzzy *Or*, overemphasized areas with multiple lower-weighted criteria. Fuzzy *Product* was similar to Fuzzy *And* but to a much more exclusive degree.

With fuzzy *Gamma*, the choice of a γ value of 0.9 was selected because it represented a reasonable balance between the endmember fuzzy *Sum* and fuzzy *Product*. A γ value of 0.5, despite being an even balance between fuzzy *Sum* and fuzzy *Product*, forced the output to lean more heavily towards the fuzzy *Product* side. The 0.9 γ value output adequately highlighted

areas of higher susceptibility while neither overemphasizing nor underemphasizing areas of lower landslide susceptibility.

Chapter 4 Results

Weighted and fuzzy overlays were used to generate the final results for this project. The weighted overlay used criteria reclassified to an equal scale, and ranks for each criterion were calculated based on the utilization frequency in other studies to determine the criterion's importance in landslide susceptibility. The fuzzy overlay ultimately used the fuzzy *Gamma* operator on fuzzy membership criteria rasters and a chosen γ value to determine landslide susceptibility.

Weighting plays a key role in both the weighted overlay and the fuzzy overlay, though more so in the former than the latter. How ranks are determined is dependent on the availability of data, the quality of the data, and how relevant a data is to the project in question. Due to the fact that landslides tend to occur in areas with changes in elevation, most authors consider slope to be of high importance with regards to assessing landslide susceptibility, and this decision is reflected in how the slope criterion was weighted for this project for the weighted overlay. It is therefore unsurprising the amount of influence it had on the weighted overlay result. As for the fuzzy overlay result, all of the criteria were given equal weight given that the *Fuzzy Overlay* tool only allows the user to add the necessary rasters and choose the desired fuzzy operator.

The results for the weighted overlay and fuzzy overlay were both expected and unexpected in that the regions of higher predicted landslide activity for the most part overlap each other. The unexpected aspects of the results were the differences in how areas with lower landslide potential was weighted as well as how bias influences results, particularly in the weighted overlay result.

4.1. Weighted Overlay Result

The weighted overlay result (Figure 32) reveals how the rankings interacted to highlight areas of higher landslide susceptibility. The scale for the overlay result was set from 1 to 5 to match the reclassification scheme, with 5 indicating high landslide susceptibility and 1 indicating low susceptibility. The color bar ranges from 2 to 5, suggesting that with the weighting of the criteria used in this project, the entirety of the area of interest is susceptible to some degree of landslide activity.

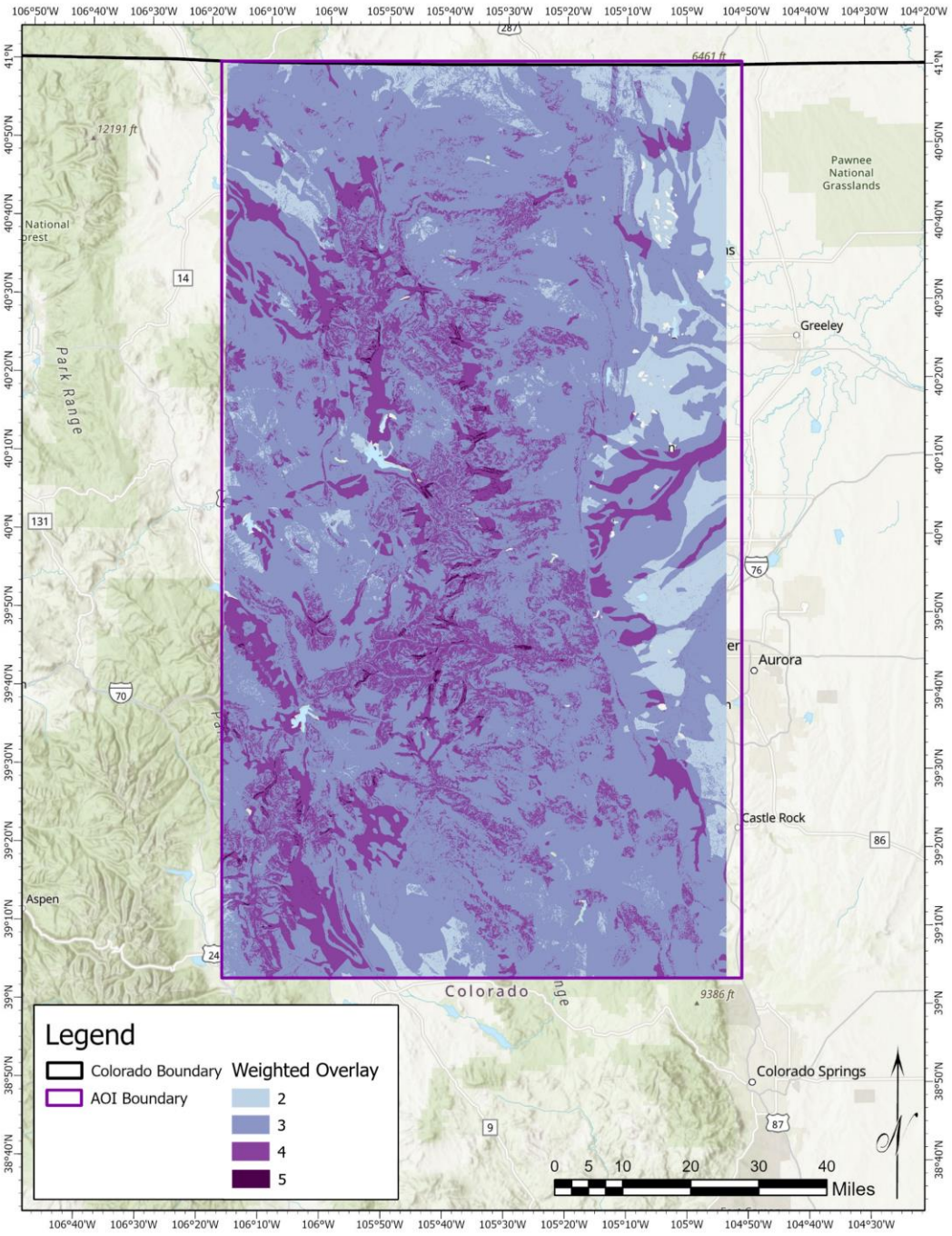

Figure 31 Weighted overlay result

A comparison of the weighted overlay result with the USGS landslide inventory (Figure 33) reveals that the results from the weighted overlay do not entirely correlate with the landslide inventory. Much of the high confidence locations in the inventory fall within areas calculated to

have medium landslide susceptibility according to the weighted overlay results. The weighted overlay result correlated much better with locations flagged by the USGS as having possible or probable landslides in the area.

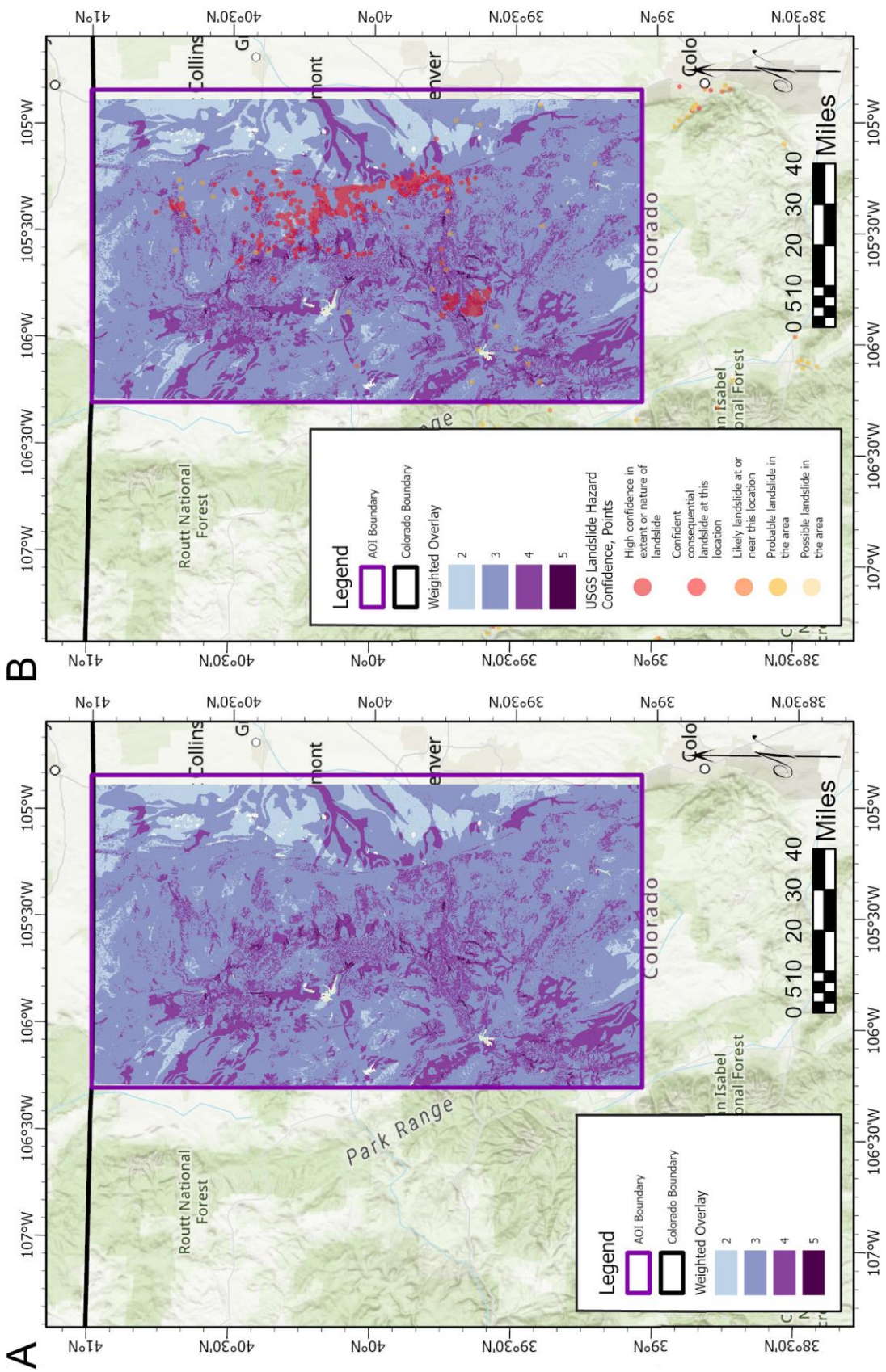

Figure 33 Comparison of (A) the weighted overlay result with (B) the USGS's landslide inventory locations superimposed

Both slope (29%) and lithology (24%), as the two most heavily weighted criteria, greatly affected the output. The mountainous areas to the west have the highest landslide susceptibility outputs, where the slope gradients are highest, with susceptibility decreased to the east until the area relatively flattens out where central Denver is located. Likewise, the fluvial deposits east of where central Denver is situated had higher susceptibility scores due to the fact that those rivers and streams are actively depositing unconsolidated sediment eroded from the Front Range.

Precipitation (13%) certainly caused an increase in landslide susceptibility, where higher amounts of rainwater are more likely to turn dry soil into slippery mud. Lineament proximity (11%), with the majority of known mapped lineaments located within the Front Range proper, primarily boost landslide susceptibility in areas that statistically have higher elevation and steeper slope gradients when compared to the relatively lower elevation and flatter area that central Denver covers. Road and river proximity (9% and 7%, respectively) both cover much of the area of interest, while river density (5%) highlights confluence areas and areas with a higher density of rivers and streams. Elevation (2%) plays a role in landslide susceptibility in that generally speaking, the higher the elevation, the more likely a landslide may occur.

Of note are the higher-ranked areas that more susceptible areas scattered around the Front Range peaks. With regards to slope, higher landslide susceptibility appears to be closely associated with slopes that range from 20° to 50° (Figure 34). This agrees with Patil et al. (2020)'s study, which indicated that slope gradients between 20° to 40° tend to have the highest landslide frequencies.

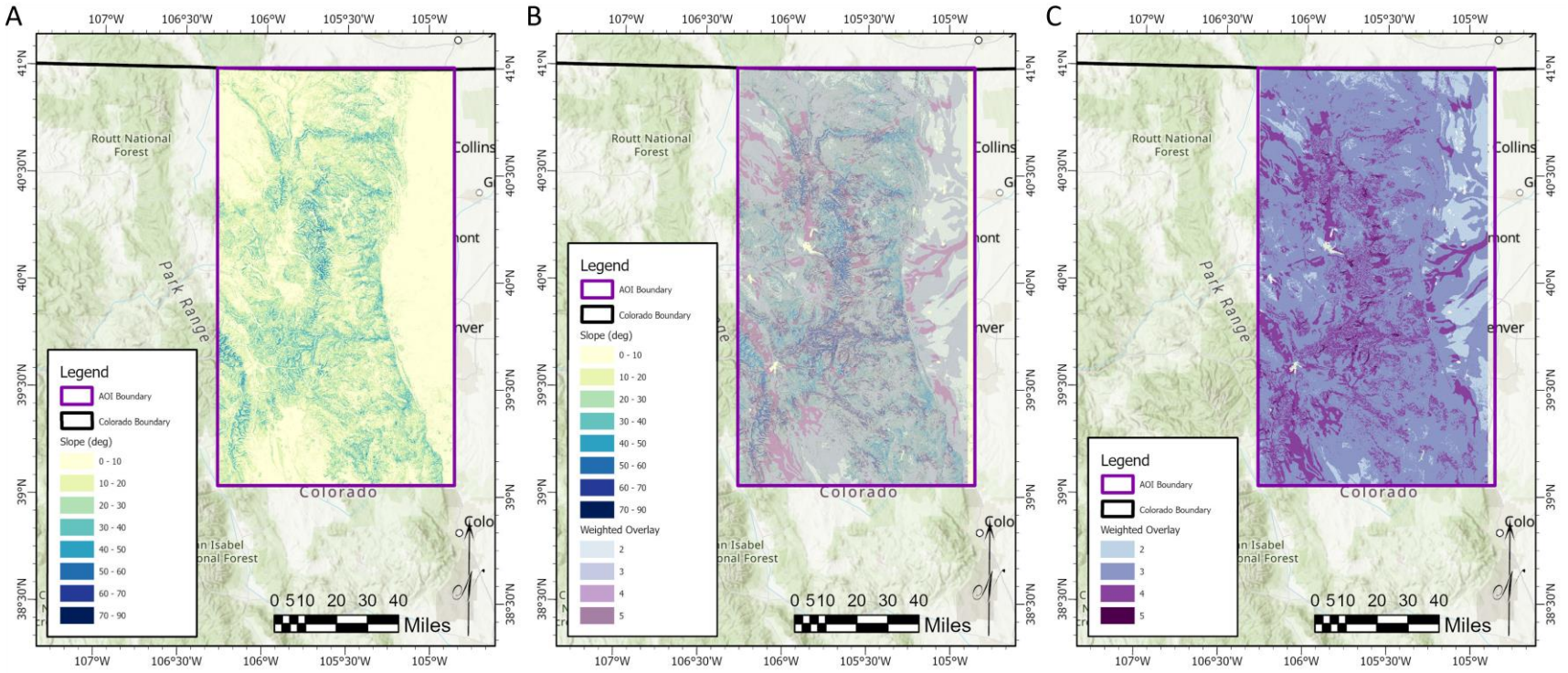

Figure 34 Slope and weighted overlay comparison: (A) slope; (B) slope with weighted overlay result semitransparent and superimposed; (C) weighted overlay result

The weighted overlay result from the slope criterion's weight was expected; the result from the lithology criterion's weight was more of a surprise given how much weight the unconsolidated sediment of the fluvial flood plains in the Denver metroplex added to the result with one river in particular – the St. Vrain River (Figure 35). The expectation was that the flood plains would not rank so highly, given that the area lies within the urbanized corridor that consists of Denver, Boulder, and Fort Collins. Unconsolidated sediment on the slopes of the Front Range – deposited in the incised valleys due to the drainage systems mentioned earlier – also increased the ranking of landslide frequency. Cross inspection of the weighted overlay result to elevation, precipitation, drainage systems, lineaments, and roads yielded no easily visible correlations.

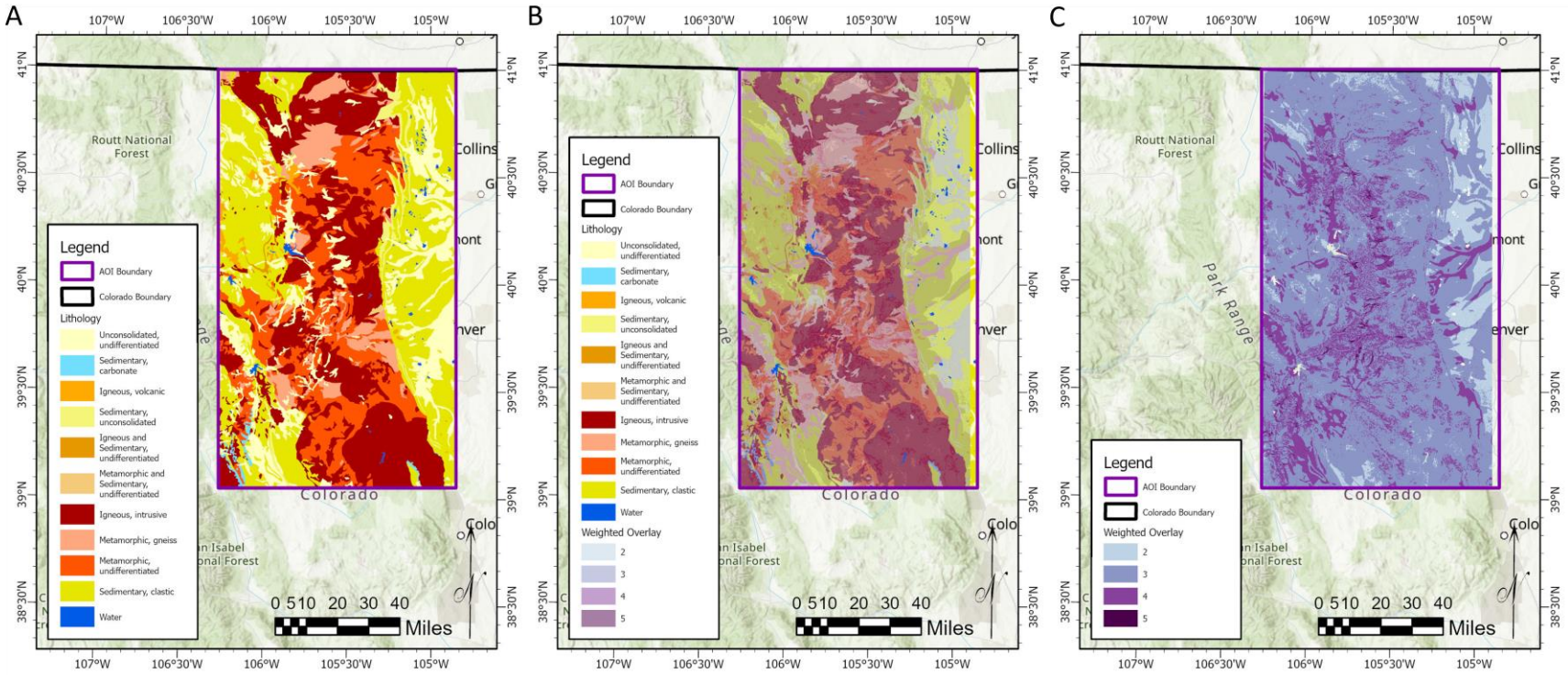

Figure 35 Lithology and weighted overlay comparison: (A) lithology; (B) lithology with weighted overlay result semitransparent and superimposed; (C) weighted overlay result

4.2. Fuzzy Overlay Result

The fuzzy overlay result (Figure 36) yielded a very different output. The γ value chosen that best displays the results of the fuzzy overlay is 0.9. The scale used for fuzzy overlay covers a range from 0 to 1, with 0 indicating very low landslide susceptibility and 1 indicating very high landslide susceptibility. Unlike the weighted overlay result, the fuzzy overlay result displays a large majority of the AOI as not particularly susceptible to landslide activity. The fact that the much larger swaths of land have a susceptibility rating closer to 0 is indicative of the fact that the fuzzy overlay's weighting result is much stricter in terms of which areas are considered more susceptible to landslides than others.

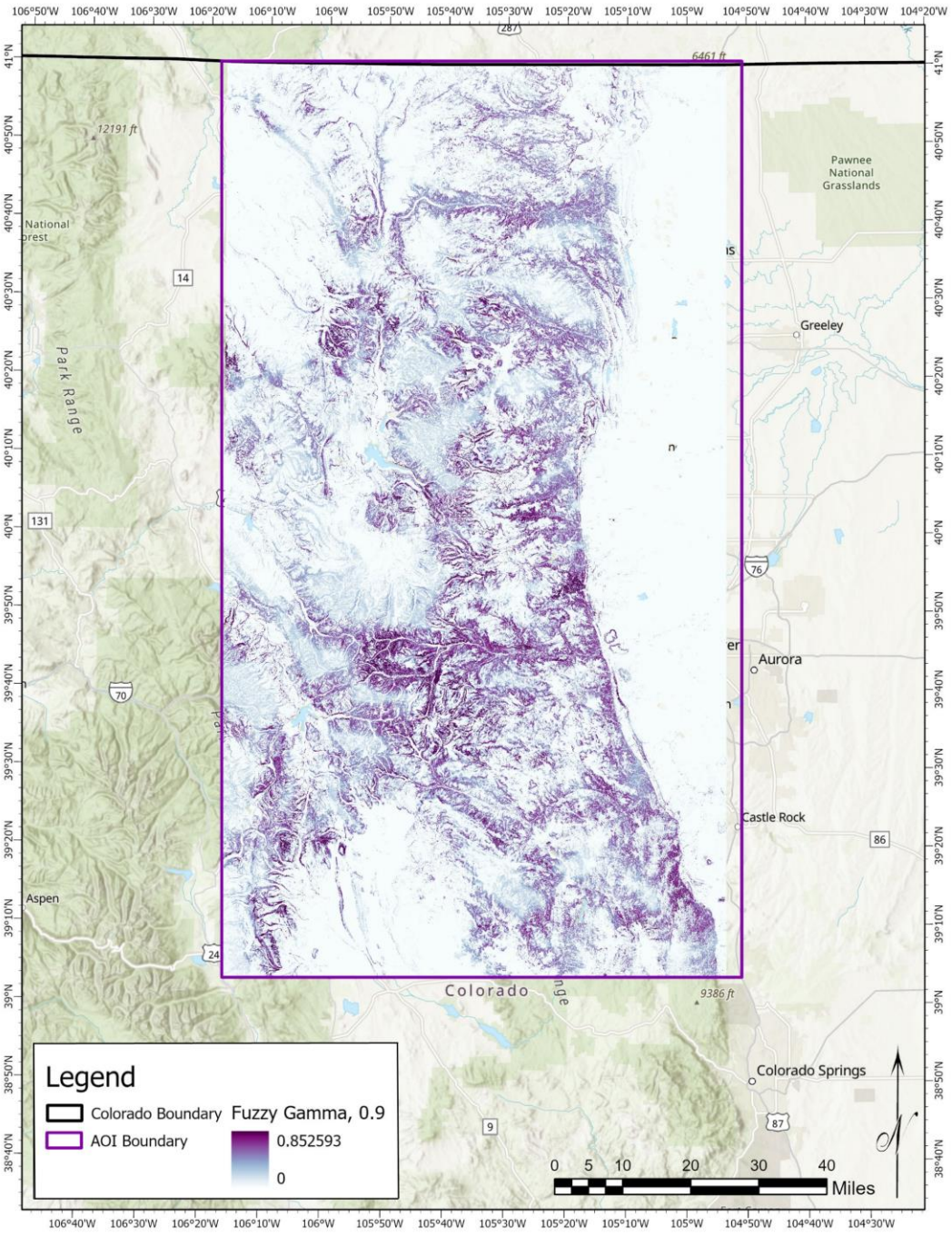

Figure 32 Fuzzy overlay result using the fuzzy *Gamma* operator with a γ value of 0.9

The comparison between the fuzzy overlay result and the USGS's landslide inventory displays greater commonality with regards to predicted landslide hazard locations (Figure 37). Areas marked as high confidence overlap with regions the fuzzy overlay result considered to have higher landslide susceptibility. To a lesser degree, areas noted as probable or possible with

regards to landslide occurrence overlap with lower landslide susceptibility in the fuzzy overlay result. This is indicative of the fact that the weighting generated through the various fuzzy membership operators seems to coincide with the predictions of external sources.

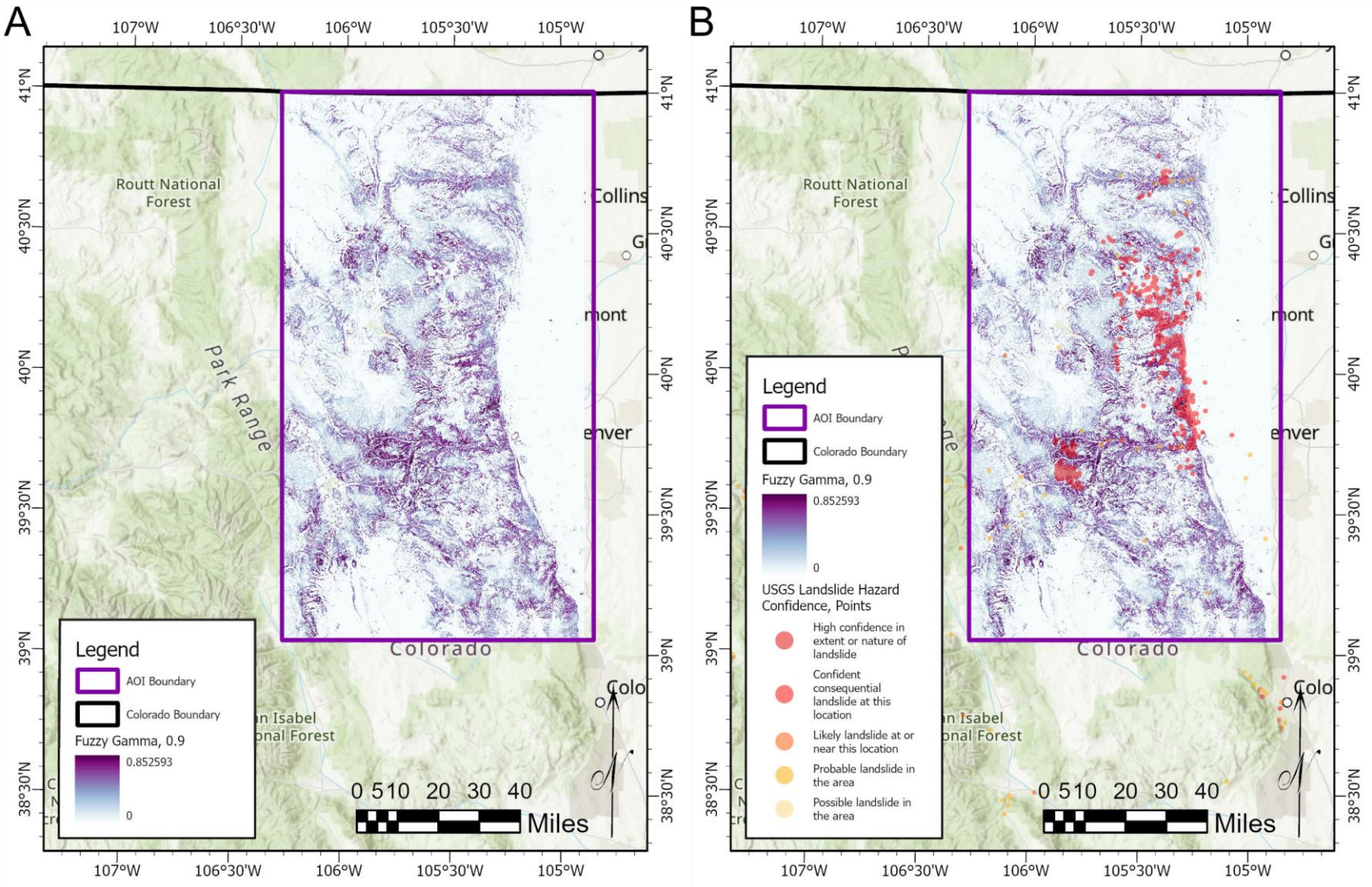

Figure 37 Comparison of (A) the fuzzy overlay result with (B) the USGS's landslide inventory locations superimposed

Two criteria in particular seem to have a higher correlation to increased landslide susceptibility than the rest: slope and drainage systems. Landslide susceptibility tends to be higher in areas with more ideal slope gradients (20°-40°), and a side-by-side comparison is displayed in Figure 38.

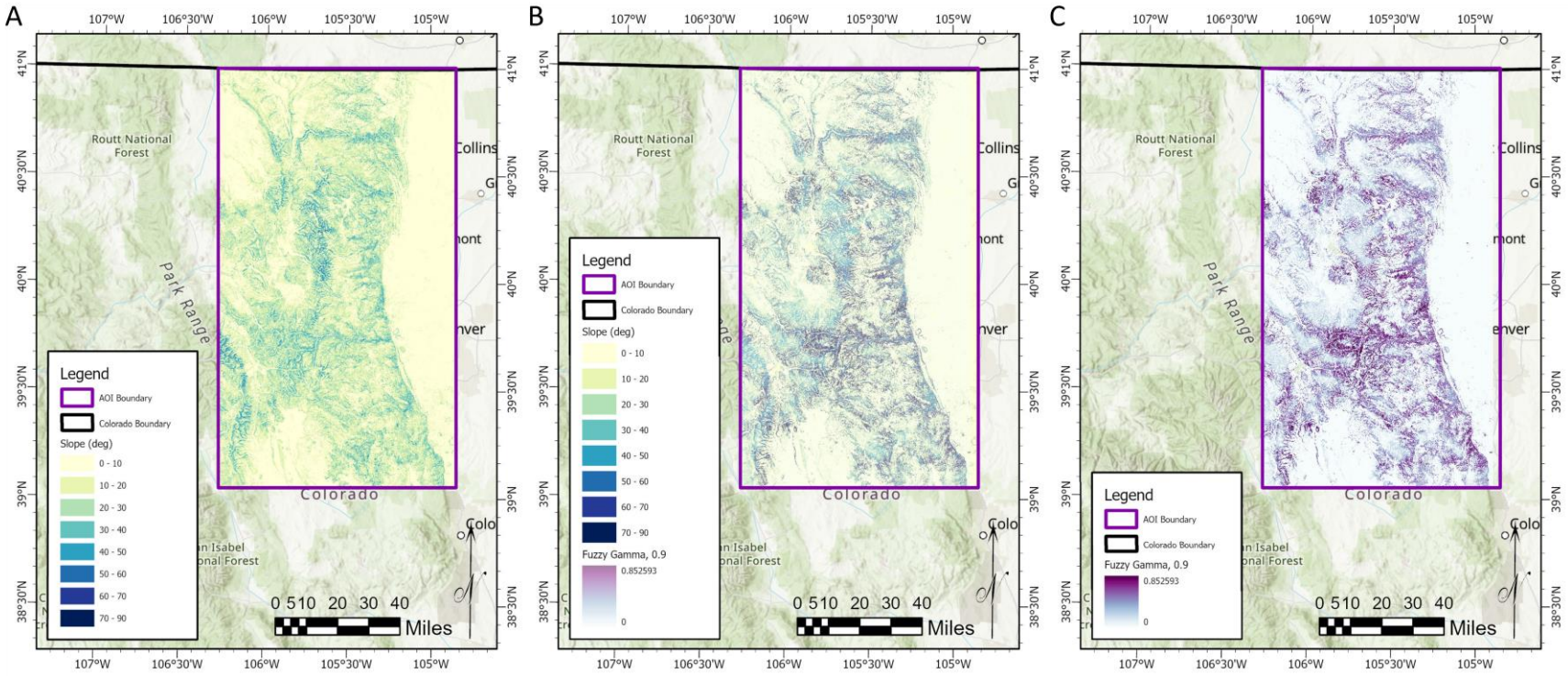

Figure 38 Slope and fuzzy overlay comparison: (A) slope; (B) slope with fuzzy overlay result superimposed; (C) fuzzy overlay result

That localized areas of particularly high landslide susceptibility also tend to coincide with incised valleys from said drainage systems is likely due to increased erosion that comes with closer proximity to drainage systems (Figure 39). The other criteria do not seem to have as much of an impact on the result than the aforementioned two.

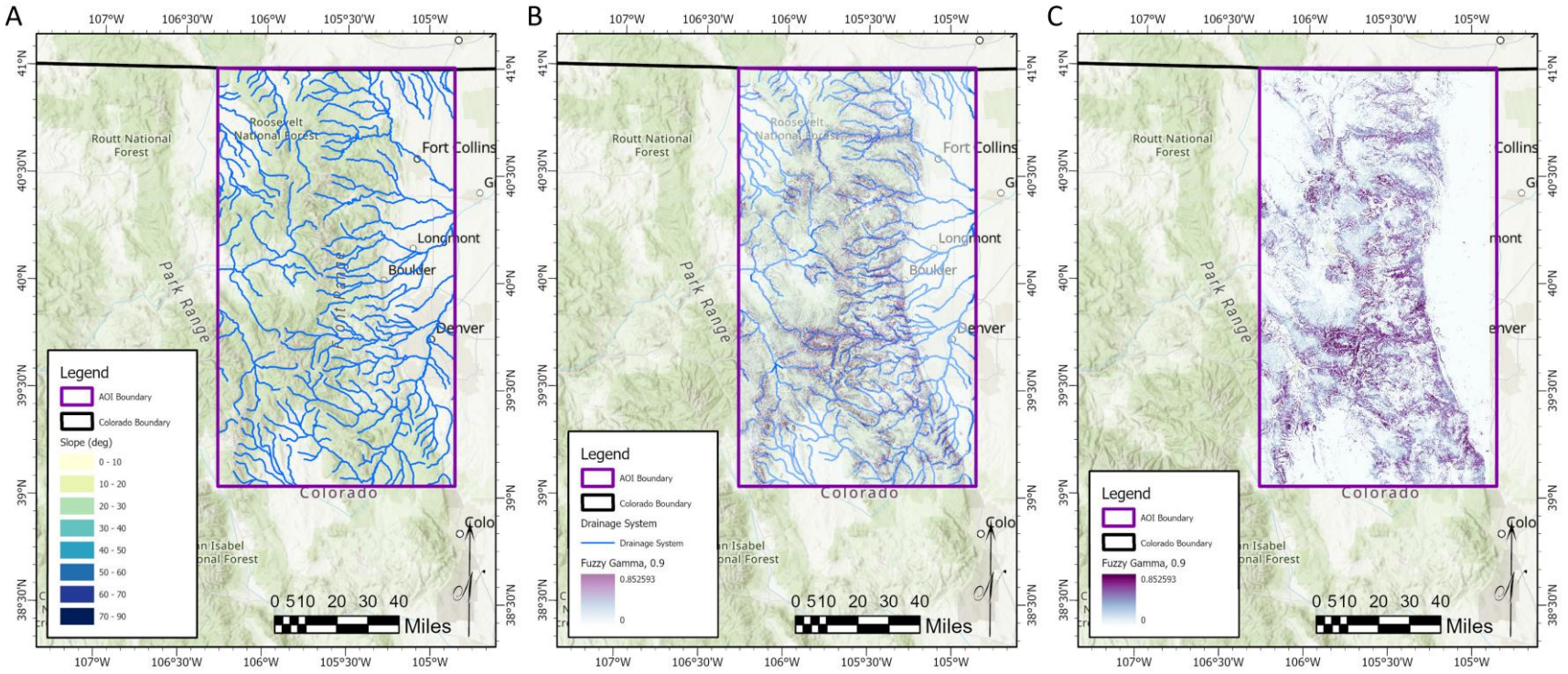

Figure 39 Drainage systems and fuzzy overlay comparison: (A) drainage systems; (B) drainage systems with fuzzy overlay result semitransparent and superimposed; (C) fuzzy overlay result

Chapter 5 Discussion and Conclusion

This project looked at two out of many different MCDA weighting schemes for landslide susceptibility mapping: weighted overlay and fuzzy overlay. These two methods were selected because there exists little in the way of direct comparisons between the two in literature with regards to landslide susceptibility. The ability for the software used to be able to handle such analyses had to also be taken into consideration. The various criteria used for this project was selected based on data availability and resolution, as well as what authors deemed important enough to include in their own studies.

Bias and limitations play a significant role in how they affect the results as they may emphasize certain criteria more than others. The fact that both rankings and fuzzy memberships may be chosen differently depending on the user means that the results, even if using the same data and same methodology, yields different outputs. This in turn affects how people's understanding of the data is perceived, which also influences how and where people may live and what kinds of laws might be put in place to protect them.

5.1. Bias and Limitations

The results of the weighted overlay and the fuzzy overlay had both similarities and differences that were visually distinct, though these distinctions were partially a result of the inclusion and weighting of specific criterion. The results revealed that the selection of the method of weighting as well as how variables are weighted play important roles in result expectations. This, in turn, hints at a cyclical influence between how weighting biases affect results, and how results can generate biases that affect the decision-making process with regards to landslide susceptibility mapping.

As noted in Chapter 2, there are a wide variety of variables that were used in landslide susceptibility studies. Because of the number of criteria collectively used, it is not possible for any given study to include all of them, and it is also likely that this project did not cover the full range of criteria used in landslide susceptibility studies. It is impractical for any study to include every possible variable used in landslide susceptibility mapping – depending on the size of the AOI, the amount of data required could be astronomically high.

Data such as elevation is readily accessible across the globe, and in varying resolutions. The suitability of a given resolution is dependent on the size of the AOI and the scale of the subject(s) of analysis. DEMs may be generated from satellite imagery, topographic maps, and LiDAR – though the former two are more likely to be "bare-earth" models while the latter probably includes surficial features such as buildings and trees (USGS, n.d.). From this, derivative variables such as slope and aspect may be generated in resolutions equal to the original DEM. Within Esri ArcGIS Pro's *Spatial Analyst* toolbox are fourteen tools specifically made to generate some derivative layer of elevation in the *Surface* toolset, not including a tool to manually add supplementary information to a surface layer. On the other hand, other variable data such as desiccation height and undesiccation height, water condition, landslide-rainfall index are specific to individual studies in which the study author(s) likely generated the data themselves. Such data on a wider scale would not be available as it does not exist outside of the AOIs of the studies in question.

In addition to variable resolutions, sourcing data is also a necessary consideration. With regards to the data, it can be either readily available to the public or proprietary, in which a user would need to purchase access to said data. Data from certain national organizations, such as the USGS, USDA, and NOAA, as well as national, state, and local governments, and universities

usually offer some data for public consumption. The data that is available may or may not be cover the study area in question, and it may also not be of viable quality depending on the project scope. The format of the data also had to be taken into consideration, as data incompatible with the software being utilized is not useful to the study. In the event that a data format could be converted without a loss in quality, such measures are likely to be taken in order to include that criterion in a study.

The eight criteria used in this project were chosen from a combination of factors. The landslide inventory from the USGS was used to search for locations within the US that had high landslide incidences. Once the location was chosen, searching for data that would be suitable for the AOI began, and the criteria listed in Chapter 2 were searched for. Of all the criteria listed in Chapter 2, the key data to any landslide susceptibility study was elevation – without elevation, derivatives such as slope would not exist. Apart from one study out of the thirty-four examined in this project, elevation was included as a criterion for their analysis. The second key criterion was aspect, of which thirty-one studies included as part of their dataset, followed by slope at twenty-nine studies.

Aspect was not included in this project because of a lack of information regarding which cardinal directions landslides were more likely to occur on. LULC data was found within the AOI, but the extent did not cover the whole of the area in question and ultimately had to be discarded. Soil composition, water saturation, and porosity were downloaded in unusable formats that could not be converted and were similarly deemed unnecessary. Census tract data were readily available but a method of distilling census data into spatially representative population density data was beyond the scope of this project, and therefore census tract data was abandoned.

Choosing rankings for the weighted overlay, and fuzzy memberships and γ values for the fuzzy overlay ingrain a subjective bias in the results. This is due to the fact that, depending on what criteria the user or decision maker deems more important than others, some variables may be weighted more heavily in the weighted overlay. The fact that no means of objectively weighting variables exists only emphasizes the fact that bias is an implicit part of the results of any analysis that uses a weighting system. The same bias comes into play when fuzzy memberships are chosen for the individual criterion, as well as which fuzzy overlay operator is used. Subjectivity is therefore introduced by the selection of fuzzy membership by tweaking its parameters, and the choice of fuzzy overlay operator is also dependent on what sort of outcome the endmember user is expecting.

With regards to this project, there exist limitations that needed to be acknowledged from the onset. Software choice is somewhat dictated by the analysis methodology to be used and vice versa – if the software cannot support the desired methodology, then either a different methodology must be chosen or created, or a change in software is required so that one capable of handling the desired methodology is selected. There is also the possibility that the number of variables must also be constrained to a quantity that the chosen analysis software can handle. Having too many variables would inevitably cause the processing time to slow dramatically. The same can be said of data size – datasets that are too large processes much slower than smaller datasets, and this could be an issue if projects are time-sensitive.

Data quality or resolution can drastically affect the results of an analysis. Working a small study area with data resolutions too coarse for the AOI may render any results unsuitable for further analysis or future work. Quality of the data in use is important, as the higher the resolution, the finer the detail and more comprehensive the results are. The downside of having

finer quality data is, as mentioned previously, the size of the data in question. File sizes too large may be a detriment to hardware storage and memory capacities – perhaps even cloud-based storage capacities – as well as processing time and speed.

Data compatibility is an issue that needs to be addressed whenever a project requires data. Different sources of data provide different formats that may or may not work with certain software. It is important to determine then what data is necessary and what is superfluous – upon which data deemed essential might require a conversion from its original format into another that is software compatible. Should a transformation into a compatible format fail, then either a separately sourced data set needs to be found, or the criterion that uses the data in question is discarded from the project.

5.2. Societal Impacts

Landslide susceptibility mapping is an important facet of disaster planning and management. As populations spread outward and encroach on the foothills of mountains, people migrate ever closer to areas prone to landslide activity. This movement towards landslide-prone areas means that more lives, as well as property and infrastructure, are at risk. With the rise in global population and climatic changes due to global warming, predicting potential landslide locations becomes increasingly important in regions already prone to landslides.

While the global average temperature is slowly climbing, local average temperatures in parts of the world have dropped. These localized changes are exaggerated at the poles and regions of high altitude, and it is for this reason that landslide susceptibility mapping – particularly in mountainous regions with nearby urban centers – is such an important of urban planning. The increasing global population has led to wider, more extensive urban sprawl. As more people move to larger cities and, in turn, choose to live in the suburbs, cities that are

already in close proximity to mountain ranges are spreading upwards into the foothills of said mountains. This puts not only people, but infrastructure and property as well, in regions of higher landslide risk. Roads that traverse through and along mountains require level surfaces, and so slopes are excavated in order to accommodate construction. This excavation, however, comes at the cost of slope stability, thereby increasing the risk of a landslide occurring.

The spreading of population centers and the creation of roads also brings along other forms of infrastructure, such as buildings both residential and commercial, electricity, water, and communications networks, and potentially other methods of rapid transit. Most of these constructions require stable, if not level, foundations for structural longevity and integrity, and destabilizing the soil under and around these new constructions must be taken into consideration. Landslide susceptibility mapping studies undertaken to better understand the slope stability of the construction of these new construction projects may also play a feature role in legislation to ensure the safety of both the infrastructure being built, as well as the people working on the construction projects. This may be further extended to legislation regarding the protection of both residents and commercial businesses, which ultimately means greater safety precautions are put into place for the protection of those with a landslide hazard zone.

The following figures respectively showcase details for both the weighted and fuzzy overlays in relation to Front Range and the Denver metroplex. The overlay layers are semitransparent to allow visibility of not only Denver and its satellite cities, but also a few of the major roads and highways that run through the cities and the hillshade from the basemap for a sense of relative relief.

The weighted overlay result (Figure 40) shows higher susceptibility within the Front Range where drainage systems exist. The weighted overlay result suggests that for the most part,

residents of Denver and its surroundings are most susceptible to landslides near where the Clear Creek drainage system exits the Front Range – the Clear Creek drainage system is the fluvial system that crosses the center of Figure 40. This means that when there is precipitation upstream in the Front Range, residents in western Denver are at higher risk, and while cities like Golden and Boulder are established along the edge of the Front Range, lawmakers may mitigate damage and injury by passing laws that require property and infrastructure to be built a certain distance away from the base of the mountains. While the weighted overlay results implies that there is an increase chance of landslide activity to the north of Denver due to the presence of unconsolidated sediment, the fact that there is minimal slope change drops the chances of a landslide significantly.

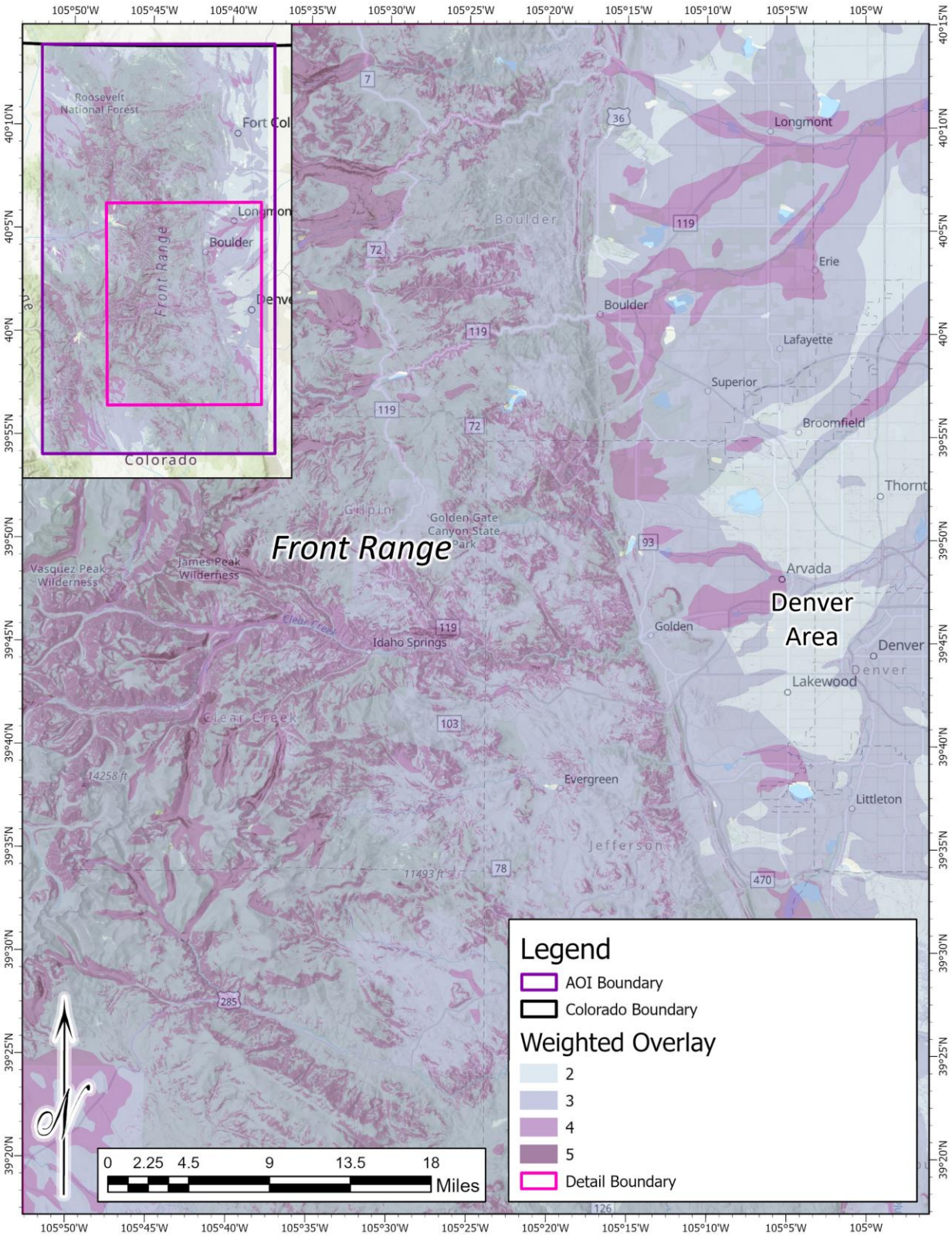

Figure 33 Detail of weighted overalay

The fuzzy overlay result (Figure 41) is similar to the weighted overlay with regards to its characterization of the Clear Creek drainage system, but there is increased emphasis on smaller drainage systems to the north that the weighted overlay does not demonstrate to the same extent. The result from the fuzzy overlay indicates that a larger percentage of the population in the Denver metroplex are more vulnerable to landslide activity. Unlike the weighted overlay, the fuzzy overlay result does not consider unconsolidated sediment within the Denver metroplex to be a landslide hazard for reasons stated before. In this way, the fuzzy overlay's result is more accurate than the weighted overlay.

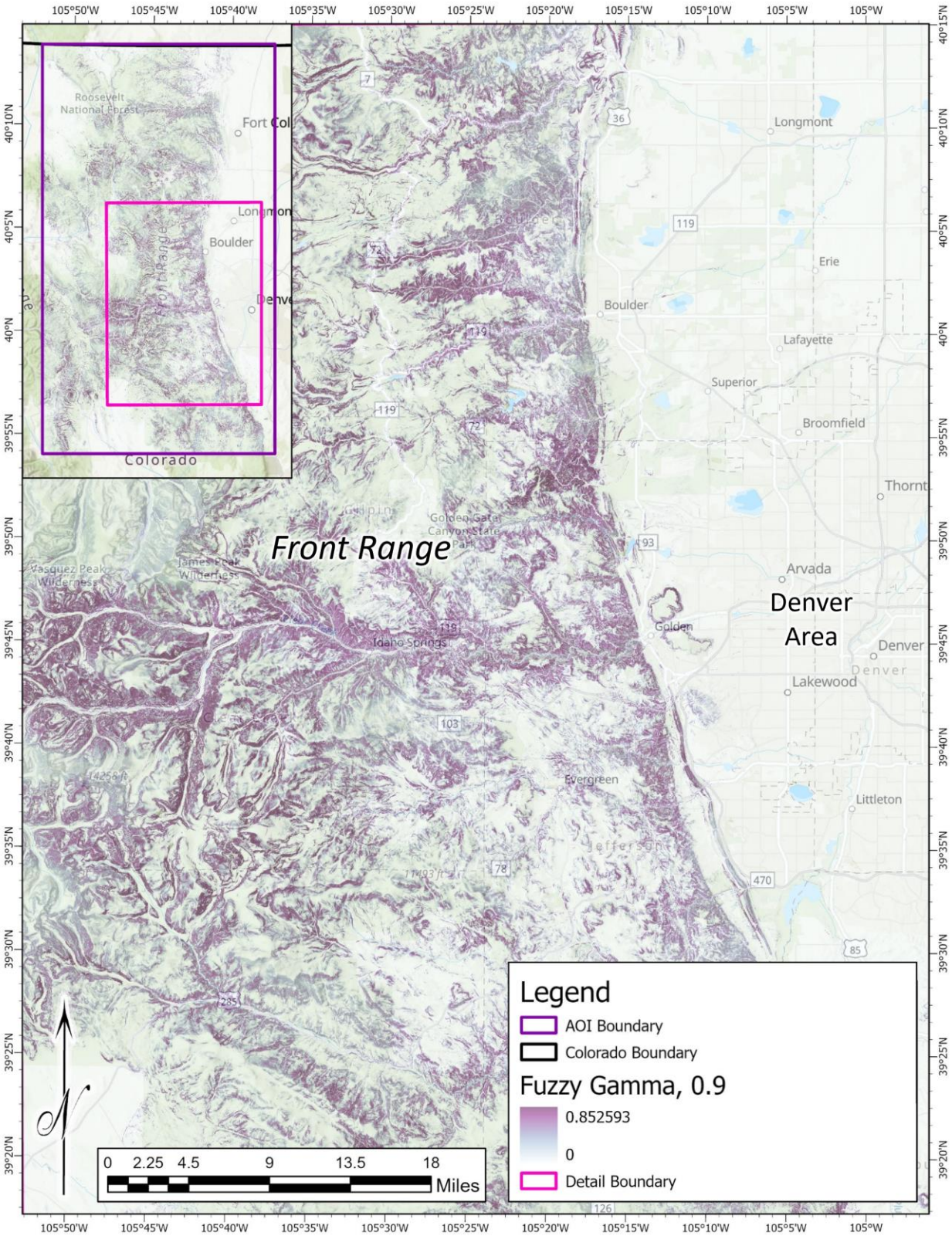

Figure 34 Detail of fuzzy overlay

5.3. Future Application and Work

Further work could be done with this project, as the results may be considered preliminary if expanded upon. The results of this project could be the first step in creating a more robust project for landslide susceptibility mapping in the Front Range. In refining this project, more variables might be added to increase the accuracy and precision of potential landslide locales. While every possible criterion should not be included, select data that was not included here, including soil composition, water saturation, LULC, population/census tracts, and aspect. Each of these variables were considered and ultimately discarded for reasons listed in Chapter 3, but their inclusion in this project would have enriched the results immensely.

The results from this project could also be used as a means of comparing methodologies. Provided the variables used are weighted as evenly as possible across methods, an analysis of which method works better or worse for landslide susceptibility analysis might be useful in narrowing down choices for similar projects in the future. As mentioned in Chapter 2, a variety of methods have been used for landslide susceptibility mapping in the past, and the results of this project might be compared to those other methodologies if they use the same data and AOI. It is also possible for the results of this project to be merged into a larger, state-wide or even nation-wide landslide susceptibility map, one that could provide greater detail if the resolution of this project's output is of better quality than what is otherwise available.

If given the opportunity or time to further or improve upon this project, the data that had been discarded would have been assimilated into the project. If available, information regarding wind direction would have also been included, as the direction of prevailing winds have a significant impact on climate – and more specifically, precipitation, weathering, and erosional patterns, as well as amount of solar radiation an area receives. It is possible that other weighting

schemes might have been included to create a more robust comparison to better flesh out both the effectiveness and accuracy of the weighting methods as well as incite deeper discussion on the relationship between variables and bias. These would be the primary reasons to further pursue research through this project, which would, in and of itself, be a hefty undertaking.

References

Ahmed, B. 2015. “Landslide Susceptibility Mapping Using Multi-Criteria Evaluation Techniques in Chittagong Metropolitan Area, Bangladesh.” *Landslides* 12: 1077–1095. https://doi.org/10.1007/s10346-014-0521-x.

American Geosciences Institute. n.d. “How Much Do Landslides Cost the U.S. in Terms of Monetary Losses?” Accessed July 15, 2021. https://www.americangeosciences.org/critical-issues/faq/how-much-do-landslides-cost-terms-monetary-losses.

Amitrano, D., R. Guida, D. Dell’Aglio, G. Di Martino, D. Di Martire, A. Iodice, M. Costantini, F. Malvarosa, and F. Minati. 2019. “Long-Term Satellite Monitoring of the Slumgullion Landslide Using Space-Borne Synthetic Aperture Radar Sub-Pixel Offset Tracking.” *Remote Sensing* 11: 369. https://doi.org/10.3390/rs11030369.

Aoudia, A., G. Costa, and P. Suhadolc. 1970. "GIS for Earthquake Hazards Mitigation in the Friuli Area (NE Italy)." *WIT Transactions on Information and Communication Technologies* 21.

Baidya, P., D. Chutia, S. Sudhakar, C. Goswami, J. Goswami, V. Saikhom, P.S. Singh, and K.K. Sarma. 2014. “Effectiveness of Fuzzy Overlay Function for Multi-Criteria Spatial Modeling—A Case Study on Preparation of Land Resources Map for Mawsynram Block of East Khasi Hills District of Meghalaya, India.” *Journal of Geographic Information System* 6: 605–612. https://doi.org/10.4236/jgis.2014.66050.

Blońska, E., J. Lasota, W. Piazczyk, M. Wiecheć, A. Klamerus-Iwa. 2018. “The Effect of Landslide on Soil Organic Carbon Stock and Biochemical Properties of Soil.” *Journal of Soils and Sediments* 18: 2727–2737. https://doi.org/10.1007/s11368-017-1775-4.

Bogaard, T., Y. Gugliem, V. Marc, C. Emblanch, C. Bertrand, and J. Mudry. 2007. “Hydrogeochemistry in Landslide Research: A Review.” *Bulletin de la Société Géologique de France* 178, no. 2: 113–126. https://doi.org/10.2113/gssgfbull.178.2.113.

Buckley, J.J. 1985. “Fuzzy Hierarchical Analysis.” *Fuzzy Sets and Systems* 17, no. 3: 233–247. https://doi.org/10.1016/0165-0114(85)90090-9.

Carver, S.J. 1991. “Integrating Multi-Criteria Evaluation with Geographical Information Systems.” *International Journal of Geographical Information System* 5, no. 3: 321–339. https://doi.org/10.1080/02693799108927858.

Çellek, S. 2013. “Landslide Susceptibility Analysis of Sinop-Gerze Region.” PhD diss. Karadeniz Technical University, Turkey.

—. 2020. “Effect of the Slope Angle and Its Classification on Landslide.” *Natural Hazards and Earth System Sciences*: Preprint. https://doi.org/10.5194/nhess-2020-87.

—. 2021 "The Effect of Aspect on Landslide and Its Relationship with Other Parameters" in *Landslides*, edited by Y. Zhang, Q. Cheng. London: IntechOpen. https://doi.org/10.5772/intechopen.99389.

Cerri, R.I., V. Rosolen, F.A.G.V. Reis, A.J. Pereira Filho, F. Vemado, L. do Carmo Giordano, and B. Maques Gabelini. 2020. "The Assessment of Soil Chemical, Physical, and Structural Properties as Landslide Predisposing Factors in the Serra do Mar Mountain Range (Caraguatatuba, Brazil)." *Bulletin of Engineering Geology and the Environment* 79: 3307–3320. https://doi.org/10/1007/s10064-020-01781-1.

Çetinkaya, C., E. Özceylan, M. Erbaş, and M. Kabak. 2016. "GIS-Based Fuzzy MCDA Approach for Siting Refugee Camp: A Case Study for Southeastern Turkey." *International Journal of Disaster Risk Reduction* 18: 218–231. https://doi.org/10.1016/j.ijdrr.2016.07.004.

Che, V.B., K. Fontijn, G.G.J. Ernst, M. Kervyn, M. Elburg, E. Van Ranst, and C.E. Suh. 2011. "Evaluating the Degree of Weathering in Landslide-Prone Soils in the Humid Tropics: The Case of Limbe, SW Cameroon." *Geoderma* 170: 378–389. https://doi.org/10.1016/geoderma.2011.10.013.

Chen, Y., R. Liu, D. Barrett, L. Gao, M. Zhou, L. Renzullo, and I. Emelyanova. 2015. "A Spatial Assessment Framework for Evaluating Flood Risk Under Extreme Climates." *Science of the Total Environment* 538: 512–523. https://doi.org/10.1016/j.scitotenv.2015.08.094.

Clague J.J. and N.J. Roberts. 2012. "Landslide Hazard and Risk." in *Landslides: Types, Mechanisms and Modeling.* Cambridge: Cambridge University Press. https://doi.org/10.1017/CBO9780511740367.

Clague, J.J. and D. Stead. 2012. *Landslides: Types, Mechanisms and Modeling*. Cambridge: Cambridge University Press. https://doi.org/10.1017/CBO9780511740367.002.

Coe, J.A., J.W. Godt, R.L. Baum, R.C. Buckham, and J.A. Michael. 2004. "Landslide Susceptibility from Topography in Guatemala." in *Landslides: Evaluation and Stabilization.* Edited by W.A. Lacerda, M. Ehrlich, S.A.B. Fontura and A.S.F. Sayão. 69–78. London: Taylor & Francis Group. https://doi.org/10.1201/b16816-8.

Colorado Geological Survey. n.d. "Landslides." Accessed August 13, 2021. https://coloradogeologicalsurvey.org/hazards/landslides/.

Cruden, D.M., and D.J. Varnes. 1996. "Landslide Types and Processes. Landslides: Investigation and Mitigation." Special Report 247: 36–75, Washington: Transportation Research Board.

Dağ, S., 2007. "Landslide Susceptibility Analysis of Çayeli (Rize) and Its Surrounding by Statistical Methods." PhD diss. Karadeniz Technical University, Turkey.

Daly, C., R.P. Nielson, and D.L. Phillips. 1993. “A Statistical-Topographic Model for Mapping Climatological Precipitation over Mountainous Terrain.” *Journal of Applied Meteorology* 33: 140–158.

De Montis, A., P. De Toro, B. Droste-Franke, I. Omann, and S. Stagl. 2004. "Assessing the Quality of Different MCDA Methods." in *Alternatives for Environmental Valuation*: 115–149. London: Routledge. https://doi.org/10.4324/9780203412879.

Dempsey, C. 2020. “What is the Difference Between Elevation and Altitude?” Last modified March 23, 2023. https://www.geographyrealm.com/what-is-the-difference-between-elevation-and-altitude/.

Denver Regional Council of Governments. n.d. “Data” Accessed: July 24, 2022. https://data.drcog.org/data?page=1&q=&sort=title.

Di Luzio, M. 2010. “Seamless Daily Precipitation for the Conterminous United States.” Accessed June 5, 2022. https://datagateway.nrcs.usda.gov/GDGHome_DirectDownLoad.aspx.

Di Maio, C., J. De Rosa, R. Vassallo, R. Coviello, and G. Macchia. 2020. “Hydraulic Conductivity and Pore Water Pressures in a Clayey Landslide: Experimental Data.” *Geosciences* 10, no. 102: 13. https://doi.org/10.3390/geosciences10030102.

Donnarumma, A., P. Revellino, G. Grelle, and F.M. Guadango. 2013. “Slope Angle as Indicator Parameter of Landslide Susceptibility in a Geologically Complex Area.” in *Landslide Science and Practice*, edited by C. Margottini, P. Canuti, and K. Sassa 425–433. Berlin: Springer-Verlag Berlin Heidelberg. https://doi.org/10.1007/978-3-642-31325-7_56.

Du, G.L., Y.S. Zhang, J. Iqbal, Z.H. Yang, and X. Yao. 2017. “Landslide Susceptibility Mapping Using an Integrated Model of Information Value Method and Logistic Regression in the Bailongjiang Watershed, Gansu Province, China.” *Journal of Mountain Science* 14, no. 2: 249–268. https://doi.org/10.1007/s11629-016-4126-9.

Eberhardt, E. 2012. “Landslide Monitoring: The Role of Investigative Monitoring to Improve Understanding and Early Warning of Failure.” in *Landslides: Types, Mechanisms and Modelling*, edited by J.J. Clague and D. Stead. 222–234. Cambridge: Cambridge University Press. https://doi.org/10.1017/CBO9780511740367.020.

Erbaş, M., M. Kabak, E. Özceylan, and C. Çetinkaya. 2018. “Optical Siting of Electric Vehicle Charging Stations: A GIS-Based Fuzzy Multi-Criteria Decision Analysis.” *Energy* 163: 1017–1031. https://doi.org/10.1016/j.energy.2018.08.140.

Ercanoglu, M. and C. Gokceoglu. 2002. “Assessment of Landslide Susceptibility for a Landslide-Prone Area (North of Yenice, NW Turkey) by Fuzzy Approach.” *Environmental Geology* 41: 720–730. https://doi.org/10.1007/s00254-001-0454-2.

Erener, A., A. Mutlu, and H.S. Düzgün. 2016. “A Comparative Study for Landslide Susceptibility Mapping Using GIS-Based Multi-Criteria Decision Analysis (MCDA),

Logistic Regression (LR) and Association Rule Mining (ARM).” *Engineering Geology* 203: 45–55. https://doi.org/10.1016/j.enggeo.2015.09.007.

Feizizadeh, B. and T. Blaschke. 2013. “GIS-Multicriteria Decision Analysis for Landslide Susceptibility Mapping: Comparing Three Methods for the Urmia Lake Basin, Iran.” *Natural Hazards* 65: 210 –2128. https://doi.org/10.1007/s11069-012-0463-3.

—. 2014. “An Uncertainty and Sensitivity Analysis Approach for GIS-Based Multicriteria Landslide Susceptibility Mapping.” *International Journal of Geographical Information Science* 28, no. 3: 610–638. https://doi.org/10.1080/13658816.2013.869821.

Florinsky, I.V., 2016. “Chapter 14 – Lineaments and Faults.” in *Digital Terrain Analysis in Soil Science and Geology (Second Edition)*, edited by I.V. Florinsky. 353–376. London: Elsevier. https://doi.org/10.1016/B978-0-12-804632-6.09991-0.

Francioni, M., F. Calamita, J. Coggan, A. De Nardis, M. Eyre, E. Miccadei, T. Piacentini, D. Stead, and N. Sciarra. 2019. “A Multi-Disciplinary Approach to the Study of Large Rock Avalanches Combining Remote Sensing, GIS and Field Studies: The Case of the Scanno Landslide, Italy.” *Remote Sensing* 11: 1570. https://doi.org/10.3390/rs11131570.

Froude, M.J. and D.N. Petley. 2018. “Global Fatal Landslide Occurrence from 2004 to 2016.” *Natural Hazards and Earth System Sciences* 18: 2161–2181. https://doi.org/10.5194/nhess-18-2161-2018.

Ghorbanzadeh, O., T. Blaschke, K. Gholamnia, S.R. Meena, D. Tiede, and J. Aryal. 2019. “Evaluation of Different Machine Learning Methods and Deep-Learning Convolutional Neural Networks for Landslide Detection.” *Remote Sensing* 11: 196. https://doi.org/10.3390/rs11020196.

The GIS Encyclopedia. n.d. “Aspect (geography).” Last modified October 23, 2013, 02:33. http://www.wiki.gis.com/wiki/index.php/Aspect_(geography).

The GIS Encyclopedia. n.d. “Elevation.” Last modified November 27, 2011, 01:23. http://www.wiki.gis.com/wiki/index.php/Elevation.

Glade, T., M. Anderson, and M.J. Crozier. 2005. *Landslide Hazard and Risk*. Chichester, England: John Wiley & Sons, Ltd. https://doi.org/10.1002/9780470012659.

Glade, T. and M.J. Crozier. 2005 “Landslide Hazard and Risk: Issues, Concepts and Approach.” in *Landslide Hazard and Risk*, edited by T. Glade, M. Anderson, and M.J. Crozier. 1–40. West Sussex: John Wiley & Sons, Ltd. https://doi.org/10.1002/9780470012659.ch1.

Gomberg, J., P. Bodin, W. Savage, and M.E. Jackson. 1995. “Landslide Faults and Tectonic Faults, Analogs?: The Slumgullion Earthflow, Colorado.” *Geology* 23, no. 1: 41–44.

Gomberg, J., W. Schulz, P. Bodin, and J. Kean. 2011. “Seismic and Geodetic Signatures of Fault Slip at the Slumgullion Landslide Natural Laboratory.” *Journal of Geophysical Research* 116: B09404. https://doi.org/10.1029/2011JB008304.

Hasekioğullari, G. D. 2011. “Assessment of Parameter Effects in Eroducing Landslide Susceptibility Maps.” MS thes. Hacettepe University, Turkey.

Hasanloo, M., P. Pahlavani, and B. Bigdeli. 2019. “Flood Risk Zonation Using a Multi-Criteria Spatial Group Fuzzy-AHP Decision Making and Fuzzy Overlay Analysis.” *Remote Sensing and Spatial Information Sciences* 42: 18. https://doi/org/10.5194/isprs-archives-XLII-4-W18-455-2019.

Hassan, I., M.A. Javed, M. Asif, M. Luqman, S.R. Ahmad, A. Ahmad, S. Akhtar, and B. Hussain. 2020. “Weighted Overlay Based Land Suitability Analysis of Agriculture Land in Azad Jammu and Kashmir Using GIS and AHP.” *Pakistani Journal of Agricultural Research* 57, no. 6: 1509–1519. https://doi.org/10.21162/PAKJAS/20.9507.

Highland, L.M. 2008. *The Landslide Handbook—A Guide to Understanding Landslides.* Reston, VA: U.S. Geological Survey. https://pubs.usgs.gov/circ/1325/.

Hu, X. and R. Bürgmann. 2020. “Rheology of a Debris Slide From the Joint Analysis of UAVSAR and LiDAR Data.” *Geophysical Research Letters* 47: e2020GL087452. https://doi.org/10.1029/2020GL087452.

Huang, I.B., J. Keisler, and I. Linkov. 2011. “Multi-Criteria Decision Analysis in Environmental Sciences: Ten Years of Applications and Trends.” *Science of the Total Environment* 409: 3578–3594. https://doi.org/10.1016/j.scitotenv.2011.06.022.

Huggel, C., N. Khabarov, O. Korup, and M. Obersteiner. 2012. “Physical Impacts of Climate Change on Landslide Occurrence and Related Adaptation.” in *GIS Landslide*, edited by H. Yamagishi and N.P. Bhandary, 121–133. Tokyo: Springer Japan. https://doi.org/10.1017/CBO9780511740367.003.

Islam, Z. and G. Metternicht. 2005. “The Performance of Fuzzy Operators on Fuzzy Classification of Urban Land Covers.” *Photogammetric Engineering & Remote Sensing* 71, no. 1: 59–68. https://doi.org/10.14358/PERS.71.1.59.

Iwahashi, J., S. Watanabe, and T. Furuya. 2003. “Mean Slope-Angle Frequency Distribution and Size Frequency Distribution of Landslide in Higashikubiki Area, Japan.” *Geomorphology* 50: 394–364. https://doi.org/10.1016.S0169-555X(02)00222-2.

Jankowski, P. 1995. “Integrating Geographical Information Systems and Multiple Criteria Decision-Making Methods.” *International Journal of Geographical Information Systems* 9, no. 3: 251–273. https://doi.org/10.1080/02693799508902036.

Johnson, B., C. Campbell, and H.J. Melosh. 2016. “The Reduction of Friction in Long Runout Landslides as an Emergent Phenomenon.” *Journal of Geophysical Research Earth Science* 121: 881–889. https://doi.org/10.1002/2015JF003751.

Kayastha, P. 2015. “LandslideSusceptibility Mapping and Factor Effect Analysis Using Frequency Ratio in a Catchment Scale: A Case Study from Garuwa Sub-Basin, East

Nepal." *Arabian Journal of Geosciences* 8: 8601–8613. https://doi.org/10.1007/s12517-015-1831-6.

Kavzoglu, T., E.K. Sahin, and I. Colkesen. 2013. "Landslide Susceptibility Mapping Using GIS-Based Multi-Criteria Decision Analysis, Support Vector Machines, and Logistic Regression." *Landslides* 11, no. 3: 425–439. https://doi.org/10.1007/s10346-013-0391-7.

Kim, J.Y. 2019. "Introduction to Fuzzy Set Theory and The Hyperplane Separation Theorem of Fuzzy Convex Sets." Masters thesis, University of Washington. https://sites.math.washington.edu/~morrow/336_20/papers19/Jon.pdf.

Knepper, Jr., D.H. 2002. "Planning for the Conservation and Development of Infrastructure Resources in Urban Areas—Colorado Front Range Urban Corridor." In *U.S. Geological Survey Circular 1219*. Denver: U.S. Geological Survey. https://pubs.usgs.gov/circ/c1219/.

Korup, O. 2012. "Landslides in the Earth System." in *GIS Landslide*, edited by H. Yamagishi and N.P. Bhandary, 10–23. Tokyo: Springer Japan. https://doi.org/10.1017/CBO9780511740367.003.

Kritikos, T., and T. Davies. 2014. "Assessment of Rainfall-Generated Shallow Landslide/Debris-Flow Susceptibility and Runout Using a GIS-Based Approach: Application to Western Southern Alps of New Zealand." *Landslides* 12, no. 6: 1–25. https://doi.org/10.1007/s10346-014-0533-6.

Lai, J.S., and F. Tsai. 2019. "Improving GIS-Based Landslide Susceptibility Assessments with Multi-temporal Remote Sensing and Machine Learning." *Sensors* 19: 25. https://doi.org/10.3390/s19173717.

Lee, S. 2005. "Application of Logistic Regression Model and Its Validation for Landslide Susceptibility Mapping Using GIS and Remote Sensing Data." *International Journal of Remote Sensing* 26, no. 7: 1477–1491. https://doi.org/10.1080/01431160412331331012.

Lehmann, P., J. von Ruette, and D. Or. 2019. "Deforestation Effects on Rainfall-Induced Shallow Landslides: Remote Sensing and Physically-Based Modelling." *Water Resources Research* 55: 9962–9976. https://doi.org/10.1029/2019WR025233.

Li, J., W. Wang, and Z. Han. 2021. "A Variable Weight Combination Model for Prediction on Landslide Displacement Using AR Model, LSTM Model, and SVM Model: A Case Study of the Xinming Landslide in China." *Environmental Earth Sciences* 80: 356. https://doi.org/10.1007/s12665-021-09696-2.

Li, Y., X. Wang, and H. Mao. 2020. "Influence of Human Activity on Landslide Susceptibility Development in the Three Gorges Area." *Natural Hazards* 104: 2115–2151. https://doi.org/10.1007/s11069-020-0426406.

Lin, C.Y., C.Y. Lin, and C. Chompuchan. 2017. “Risk-Based Models for Potential Large-Scale Landslide Monitoring and Management in Taiwan.” *Geomatics, Natural Hazards and Risk* 8, no. 2:1505–1523. https://doi.org/10.1080/19475705.2017.1345797.

Lombardo, L., and P.M. Mai. 2018. “Presenting Logistic Regression-Based Landslide Susceptibility Results.” *Engineering Geology* 244: 14–24. https://doi.org/10.1016/j.enggeo.2018.07.019.

Ma, Y., J. Zhao, Y. Sui, S. Liao, and Z. Zhang. 2020. “Application of Knowledge-Driven Methods for Mineral Prospectivity Mapping of Polymetallic Sulfide Deposits in the Southwest Indian Ridge between 46° and 52°E.” *Minerals* 10: 970. https://doi.org/10.3390/min10110970.

Madison, A., E. Fielding, Y. Sheng, and K. Cavanaugh. 2019. “High-Resolution Spaceborne, Airborne and In Situ Landslide Kinematic Measurements of the Slumgullion Landslide in Southwest Colorado.” *Remote Sensing* 11: 265. https://doi.org/10.3390/rs11030265.

Maes, J., M. Kervyn, A. de Hontheim, O. Dewitte, L. Jacobs, K. Mertens, M. Vanmaercke, L. Vranken, J. Poesen. 2017. “Landslide Risk Reduction Measures: A Review of Practices and Challenges for the Tropics.” *Progress in Physical Geography* 4, no. 2: 191–221. http://doi.org/10.1177/0309133316689344.

Mallick, J., R.K. Singh, M.A. AlAwadh, S. Islam, R.A. Khan, and M.N. Qureshi. 2018. “GIS-Based Landslide Susceptibility Evaluation Using Fuzzy-AHP Multi-Criteria Decision-Making Techniques in the Abha Watershed, Saudi Arabia.” *Environmental Earth Sciences* 77: 276. https://doi.org/10.1007/s12665-018-7451-1.

Malczewski, J. 2004. “GIS-Based Land-Use Suitability Analysis: A Critical Overview.” *Progress in Planning* 62: 3–65. https://doi.org/10.1016/S0305-9006(03)00079-5.

Malczewski, J. and C. Rinner. 2015. *Multicriteria Decision Analysis in Geographic Information Science*. New York: Springer. https://doi.org/10.1007/978-3-540-74757-4.

Martel, S.J. 2004. “Mechanics of Landslide Initiation as a Shear Fracture Phenomenon.” *Marine Geology* 203: 319–339. https://doi.org/10.1016/S0025-3227(03)00313-X.

McKean, J. and J. Roering. 2004. “Objective Landslide Detection and Surface Morphology Mapping Using High-Resolution Airborne Laser Altimetry.” *Geomorphology* 57: 331–351. https://doi.org/10.1016/S0169-555X(03)00164-8.

Moreiras, S.M. and A. Coronato. 2010. “Landslide Processes in Argentina.” in *Natural Hazards and Human-Exacerbated Disasters in Latin America*, edited by Edgardo M. Latrubesse. 301–332. Amsterdam: Elsevier. https://doi.org/10.1016/S0928-2025(08)10015-3.

National Oceanic and Atmospheric Administration. 2007. “Full Set of Rivers.” Last modified May 16, 2007. https://www.weather.gov/gis/Rivers.

National Renewable Energy Laboratory (NREL). n.d. “Wind Prospector.” Accessed July 27, 2022. https://maps.nrel.gov/wind-prospector/?aL=w_eWZI%255Bv%255D%3Dt%26P0Tu_1%255Bv%255D%3Dt%26P0Tu_1%255Bd%255D%3D1&bL=ujuxuD&cE=0&lR=0&mC=38.28131307922966%2C-106.23779296875&zL=6

Nelson, P.H., and S.L. Santus. 2011. “Gas, Water, and Oil Production from Wattenberg Field in the Denver Basin, Colorado.” In *U.S. Geological Survey Open-File Report 2011-1175.* Reston, Virginia: U.S. Geological Survey. https://pubs.usgs.gov/of/2011/1175/pdf/OF11-1175.pdf.

Ott, R.F. 2020. “How Lithology Impacts Global Topography, Vegetation, and Animal Biodiversity: A Global-Scale Analysis of Mountainous Regions.” *Geophysical Research Letters* 47: e2020GL088649. https://doi.org/10.1029/2020GL088649.

Padilla, C., Y. Onda, T. Iida, S. Takahashi, and T. Uchida. 2014. “Characterization of the Groundwater Response to Rainfall on a Hillslope with Fractured Bedrock by Creep Deformation and Its Implication for the Generation of Deep-Seated Landslides on Mt. Wanitsuka, Kyushu Island.” *Geomorphology* 204: 444–458. https://doi.org/10.1016.j.geomorph2013.08.024.

Palcic, I. and B. Lalic. 2009. “Analytical Hierarchy Process as a Tool for Selecting and Evaluating Projects.” *International Journal of Simulation Modelling* 1: 16–26. https://doi.org/10.2507/IJSIMM08(1)2.112.

Park, J.H. 2015. “Analysis on the Characteristics of the Landslide – With a Special Reference on Geo-Topographical Characteristics –.” *Journal of Korean Society of Forest Science* 104, no. 4: 588–597. https://doi.org/10.14578/jkfs.2015.104.4.588.

Pawluszek, K. and A. Borkowski. 2016. “Impact of DEM-Derived Factors and Analytical Hierarchy Process on Landslide Susceptibility Mapping in the Region of Rożnów Lake, Poland.” *Natural Hazards* 86: 919–952. https://doi.org/10.1007/s11069-016-2725-y.

Petley, D. 2012. “Remote Sensing Techniques and Landslides.” in *Landslides: Types, Mechanisms and Modelling,* edited by J.J. Clague and D. Stead, 159–171. Cambridge: Cambridge University Press. https://doi.org/10.1017/CBO9780511740367.015.

Pourghasemi, H.R., B. Pradhan, and C. Gokceoglu. 2012. "Application of Fuzzy Logic and Analytical Hierarchy Process (AHP) to Landslide Susceptibility Mapping at Haraz Watershed, Iran." *Natural hazards* 63, no. 2: 965–996. https://doi.org/10.1007/s11069-012-0217-2.

Preuth, T., T. Glade, and A. Demoulin. 2009. “Stability Analysis of a Human-Influenced Landslide in Eastern Belgium.” *Geomorphology* 120: 38–47. http://doi.org/j.geomorph.2009.09.013.

Qiu, C., and Y. Mitani. 2017. “Development of a GIS-Based 3D Slope Stability Analysis System for Rainfall-Induced Landslide Hazard Assessment.” in *GIS Landslide,* edited by H.

Yamagishi and N.P. Bhandary, 71–93. Tokyo: Springer Japan. https://doi.org/10.1007/978-4-431-54391-6.

Roslee, R., A.C. Mickey, N. Simon, and M.N. Norhisham. 2017. "Landslide Susceptibility Analysis (LSA) Using Weighted Overlay Method (WOM) Along the Genting Sempah to Bentong Highway, Pahang." *Malaysian Journal of Geosciences* 1 no. 2: 13–19. https://doi.org/10.26480/mjg.02.2017.13.19.

Regmi, N.R., J.R. Giardino, and J.D. Vitek. 2013. "Characteristics of Landslides in Western Colorado, USA." *Landslides* 11: 589–603. https://doi.org/10.1007/s10346-013-0412-6.

Reid, M.E., R.G. LaHusen, R.L. Baum, J.W. Kean, W.H. Schulz, and L.M. Highland. 2012. *Real-Time Monitoring of Landslides.* Denver: U.S. Geological Survey. https://doi.org/10.3133/FS20123008.

Rengers, F.K., L.A. McGuire, J.A. Coe, J.W. Kean, R.L. Baum, D.M. Staley, and J.W. Godt. 2016. "The Influence of Vegetation on Debris-Flow Initiation During Extreme Rainfall in the Northern Colorado Front Range." *Geology* 44, no. 10: 823–826. https://doi.org/10.1130/G38096.1.

Roodposhti, M.S., J. Aryal, H. Shahabi, and T. Safarrad. 2016. "Fuzzy Shannon Entropy: A Hybrid GIS-Based Landslide Susceptibility Mapping Method." *Entropy* 18: 343. https://doi.org/10.3390/e18100343.

Rotaru, A., D. Oajdea, and P. Răileanu. 2007. "Analysis of the Landslide Movements." *International Journal of Geology* 3, no. 1: 70–79. https://naun.org/multimedia/NAUN/geology/ijgeo-10.pdf.

Saaty, R.W. 1987. "The Analytic Hierarchy Process—what it is and how it is used." *Mathl Modelling* 9, no. 3–5: 161–176.

Saha, A.K., R.P. Gupta, I. Sarkar, M.K. Arora, and E. Csaplovics. 2005. "An Approach for GIS-Based Statistical Landslide Susceptibility Zonation—with a Case Study in the Himalayas." *Landslides* 2: 61–69. https://doi.org/10.1007/s10346-004-0039-8.

Schulz, W.H., J.P. McKenna, J.D. Kibler, and G. Biavati. 2009. "Relations between Hydrology and Velocity of a Continuously Moving Landslide—Evidence of Pore-Pressure Feedback Regulating Landslide Motion?" *Landslides* 6: 181–190. https://doi.org/10.1007/s10346-009-0157-4.

Shit, P.K., G.S. Bhunia, and R. Maiti. 2016. "Potential Landslide Susceptibility Mapping Using Weighted Overlay Model (WOM)." *Modeling Earth Systems and Environment* 2: 21. https://doi.org/10.1007/s40808-016-0078-x.

Shou, K.J. and J. Chen. 2021. "On the Rainfall Induced Deep-Seated and Shallow Landslide Hazard in Taiwan." *Engineering Geology* 288: 106156. https://doi.org/10.1016/j.enggeo.2021.106156

Shou, K.J. and J.F. Lin. 2016. “Multi-Scale Landslide Susceptibility Analysis Along a Mountain Highway in Central Taiwan.” *Engineering Geology* 212: 120–135. https://doi.org/10.1016/j.enggeo.2016.08.009

Stanley, T., and D.B. Kirschbaum. 2017. “A Heuristic Approach to Global Landslide Susceptibility Mapping.” *Natural Hazards* 87, no. 1: 145–164. https://doi.org/10.1007/s11069-017-2757-y.

State of Colorado. 2011. “Major River Basin Boundaries.” Last modified February 9, 2011. https://cdss.colorado.gov/gis-data/gis-data-by-category.

—. 2015. “Counties in Colorado.” Last modified January 17, 2023. https://data.colorado.gov/Transportation/Counties-in-Colorado/67vn-ijga.

—. 2015. “Major Roads in Colorado.” Last modified January 17, 2023. https://data.colorado.gov/Transportation/Major-Roads-in-Colorado/e7ye-tasg.

Suchet, P.A., J.L. Probst, and W. Ludwig. 2003. “Worldwide Distribution of Continental Rock Lithology: Implications for the Atmospheric/Soil CO_2 Uptake by Continental Weathering and Alkalinity River Transport to the Oceans.” *Global Biogeochemical Cycles* 17, no. 2: 1083. https://doi.org/10.1029/2002GB001891.

Tan, Q., M. Bai, P. Zhou, J. Hu, and X. Qin. 2020. “Geological Hazard Risk Assessment of Line Landslide Based on Remotely Sensed Data and GIS.” *Measurement* 169: 10. https://doi.org/10.1016/j.measurement.2020.108370.

Triantaphyllou, E. and K. Baig. 2005. “The Impact of Aggregating Benefit and Cost Criteria in Four MCDA Methods.” *IEEE Transactions on Engineering Management* 52, no. 2: 213–226. https://doi.org/10.1109/TEM.2005.845221.

Tweto, O. 1979. “MI-16 Geologic Map of Colorado.” Accessed May 10, 2022. https://mrdata.usgs.gov/geology/state/state.php?state=CO.

United States Census Bureau, Department of Commerce. 2019. “TIGER/LineShapefile, 2019, Primary and Secondary Roads State-based Shapefile.” Updated: January 15, 2021. https://catalog.data.gov/dataset/tiger-line-shapefile-2019-state-colorado-primary-and-secondary-roads-state-based-shapefile.

United States Geological Survey. 2018. “U.S. Landslide Inventory.” Last modified April 5, 2022. https://uscssi.maps.arcgis.com/home/search.html?q=owner%3A%22esjones_USGS%22&t=content&restrict=false.

—. 2022. “Elevation Products (3DEP): 1/3 arc-second DEM.” Last modified July 07, 2022. https://apps.nationalmap.gov/downloader/.

—. n.d. “Lithclass polygon colors.” Accessed November 14, 2022. https://mrdata.usgs.gov/catalog/lithclass-color.php.

—. n.d. “How Many Deaths Result from Landslides Each Year?” Accessed July 15, 2021. https://www.usgs.gov/faqs/how-many-deaths-result-landslides-each-year?qt-news_science_products=0#qt-news_science_products.

—. n.d. “What is a digital elevation model (DEM)?” Accessed February 8, 2023. https://www.usgs.gov/faqs/what-digital-elevation-model-dem#:~:text=DEMs%20are%20created%20from%20a,IfSAR%20(Alaska%20only)%20data.

University of Colorado. 2015. “Colorado Watershed Boundary Dataset (WBD) Hydrologic Unit 8.” Last modified December 16, 2015. https://ark.colorado.edu/ark:/47540/5c8ff914a84a6c000a68f3a8.

—. 2017. “BLM - Colorado State Boundary.” Last modified January 9, 2017. https://geo.colorado.edu/catalog/47540-pf100p61s2w3.

Wang, G. and K. Sassa. 2009. “Seismic Loading Impacts on Excess Pore-Water Pressure Maintain Landslide Triggered Flowslides.” *Earth Surface Processes and Landforms* 34: 232–241. https://doi.org/10.1002/esp.1708.

Wayllace, A., B. Thunder, N. Lu, A. Khan, and J.W. Godt. 2019. “Hydrological Behavior of an Infiltration-Induced Landslide in Colorado, USA.” *Geofluids* 2019: 14. https://doi.org/10.1155/2019/1659303.

Wieczorek, G.F. and P.P. Leahy. 2008. “Landslide Hazard Mitigation in North America.” *Environmental & Engineering Geoscience* 14, no. 2: 133–144. https://doi.org/10.2113/gseegeosci.14.2.133.

Wiki.GIS.com: The GIS Encyclopedia. Updated 27 November 2011, 02:23 UTC. Encyclopedia on-line. Available from http://wiki.gis.com/wiki/index.php/Elevation. Internet. Retrieved 10 September 2022.

Winter, M.., D. Peeling, D. Palmer, and J. Peeling. 2019. “Economic Impacts of Landslides and Floods on a Road Network.” *AUC Geographica* 54, no. 2: 201–207. https://doi.org/10.14712/23361980.2019.18.

Yamagishi, H. 2017. “Identification and Mapping of Landslides.” in *GIS Landslide*, Edited by H. Yamagishi and N.P. Bhandary, 3–11. Tokyo: Springer Japan. https://doi.org/10.1007/978-4-431-54391-6_1.

Zakaria, Z., I. Sophian, Z.S. Sabila, and L.H. Jihadi. 2018. “Slope Safety Factor and Its Relationship with Angle of Slope Gradient to Support Landslide Mitigation at Jatinangor Education Area, Sumedang, West Java, Indonesia.” *IOP Conference Series: Earth and Environmental Science* 145: 012052. https://doi.org/10.1088/1755-1315/145/1/012052.

Zhao, H., L. Yao, G. Mei, T. Liu, and Y. Ning. 2017. “A Fuzzy Comprehensive Evaluation Method Based on AHP and Entropy for a Landslide Susceptibility Map.” *Entropy* 19: 396. https://doi.org/10.3390/e19080396.

Zhou, W., M.D. Minnick, J. Chen, J. Garrett, and E. Acikalin. 2021. “GIS-Based Landslide Susceptibility Analyses: Case Studies at Different Scales.” *Natural Hazards Review* 22, no. 3: 16. https://doi.org/10.1061/(ASCE)NH.1527-6996.0000485.

Zhu, A.X., R. Wang, J. Qiao, C.Z. Qin, Y. Chen, J. Liu, F. Du, Y. Lin, and T. Zhu. 2014. “An Expert Knowledge-Based Approach to Landslide Susceptibility Mapping Using GIS and Fuzzy Logic.” *Geomorphology* 214: 128–138. https://doi.org/10.1016/j.geomorph2014.02.003.